SIBERIA

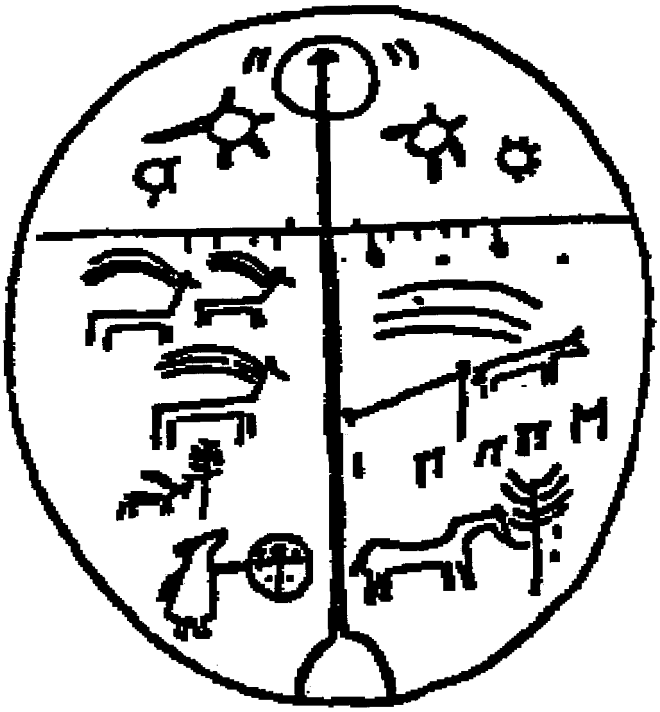

SAR Imaging for Boreal Ecology and Radar Interferometry Applications

EC ENVIRONMENT AND CLIMATE PROGRAMM

THEME 3: SPACE TECHNIQUES APPLIED TO ENVIRONMENTAL MONITORING

AREA 3.3: CENTER FOR EARTH OBSERVATION

Final Report

SIBERIA

SAR IMAGING FOR BOREAL ECOLOGY AND RADAR INTERFEROMETRY APPLICATIONS

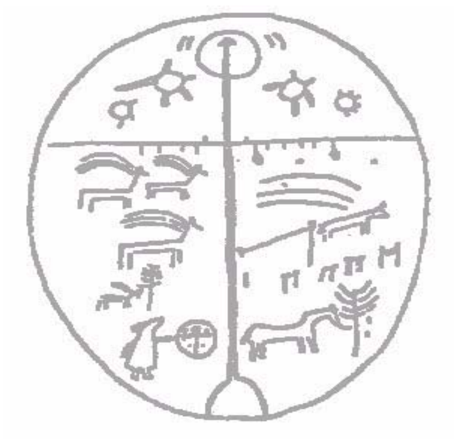

List of Partners:

Country	DE	FR	UK	FI	SE	AT	RU	CH
Teams	**2**	**1**	**3**	**1**	**1**	**1**	**3**	**1**

June 2001

This report describes the work done during the full period of the SIBERIA project (August 1998 to December 2000). SIBERIA is financed through the 4th Framework Programme of the European Commission, Environment and Climate, Area 3.3: Centre for Earth Observations.

Contract No.: ENV4-CT97-0743-SIBERIA

Project Co-ordination: Remote Sensing Unit, Institute for Geography, Friedrich-Schiller-University Jena, Germany.

Authors: J. Baker, H. Balzter, M. Davidson, L. Eriksson, D. Gaveau, M. Gluck, A. Holz, A. Luckman, U. Marschalk, I. McCallum, S. Nilsson, A. Öskog, S. Quegan, Y. Rauste, A. Roth, C. Schmullius, A. Shvidenko, K. Tansey, T. Le Toan, J. Vietmeier, W. Wagner, U. Wegmüller, A. Wiesmann, J. J. Yu.

Edited by C. Schmullius, FSU Jena.

Table of contents

List of Symbols

A	Area
B_{eff}	Effective baseline
$\mathbf{C}$	Covariance matrix
c	Class
$\mathbf{D}$	Weighting coefficient matrix
h	Elevation height
I	Intensity
K	Number of classes or input channels
M	Number of images
MSC	Mean square change
N	Number of pixels
N_{stand}	Number of stands
n_δ	Window size (total number of pixels)
p_0	Overall accuracy (percentage of correctly classified polygons)
p_e	Expected chance agreement
$p(c\|x)$	A posteriori probability
$p(x\|c)$	Probability distribution or likelihood
p(c)	A priori probability
q	Ground-truth value
RMSE	Root mean square error
StDev	Standard deviation
s	complex SAR image
T	Normalised log measure (here used as texture measure)
w	Width or height of window (in pixels)
α	Rejection threshold
γ	Interferometric coherence
γ_0	Coherence at $\nu=0$
γ_∞	Coherence at $\nu\to\infty$
Δg	Ground offset for the SAR images
ε	White noise process
η	True total growing stock volume
θ	Look angle of sensor
θ_i	Incidence angle, defined with respect to global vertical
θ_{loc}	Local incidence angle, defined with respect to local vertical
κ	Kappa coefficient, measure of agreement between classification result and ground truth data
κ_w	Weighted kappa coefficient
λ	Wavelength
μ	Mean value
ν	Growing stock volume in m^3/ha
ξ	True class parameter in Bayes' theorem
ρ_a	Estimated autocorrelation in azimuth
ρ_r	Estimated autocorrelation in range
$\boldsymbol{\sigma}$	Mean intensity vector
σ^0	Backscatter coefficient (sigma nought)
σ_0	Backscatter coefficient at $\nu=0$
σ_∞	Backscatter coefficient at $\nu\to\infty$
σ_ε	Standard deviation of the white noise process ε
ϕ	Interferometric phase

Acronyms and Abbreviations

AGC	Automatic Gain Control
AVHRR	Advanced Very High Resolution Radiometer?
BRDF	Bi-directional Reflectance Distribution Function
CEH	Centre for Ecology and Hydrology (SIBERIA project partner in UK)
CEO	Centre for Earth Observation
CESBIO	Centre d'Etudes Spatiales de la Biosphère (SIBERIA project partner in France)

DEM	Digital Elevation Model
DLR-DFD	Deutsches Zentrum für Luft und Raumfahrt, Deutsches Fernerkundungsdatenzentrum
DLR-HF	und Institut für Hochfrequenztechnik, (SIBERIA project partners in Germany)
EC	European Commission
ENL	Equivalent Number of Looks
ERS	European Remote Sensing Satellite
ESA	European Space Agency
FFS	Federal Forest Service of the Russian Federation
FF	Forest Fund
FL	Forest Land
GAMMA	Gamma Remote Sensing Research and Consulting AG (SIBERIA project partner, Switzerland)
GCP	Ground Control Point
GEC	Geocoded Ellipsoid Corrected Image
GIM	Geocoded Incidence Angle Mask
GIS	Geographical Information Systems
GLOBE	Global Land One kilometer Base Elevation?
GTC	Geocoded Terrain Corrected Image
GTOPO30	Global digital elevation model with 30-arc seconds grid spacing
HH	Horizontal polarisation transmitted, Horizontal polarisation received
HRPT	High Resolution Picture Transmission
ICP	Iterated Contextual Probability Classifier
ICM	Iterated Conditional Mode
IEEE	The Institute of Electrical and Electronics Engineers, Inc
IGARSS	IEEE Geoscience And Remote Sensing Symposium
IGBP	International Geosphere-Biosphere Programme
IIASA	International Institute for Applied Systems Analysis (SIBERIA project partner in Austria)
InSAR	Interferometric Synthetic Aperture Radar
ISP	Interferometric SAR Processor; (software from GAMMA)
JERS	Japanese Earth Resources Satellite
ML	Maximum Likelihood
MSC	Mean Square Change
MSP	Modular SAR Processor (software from GAMMA)
NASDA	National Space Development Agency of Japan
NDVI	Normalised Difference Vegetation Index
NFL	Non-Forest Land
NGO	Non Governmental Organisation
NOAA	National Oceanographic and Atmospheric Administration
PRI	SAR Precision Image
RFI	Radio Frequency Interference
RMS	Root Mean Square
SAR	Synthetic Aperture Radar
SCEOS	Sheffield Centre for Earth Observation Science (SIBERIA project partner in UK)
SFMP	Sustainable Forest Management Paradigm
SIBERIA	CEO Project "SAR Imaging for Boreal Ecology and Radar Interferometry Applications"
SLC	SAR Single Look Complex
SLCI	SAR Single Look Complex Image
SMAC	Simplified Method for Atmospheric Correction
SSC	Swedish Space Corporation (SIBERIA project partner in Sweden)
STC	Sensitivity Time Control?
StDev	Standard deviation
SQR	Square root
TM	Thematic Mapper; instrument on the recent Landsat Satellites
TT	Test Territory
UFA	Unforested Area
UNCED	United Nations Conference on Environment and Development
UTM	Universal Transverse Mercator
UWS	University of Wales, Swansea (SIBERIA project partner in Wales)
VTT	VTT Technical Research Centre (SIBERIA project partner in Finland)
VV	Vertical polarisation transmitted, Vertical polarisation received
WP	Work Package

Executive Summary

The boreal forest belt of Russia is a significant carbon pool. Siberian forests contain roughly half of the world's growing stock volume of coniferous species, making them an economically and ecologically precious resource. Due to slow growth rates and the relative fragility of taiga ecosystems, Siberian forests are susceptible to degradation caused by inappropriate harvesting technologies, forest fires and other disturbances. Because of the less developed infrastructure and remoteness of Siberia, forest inventories are not carried out frequently enough to provide timely information on the boreal ecosystem. In a frequently cloud covered large region like this, only cloud-penetrating radar can operationally be used to provide large-area coverage. The potential of synthetic aperture radars(SAR) for mapping boreal forests has been highlighted in many studies, but very little use of the data was yet made in practice .

The satellite data for this project were acquired with a mobile receiving station of the German Remote Data Center (DLR-DFD) in Ulan Bator during two campaigns in fall 1997 and summer 1998. This effort provided for the first time a near complete coverage of the main area of interest (51-60°N, 85-110°E) with ERS tandem pair and single-pass JERS images. As a result interferometric coherence images from ERS and calibrated JERS images became available which are of particular interest in forestry applications. The tandem data were interferometrically processed at DLR-DFD. DEMs could only be generated for about 40 % of all 122 ERS frames. Where available, the interferometric DEM was used to produce geocoded terrain corrected imagery and to calibrate the backscatter images. For the remaining frames, GTOPO30 with a raster width of 30 arc seconds was used to perform a crude geometric correction of the images. JERS SAR data from summer 1998 were processed at the National Space Agency of Japan (NASDA) and at Gamma Remote Sensing, Bern, Switzerland. Over mountainous areas all image products from ERS and JERS are heavily distorted and cannot be used for forest classification. Therefore, these areas were masked out using a simple threshold procedure based on the GTOPO30.

Backscatter model development and validation was carried out using data from the Russian forest inventory. Thirty-five testsites, each covering between 20,000 and 100,000 ha, were selected for model development and another 15 sites for validation purposes. The forest data base was assembled in a joint effort of the International Institute for Applied System Analysis (IIASA), Laxenburg, Austria and several Russian partners. The data stem from the Russian forest accounting inventory and are polygon-based. For each polygon, so called primary inventory units, attributes like land category, relative stocking, growing stock volume, age, or species composition are available. The sites were chosen subjectively to represent landscape and forest diversity over the entire study area. Total growing stock volume proved to be the parameter, which is physically most directly related to radar backscatter and resulted in best correlations.

Following explorative database analyses, the classes "Water", "Smooth open areas" (including bogs, agriculture and grassland) and four total growing stock classes, "≤20 m^3/ha", "20-50 m^3/ha", "50-80 m^3/ha" and ">80 m^3/ha" were defined as target classes. The lowest total growing stock class includes tundra, fire scars, shrublands and clearings with birch regrowth. The two intermediate classes represent stages of secondary regrowth, and the highest class shows potentially exploitable forest stands. Two exponential models were used to estimate signatures of coherence and backscatter for the four forest classes. Image-specific parameters in the model equations accounted for image-to-image variation. "Water" and "smooth open areas" showed constant signatures. Each image was classified using a maximum likelihood algorithm trained on the model input, followed by a new contextual classification algorithm, the Iterated Contextual Probability (ICP) algorithm. The entire classification process was automated for UNIX workstations. Reclassifying the whole 1,2 Mio km^2 area (or 960 overlaying images) takes only 24 hrs. The total area was divided into 98 map sheets with a scale 1 : 200.000. The printed map sheets (cover classes and color composites) will serve Russian forest enterprises without GIS capabilities as an information basis for sustainable forest management.

To assess the map accuracy, confusion matrices of all test sites were generated by tabulating the correspondence of forest inventory polygons with the radar-derived classes. The weighted Kappa coefficient κ_w was used to estimate the agreement between classified map and ground data. It varies between 0.73 and 0.97 (pooled κ_w = 0.94). The user accuracies for each individual class are all greater than 80%. The Russian experts concluded that the radar-derived forest cover map has a satisfactory quality for practical applications, e.g. for monitoring of reforestation and updating old forest inventory data. The provided methods can potentially be used in future forest mapping projects. First tests on sites in Brazil, the UK and Finland showed promising accuracies between 70% and 83%.

1 Objectives of the Project

The main objective of the European Commission (EC) Center for Earth Observation (CEO) Environment and Climate Programme is the generation of information for dedicated customers using Earth observation data sources and techniques. In line with this objective, the aims of the SIBERIA project are to produce an extensive forest map of a large geographical region in Russia for which only limited information is currently available. The detailed information that the SIBERIA project produces is of immense scientific, environmental and commercial interest. SIBERIA's forest map will serve as a unique planning and monitoring tool for the sustainable management of the natural resources of Siberia, for its socio-economic development and for a better understanding of the role of boreal forests in climate change.

The *primary objective* of the SIBERIA project is to support the development of sustainable management policies at the strategic and operative levels in order to manage the Russian forest resources in an efficient and ecological way. This development is based on up-to-date information on forest resources and related variables where existing inventory data is to be validated and confirmed. The scientific and commercial importance of this project is supported by Letters of Interest from strategically important organisations.

The forest map is being derived primarily from satellite data and remote sensing techniques. These include multitemporal and interferometric data from dual-frequency spaceborne radar instruments, which, although relatively recent in development, have shown huge potential for the mapping and monitoring of the Earth's surface. The advantage of using radar remote sensing methods is that the information can be acquired independently of cloud cover or solar illumination. Strong ties with the project consortium members and the European (ESA) and Japanese (NASDA) space agencies ensured that this data would be acquired.

SIBERIA is a shared-cost action (SCA) proposal for Area 3.3 of the Environment and Climate programme that benefits from close cooperation with a dedicated customer. One partner of the SIBERIA consortium is a customer whose role is both as a user of the project output, but also, together with Russian associates, to actively define the project deliverables, observe closely the working procedure and evaluate their cost-effectiveness. Additionally, the SIBERIA project makes important contributions to various components of the CEO, including, in order of relevance, Application support (3.3.1), User support (3.3.2) and Enabling services (3.3.3).

1.1 The Russian Forest Sector and the Need for Accurate Maps

Russia's vast forests are a natural resource of global importance, both economically and ecologically. They serve Russia and neighbouring countries as a source of wood, a symbol of wilderness, and a critical stabilizer of the global climate. They sprawl over 11 time zones from the Baltic Sea to the Pacific. Russia has 23% of the Earth's forest areas ('forest area' defined according to the FAO, 1995). According to Shvidenko and Nilsson (1996), these forested areas host 21-22% of the world's growing stock (the volume of woody material in the forest) and contain 11% of the world's live forest biomass (Shvidenko, 1997). In comparative terms, this amount of biomass equates to the total amount of stored carbon in the tropical forests of Asia (FAO, 1995). In addition, Russian forests contain more then 55% of the world's growing stock of coniferous species (UN, 1992; Shvidenko and Nilsson, 1996). The boreal forests of central and western Siberia represent the largest unbroken tracts of forest on Earth and are listed as 'Last Frontier Forests' by the World Resources Institute (Bryant et al., 1997). Hence the region is of increasing interest to international organisations with conservational and climatological objectives as well as for political and industrial reasons.

Forest maps covering Russia are today only available at a scale of 1:2.5 Mio, with the latest issue printed in 1990. For about 100 million hectares of this map, only data from rough surveys have been carried out during the period 1948-1956. Due to numerous large-scale disturbances, both natural and human induced, the actual state of vast territories is unknown. For example, in 1994 large areas of forest in the Krasnoyarsk Kray (a Russian territory located in central Siberia) were devastated by the Siberia moth (*Dendrolimus superans sibiricus*), the most destructive defoliator of coniferous forests in northern Asia. The larvae of the moth feed on most conifers in the pine family as well as attacking fir, spruce and larch forest (from US Forestry Service, http://www.fs.fed.us/ne/home/research/themes/siberian_moth.html). Another major disturbance to the forest ecosystem is fire. The Russian foresters state that their biggest concern is human-induced forest fires that add up to an estimated 95% of all fires. The summer of 1998 was considered a bad year for forest fires in Siberia, but initial estimates of the extent of fires occurring in 1999 yielded an area ten times that of 1998. On July 14, 1999 a state of emergency was declared in the Krasnoyarsk Kray where fires had ravaged an estimated 54,000 hectares.

No accuracy assessments of the available forest map products exist. Until now remote sensing data has been limited to high spatial resolution, small area areal surveys and some satellite imagery. The usefulness of optical data is limited due to excessive cloud cover or, such as from NOAA AVHRR, to their low geometric resolution.

1.2 Anticipated Advances in Earth Observation Techniques

Radar remote sensing has become increasingly important for observations of forest ecosystems. Current available spaceborne SAR data have been used in several large programmes to observe tropical, temperate and boreal forest. In recent years, the use of multitemporal images and SAR interferometry has led to the biggest advances in the field. Multitemporal images have been used to differentiate forest from non-forest and to distinguish other land classes, based on the temporal characteristics of each surface type. In addition, it is possible to distinguish coniferous from deciduous forest, and areas with fluctuating exposures to freeze-thaw processes can also be detected. The use of SAR interferometry also allows classification of forest and non-forest classes to be made. Tandem SAR interferometry makes use of the short time gap (24 hours) between consecutive overpasses of the same area by the ERS-1 and ERS-2 satellites. In many cases, a high-resolution digital elevation model (DEM) can also be generated during the interferometric processing of Tandem radar images.

Until the proposal writing, neither data from the ERS-1/ERS-2 (European) or the JERS-1 (Japanese) satellites were available over central and eastern Russia due to the lack of a receiving station within range of this area. Thanks to an unprecedented fast international effort, extensive dual frequency and interferometric radar images were acquired during autumn 1997 and the summer of 1998. This represents the largest continuous area ever covered by three radar satellites in concert and has been facilitated by (i) the deployment of a mobile receiving station in Mongolia to close the acquisition gap in central Siberia, (ii) ESA's initiation of a full ERS-1 and ERS-2 Tandem cycle for the stations visibility circle and (iii) NASDA's commitment to JERS-1 images for their global boreal forest mapping project (GBFM).

The SIBERIA project merges the advantages of operational SAR satellites by analysing dual frequency composites and interferometric products. The project is a world first for the analysis of over 550 ERS images and 600 JERS-1 images over an area of 1 million square kilometres. Therefore, the ***second main objective*** of SIBERIA is to demonstrate the feasibility of radar remote sensing for large-scale vegetation mapping. A fully validated, robust and adaptive algorithm for forest mapping is one of SIBERIA's main deliverables. The ***third objective*** of the SIBERIA project is the construction of an up-to-date geographical information system (GIS) containing SAR image parameters as well as forest inventory information down to the forest stand level. In digital format, updating of the forest inventory and image GIS can easily be carried out.

1.3 Sustaining the Work

The acquired radar images and derived 1 Mio km^2 forest map establish an initial data set to enable research about the dynamics of boreal ecosystems to be undertaken for many years in the future. This research may include natural factors such as forest fire and insect damage as well as anthropogenic factors such as timber harvesting. Russia currently does not have any sufficient forest monitoring system. Only 60% of the Forest Fund Area is under fire protection. Results of the SIBERIA project improve information on the state of the Russian boreal terrestrial biota (specifically forests) and provide data for the development of special forecasting models, e.g. to predict forest fire risk.

Long term monitoring, for example with the next generation European ENVISAT or the Japanese ALOS missions can be accomplished in the future. The participating and associated customers, who had not used remote sensing as an environmental monitoring tool, gained understanding and underwent training in radar remote sensing techniques. The SIBERIA project created the basis for further development of an operative forest information system with monitoring capabilities in a GIS environment to be used at local and regional levels.

2 Scientific and Technical Description of the Results

2.1 Study Site

The taiga forests of central Siberian in Russia, between 88 and 112 E and 50 and 62 N, covering an area of almost 1 million km^2 were studied in the SIBERIA project. Two Russian territories were located in the project area, the Krasnoyarsk kray and the Irkutsk oblast. Lake Baikal is located in the south east of the study area. The cities of Irkutsk and Krasnoyarsk are the two centres of urbanisation and development. The Yenisey and Angara rivers make steady progress north into the Arctic Ocean. These two rivers and their tributaries are largely responsible for the drainage of the central Siberian boreal forests. The project area also covers smaller areas of the Burjatija and Touva Republics.

This study area was chosen for two main reasons. In 1997, vast expanses of the Siberian boreal forest were classified by the World Resources Institute as being frontier forests under medium or high threat (Bryant et al. 1997). Two large areas, one in Irkutsk oblast and the other in the Krasnoyarsk kray, that are under medium or high threat, are shown in Figure 2.1 within the yellow polygon indicating the extent of the project area. Large area mapping and monitoring of these threatened frontier forests is therefore both timely and important. The high commercial and economic value of the timber was the second reason for the selection of the study area. For efficient and economic management of timber resources, up-to-date and accurate information on the state of the forests are required. As well as providing information on the extent of timber harvesting, it was hoped the project's investigations would yield information on the extent of natural disturbances caused by fire or insect outbreaks.

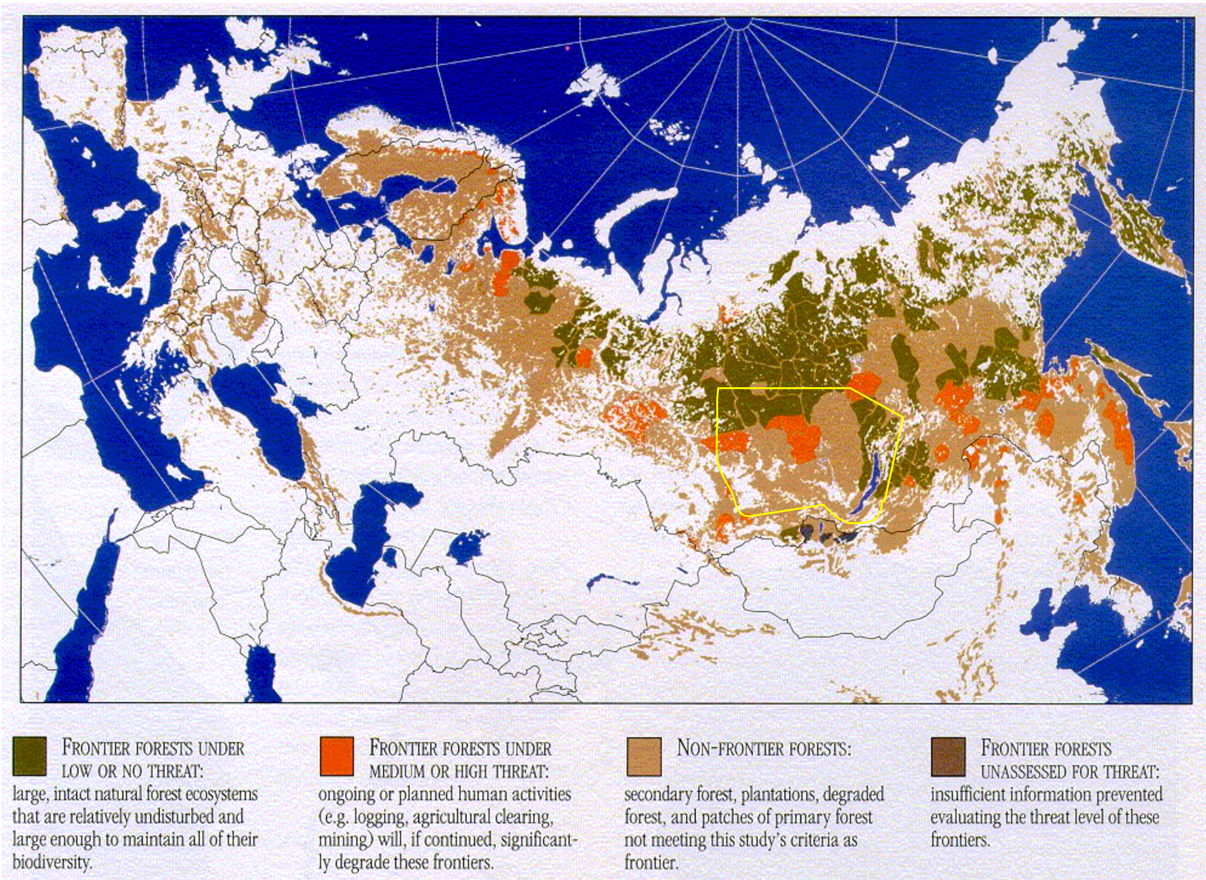

Fig. 2.1 *Threatened frontier forests of Europe and Russia. Map published by World Resource Institute (Bryant et al, 1997). Map projection: Equidistant. Data sources (i) Forest cover data provided by World Conservation Monitoring Centre. (ii) Forest frontiers data derived through expert assessment and from other sources. The added yellow polygon indicates the extent of the area of interest for the SIBERIA project.*

2.1.1 Ground-Truth Areas

The establishment of ground truth areas had two major objectives: 1) to provide ground data of the region investigated, with a special emphasis on forests, which would be sufficient for development of methods for classification and quantification of major types of land/forest cover using radar imagery, and 2) to initiate the generation of a unified network of ground-truth data for Russian forests which could be used for further examination of different remote sensing sensors and systems.

The following major requirements were set for the ground truth area selection: 1) they should include basic bio-climatic zones of the region, land forms and landscape types; 2) they should include regions with different levels of infrastructure developments; 3) major land cover classes, forest formation, forest type, species composition, age distribution and levels of productivity should be represented in the test territories; and 4) special attention should be paid to human and naturally disturbed areas, including types, severity and frequency of disturbances (largely, forest fire and harvest).

The vast areas investigated are situated between the Yenisey River in the west and the Baikal Lake basin in the east and cover territories of 4 administrative regions of Russia (*Krasnoyarsk kray* and *Irkutsk oblast*; relatively small parts of *Republics Burjatija* and *Touva* are also included). Diverse landforms - plains, plateaus, mountains - are represented in the region. A mountainous area stretches along the southern boundary of the region, represented by *Kuznezky Ala-Tau* (the eastern slope), *Zapadny Sayan,* and *Vostochny Sayan*. A major part of the territory belongs to typical boreal forests, represented by middle and southern taiga sub-zones. The percentage of forest cover is high even for the taiga zone, and as a rule reaches 60-70%. To the south from Krasnoyarsk (about 57^{o} N.), deciduous forests are common, mixed with islands of forest steppe and steppe; to the east these areas decrease. While landscape diversity is very high, ecosystem and species biodiversity is low: there are approximately 25 tree and 80 shrub indigenous species in the forests of the region. Major tree species of non-mountain forests - Larch (*Larix dahurica and L. sibirica*) and Pine (*Pinus sylvestris*), cover approximately 2/3 of the forested areas. Larch usually dominates in northern regions, but is usually present in all forest formations. Spruce (*Picea sibirica*) grows in river valleys and on watersheds above 400-500 m a.s.l. Cedar (*Pinus sibirica*) is typical of "mist" forests and occupies high plateaus. Secondary deciduous forests (mostly dominated by Birch) cover significant areas, but do not generate an explicitly delineated zone. Mountain regions have a very diverse vegetation cover, with clearly expressed altitudinal zonality. Foothill Pine and Spruce forests change from 600 m a.s.l. to dark coniferous forests dominated by Cedar, Fir and Spruce. This well defined belt changes to sparse sub-alpine forests, and sub-alpine and alpine meadows and mountain tundra from 1300-1500 m a.s.l. (for more information see, e.g., Smirnov, 1969; Sokolov, 1997; Sokolov et al., 1998; Vaschuk, 1997; Zhukov et al., 1969).

Productivity of forests increases from north to south. Growing stock volume of mature forests is approximately 150 $m^{3} \cdot ha^{-1}$ in middle taiga and 230-250 $m^{3} \cdot ha^{-1}$ in the southern taiga. A major part of the forests is represented by mature forests (more than 60% for large regions). The main types of disturbances include fires, insect outbreaks and harvests. The most disturbed forests are distributed along the Trans-Siberian railway and around cities and industrial centres (Krasnoyarsk, Irkutsk, Bratsk, etc.). Regeneration of forests after disturbances usually (especially after clear cut harvests) goes through a change of species, which explains the large areas of Birch and Aspen forest.

Table 2.1 *Characteristics of Test Territories*

Test Territory Names	Location (decimal degrees)				Number of Test Areas		
	Lower Left Coordinates		Upper Right Coordinates		total	including	
						used by meth-team	used for acc.assess.
	East	North	East	North			
Bolshe-Murtinsky	91.83	56.83	94.00	57.33	4	4	0
Chunsky	95.17	57.42	98.25	58.08	5	5	0
Ermakovsky	91.48	52.85	93.20	53.17	4	4	0
Hrebtovsky	98.37	58.64	99.74	59.98	4	4	0
Irbeisky	95.25	54.50	96.83	55.67	5	3	2
Mansky	93.00	55.00	94.00	55.67	4	0	4
Nizhne-Udinsky	95.83	53.00	100.00	55.83	4	4	0
Primorsky	102.09	55.58	102.56	55.99	4	4	0
Sayano-Shushensky	90.50	52.25	92.42	53.08	4	0	4
Shestakovsky	102.94	56.10	104.51	56.68	4	4	0
Juzhno-Baikalsky	103.08	51.33	104.75	51.83	3	3	0
Ulkansky	107.75	55.00	108.83	55.92	4	2	2
Ust-Ilimsky	102.67	58.83	103.83	59.83	1	1	0
Total					50	38	12

In order to reach the above mentioned requirements, taking into account the specifics of landscapes and forests, as well as the required accuracy of ground data for SAR images, the following scheme for ground truth data selection was developed.

- The region investigated was selected from the overall IIASA data set, which is comprised of numerous databases and related GIS components for all of Russia. Vegetation, land use-land cover, landscape, forest and soil databases (with corresponding digitized maps at a scale of 1:1 Mio to 1: 2.5 Mio) were used for the primary selection.
- Based on the requirements mentioned above, 13 *test territories* (TT) were selected, representing major vegetation zones, landforms and levels of land transformation. Each TT is represented by an area of 1-3 million ha. It was decided, as a rule, to use individual forest enterprises as TTs.
- Inside each TT, 3-5 *test areas* were selected in order to represent data for each primary land cover (forest inventory) unit. The forest inventory data were used as the major information source. The area of each test area comprised from 40,000 to 150,000 ha and is divided into about 700-3000 primary land cover units. Based on available forest inventory data (about 400 Bytes of information for each primary inventory unit) and initial forest maps (scale 1:50,000), the corresponding database was developed.

The information implemented in the database, by its content, details and accuracy, exceeds the explicit information requirements of this Study, and contains: 1) land cover categories; 2) area of primary units; 3) short description of land cover; 4) detailed information for forests which includes species composition, age, average diameter and height, relative stocking, growing stock, forest types, etc., by each stand delineated according to the latest Russian forest inventory manual (1995); 5) description of elevation and slopes. The database was validated by using the latest forest inventory data, air photography and other available sources. A visit to about 15 different test areas in June 1999 by a group of scientists representing 6 countries of the study team confirmed that the quality of the ground data is high.

In total, the database includes 50 test areas (Table 2.1**,** Fig. 2.2), of which 38 were used by the Project methodological team for the development of models and tools for mapping, and 12 were used for independent control and evaluation of the methodologies developed.

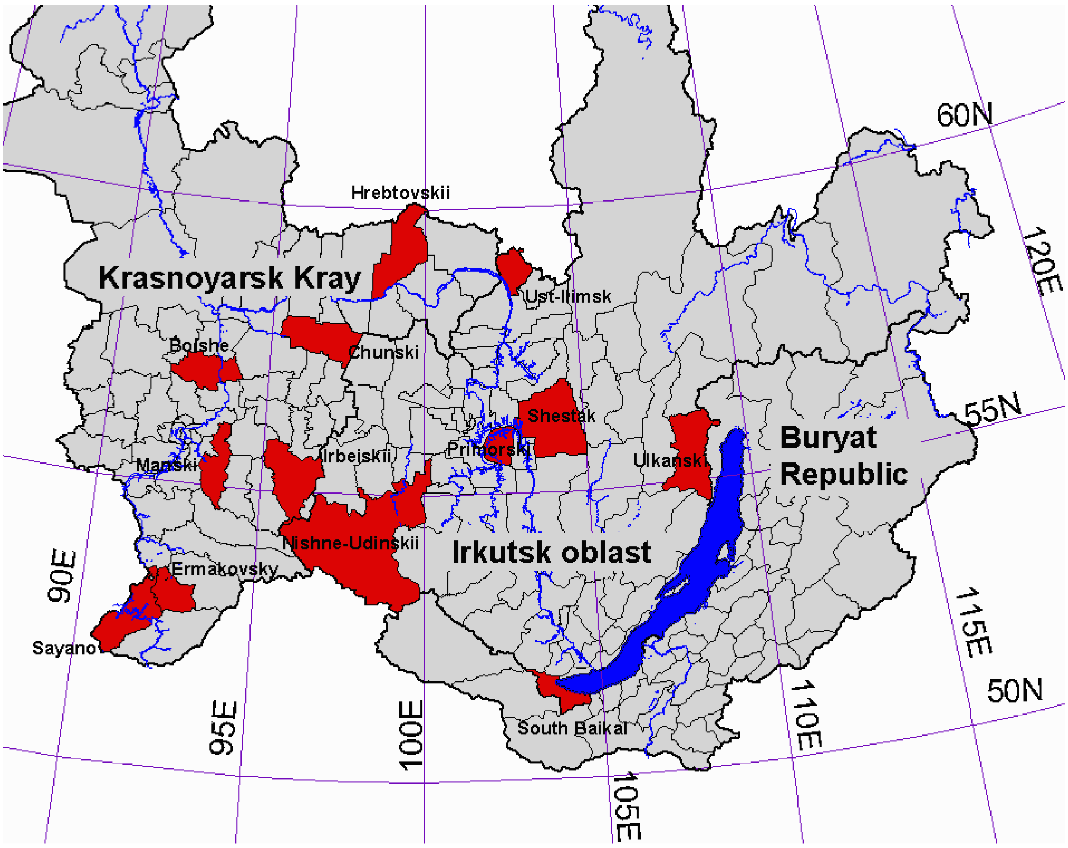

Fig. 2.2 *Ground data in the database come from selected test territories (red regions on the map).*

2.1.2 Meteorological Database

To aid the interpretation and analysis of the radar images meteorological data from 113 stations spread over an area from about 49 to 62°N and 84 to 115°E were acquired from the "Deutscher Wetterdienst". The location of the stations can be seen in Fig. 2.3.

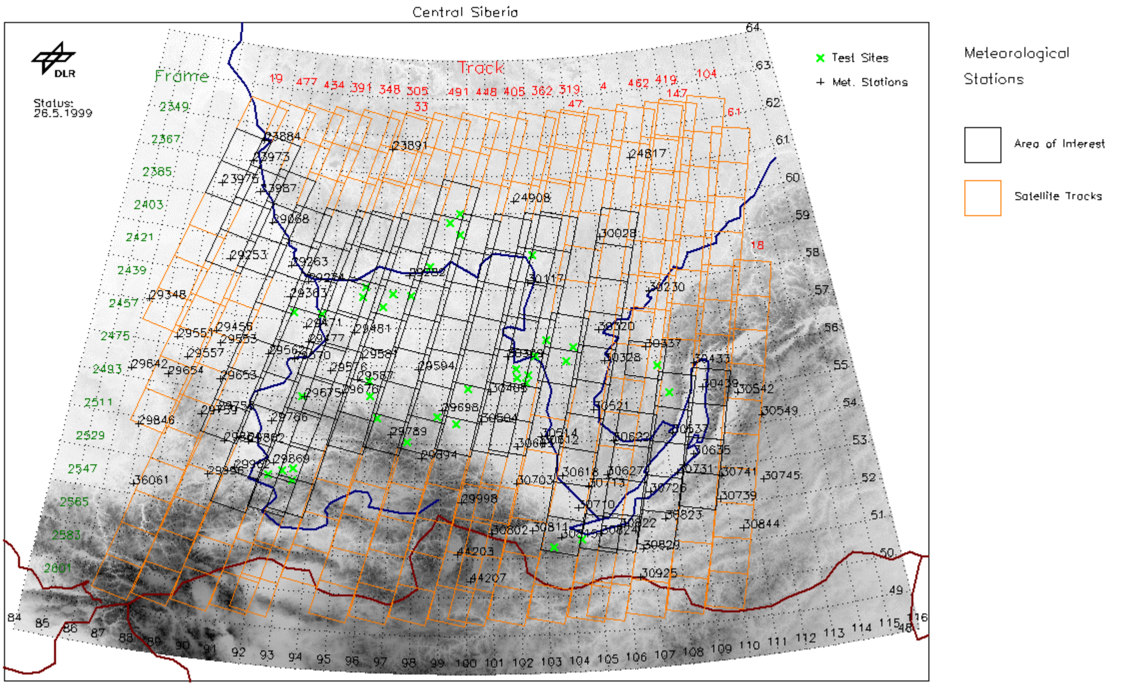

Fig. 2.3 The location of the meteorological stations in the SIBERIA study area.

The meteorological data span the time periods from September 15 to October 31, 1997 and from May 1 to August 15, 1998. The nominal time step of the records is 3 hours, but depending on the variable or station other time steps (6, 12, 24 hours) occur. In some cases the series were incomplete. The data base contains the following variables: pressure, windspeed, temperature, dew point, weather, cloudiness, precipitation and others. To allow easy checking of the meteorological conditions during the satellite acquisition dates, plots of temperature and precipitation series were prepared and put on the project web page. An example is given in Fig. 2.4. If an ERS scene was within 50 km of the geographic location of the meteorological station then the acquisition dates of the three ERS images were indicated by a vertical line in the plots.

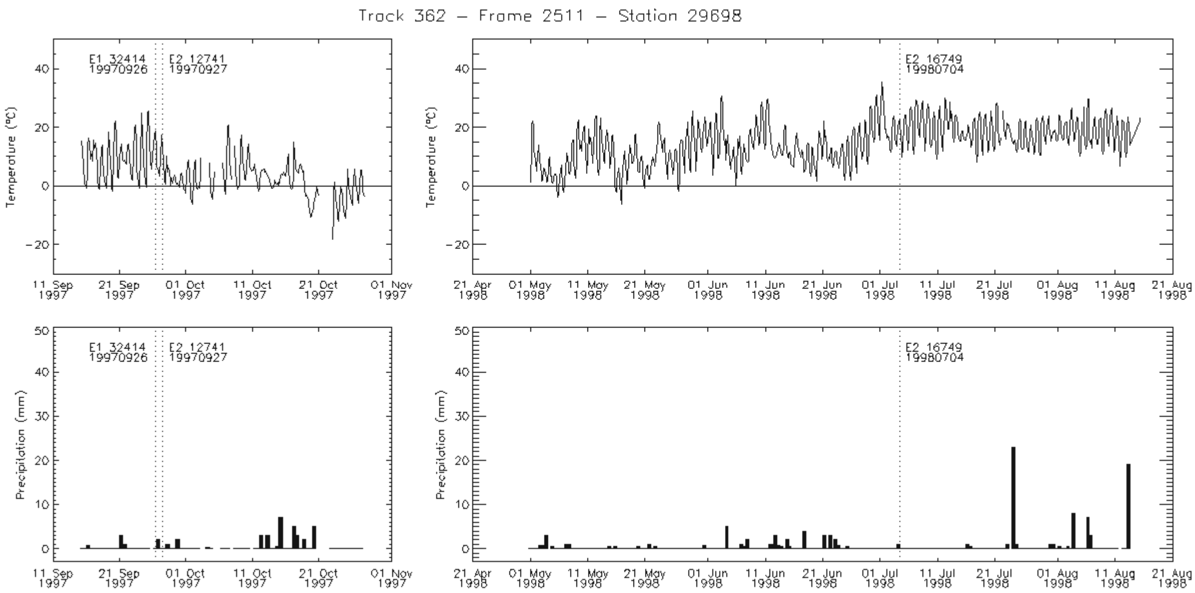

Fig. 2.4 *Temperature and precipitation series from station 29698 near Nizhneudinsk (99.03°E, 54.88°N).*

2.2 Remote Sensing Data

2.2.1 Radar Data

2.2.1.1 Acquisition

All SAR data utilised in this project were acquired by DLR's mobile ground station in Ulan Bator. The station is located within the capital of Mongolia at an elevation of 1450 m. It is operated in campaigns and it is capable to acquire ERS-1/2, JERS, Landsat and Radarsat data. The data are either stored on HDDT or DLT tapes. The ERS and JERS data were shipped to Oberpfaffenhofen for further processing. Landsat and Radarsat data are transferred to the corresponding distribution facility. Fig. 2.5 shows the station's visibility circle. The blue lines indicate the theoretical visibility. However buildings and the surrounding terrain limit the area really covered to the part within the red line.

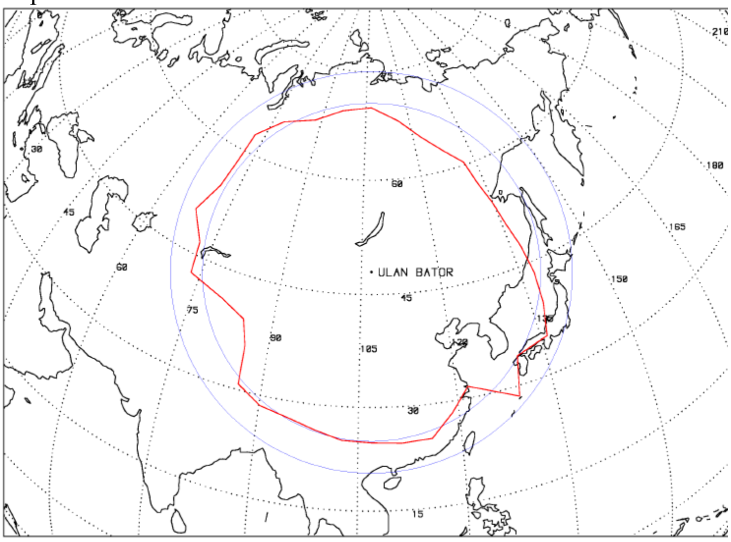

Fig. 2.5 *Visibility circle of Ulan Bator ground station*

Fig. 2.6 *Station set up*

The receiving station was installed closed to the national seismographic institute. Fig. 2.6 was taken during the set up of the satellite dish and illustrates the irregular shape of the visibility line.
The data relevant to this project were acquired in two campaigns, September 22nd to October 27th, 1997 and May 10th to August 10th, 1998. During these two campaigns 164 (116) passes of ERS-1, 169 (294) of ERS-2 were acquired. Additionally 197 passes of JERS were made available.

2.2.1.2 ERS-1 and ERS-2

DLR-DFD developed an interferometric processing system mainly designed for the operational derivation of digital elevation models (DEM) from ERS, SRTM and ENVISAT-ASAR (Roth et al, 1998). It consists of a line of processors (Fig. 2.7) allowing the ingestion of different input products. The media of the ground stations - HDDT and DLT tapes - are supported as well as D2 cassettes on which the SRTM data are stored. Input to the interferometric processor (GENESIS) is complex SAR data. The base for the SIBERIA project was ESA's SLCI (Single Look Complex Image) standard products.

The interferometric processor GENESIS (Eineder et al, 1997) derives the intensity images, the coherence and the interferogram and finally performs the phase unwrapping. The absolute phase values, together with the intensity images and the coherence map are passed to the geocoding and mosaicking system (GeMoS). This system determines of each pixel the three-dimensional position on ground and resamples them to a regular map grid. Tie-pointing and a geometric adjustment allow an improvement of the initial geometry and the phase measurements (Roth et al, 1999). Then the same imaging geometry is used to transform the elevation data as well as the images and the coherence.

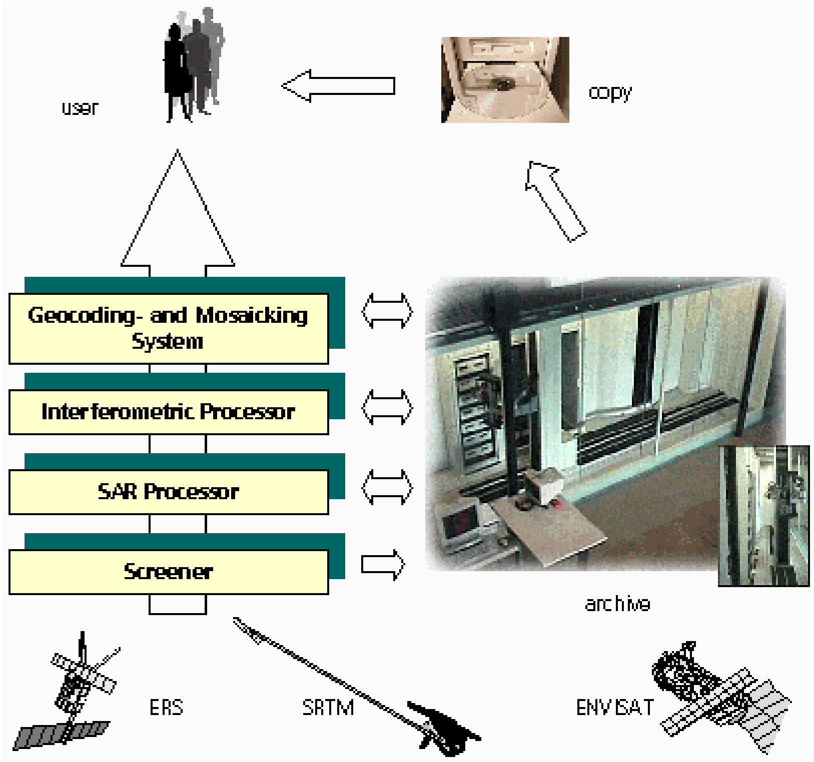

Fig. 2.7 *Interferometric processing system*

Tasks of the interferometric processing of the ERS data are the generation of a reference DEM, the improvement of the location accuracy by a terrain correction, the derivation of the local slopes in order to enable a precise radiometric calibration and the determination of the coherence values as additional classification information.

Several functions of the system were modified for SIBERIA. Originally the system was designed to process a pair of SAR data. The ERS tandem pairs for SIBERIA were acquired in autumn 1997. As the mapping requires an additional data set of the spring campaign 1998 for multi-temporal investigations, the system was modified to handle also a third ERS data set. The tandem images are co-registered with an accuracy of fractions of a pixel and the third image is registered to the tandem pair with pixel accuracy. The spring data therewith fit to the interferometrically derived DEM and the ortho-rectification of all data sets is performed in one step. Additionally the co-registration procedure was improved regarding low coherent data sets.

The coherence map contains information regarding the similarity of the tandem data sets (ERS-1 and ERS-2). Amongst other factors, the land coverage influences the coherence values and therefore shows a high potential for the improvement of the classification results. The coherence is estimated from a group of neighbouring pixels. Its accuracy mainly depends on the considered number of pixels. 80 image pixels (20x4) of the SLCI product were used to estimate the coherence. Additionally the coherence value is influenced by the topography. A terrain correction of the coherence based on the fringe frequency was implemented. In the case of low coherence preventing the derivation of a DEM a backup procedure was applied. The coarse GTOPO30 DEM, which is available globally with a grid spacing of 30 arcseconds, was used to register the intensity and coherence images. This leads to a better geometric precision and especially enables the mosaicking of the individual data sets. However, the coherence was not corrected for terrain effects in order to avoid artefacts introduced by an insufficient description of the relief.

In case of ERS tandem the baseline parameters (length and tilt angle) are variable and have to be determined from the orbits. However, the ERS orbits are only known with a few dm accuracy. This requires control point measurement and an adjustment. For the whole project area colour copies of topographic maps were acquired with a scale of 1:200.000. Tie-points could only be measured with approximately 1mm accuracy, equivalent to 200 m. As ERS provides a location accuracy of better then 100 m, timing parameters were not considered. Only the phase values were corrected.

The quality of the DEMs was ensured by the inspection of a difference image to the GTOPO30 DEM. A detailed analysis was not possible, but systematic errors like phase ramps would be visible and could be corrected if they appeared. Additionally control points from the maps were measured in the intensity image of either the ERS-1 or ERS-2 data set of the tandem pair. Table 2.2 shows the validation results of three typical data sets:

Orbit 32529, frame 2421 (13 GCPs)	Max	Min	Mean	StDev	RMS
Northing	49	-115	-34	79	59
Easting	122	-121	33	50	83
Orbit 32543, frame 2475 (12 GCPs)	Max	Min	Mean	StDev	RMS
Northing	146	-133	4	90	87
Easting	159	-196	30	127	125
Orbit 32572, frame 2367 (7 GCPs)	Max	Min	Mean	StDev	RMS
Northing	139	-70	3	69	64
Easting	71	-74	16	51	50

Table 2.2 *Validation results. All values in meters.*

The output products were sampled to 50 m pixel size. Maximum and minimum deviations are in order of 4 pixels. As the DEM production was possible only in areas of moderate relief the differences are in the expected order. It should also be considered, that control points were sometimes difficult to find. In total 48 products could be processed to DEMs and terrain corrected products while for 70 ERS-triples only a GTOPO30 correction was possible due to low coherence. 4 products were ellipsoid corrected. Fig. 2.8 shows the total coverage of the project area and the distribution of terrain and GTOPO30 corrected products. The terrain corrected products were called GTCs (Geocoded Terrain Corrected) and the products corrected with GTOPO30 or ellipsoid were grouped together and referred to as GECs (Geocoded Ellipsoid Corrected).

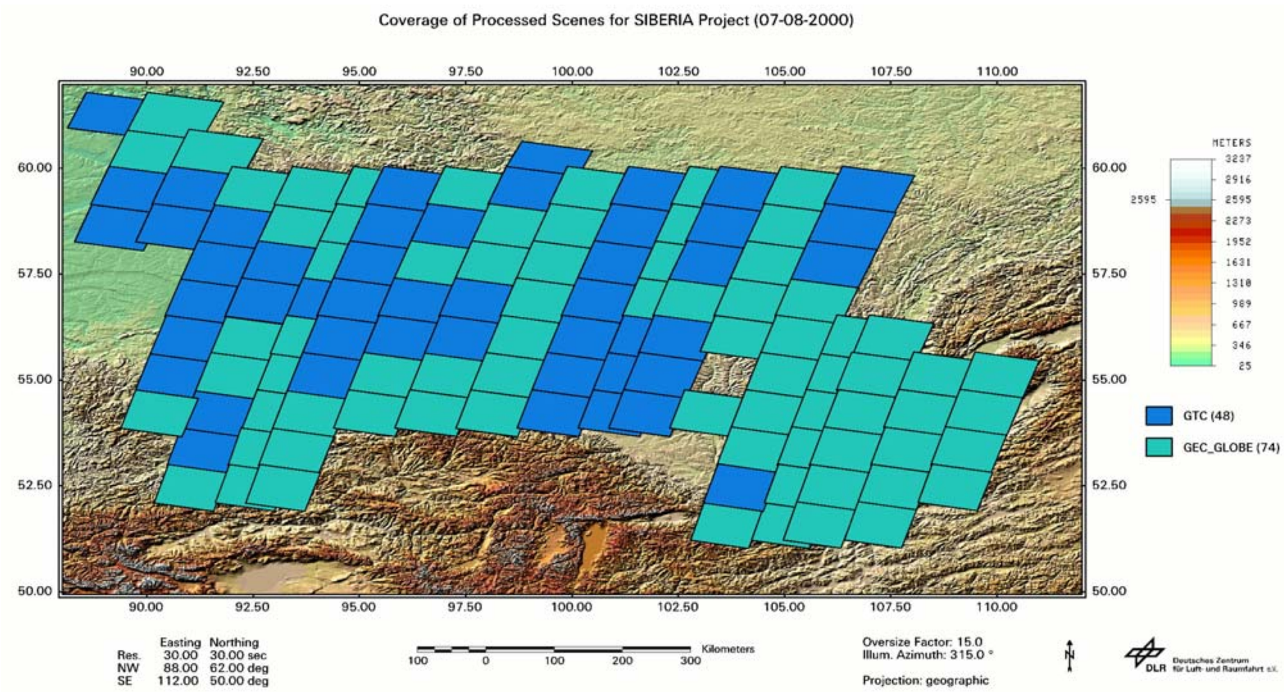

Fig. 2.8 *Coverage of processed scenes for the SIBERIA project area. The coverage is plotted onto a colour-shaded presentation of the GTOPO30 model.*

2.2.1.3 JERS-1

2.2.1.3.1 JERS Data Selection

JERS data for SIBERIA were available from two sources, the NASDA archive and from the German special receiving station at Ulan Bator (Mongolia):

Archive data:

- Available from NASDA
- Available from 1992 until 1997
- Archive online: telnet://eustty.nasda.go.jp, login: nasdadir, user: guest

Ulan Bator data:

- From mobile DLR receiving station at Ulan Bator
- Available from autumn 1997 to summer 1998
- No data catalogue available
- Special format, data must be synchronized by DLR, and orbit information added and converted to level 0 format by NASDA.

The data was selected to meet the following requirements:

- Global coverage of the test area
- INSAR coverage of selected sites
- Multi-temporal coverage of selected test sites

For signal interpretation it is important that

- No melt-freeze or snowfall events occur
- The coverage is within one season
- The temporal baseline between in-situ observation and SAR data acquisition is small

Additionally for interferometry the following constraints apply:

- Succeeding orbits (44 days)
- A spatial baseline of less than about 2 km

In the Siberia project the Ulan Bator data are preferred for its almost complete coverage in spring and summer 1998. But archive data have also been processed to investigate temporal changes and because no Ulan Bator data were available at the beginning of the project. Multitemporal data is available for a few tracks.

Within the SIBERIA project Gamma Remote Sensing processed 26 different tracks, 16 of them interferometrically, corresponding to more than 600 JERS frames, or 5 times what was promised by Gamma in the proposal.

2.2.1.3.2 JERS Radiometric Calibration

Special care was put on the radiometric calibration of the JERS backscattering because of its importance in the distinction of forest classes. The calibration factor required for the absolute radiometric calibration of JERS SAR processing was determined based on active calibrator data made available by M. Shimada (NASDA), and validated by cross-comparison with NASDA processed data over a tropical forest site (Wiesmann et al. 1999a). The very small corrections in the mosaicking confirm the excellent calibration.

2.2.1.3.3 JERS Processing

Fig. 2.9 shows the JERS data processing chain. Data are processed track by track. Interferometric pairs are processed together.

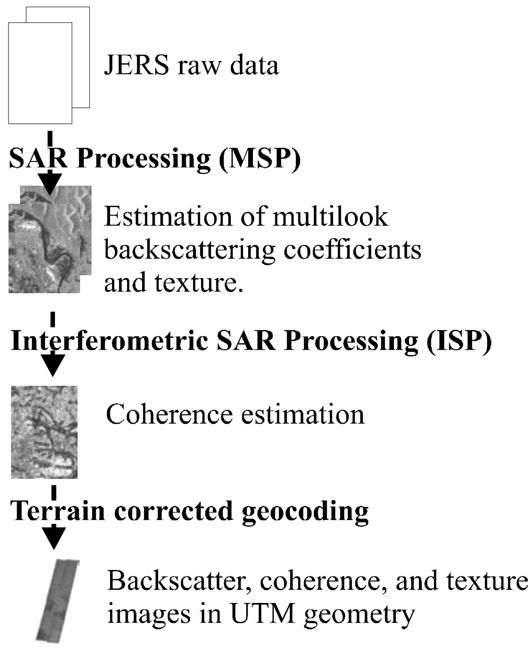

Fig. 2.9 *JERS data processing chain.*

SAR processing, radiometric calibration, and fine registration:
The SAR processing with Gamma's Modular SAR Processor (MSP) (Wegmüller and Werner, 1997) includes radio frequency interference (RFI) filtering. The radiometric calibration accounts for JERS sensitivity time control (STC), and automatic gain control (AGC). In addition it corrects for JERS range antenna pattern. Gain saturation correction was not applied. A MSP calibration constant of 22.1 dB was used as derived in the calibration experiment.
Multitemporal SLC (SAR single look complex) images are registered to common slant range geometry. The resolution is 14 m in slant range and 5,6 m in azimuth. For the backscattering images 4 looks in slant range and 12 looks in azimuth are taken. To investigate the information content of the texture for forest applications, a texture image is generated.

Interferometric Processing:
The InSAR Processing is done with Gamma’s Interferometric SAR Processor (ISP). Common band filtering is applied. As expected from the large temporal baseline of 44 days, the coherence is generally low. In spite of the low coherence, we succeeded in generating InSAR DEMs for a few test areas.

Terrain corrected geocoding:
Geocoding is used for the registration of the JERS with the ERS images and the available ground truth data. During the map production phase geocoding is important for the mosaicking process.
For the geocoding the GAMMA Differential Interferometry and Geocoding Software (DIFF&GEO) was used. The global DEM “GTOPO30” was used as geometric reference. Quadratic spline interpolation algorithms were used for the data interpolation necessary in the resampling step. The effective number of looks, determined with the method of moments, is about 25. An error of 200m in height in the “GTOPO30” DEM results in an error of 220m (far range) to 270m (near range) in localization (Wiesmann et al. 2000b).

2.2.1.3.4 JERS Data Products

The final JERS data products are in UTM coordinates with a pixel spacing of 50m in easting and northing. To keep the image files a reasonable size, the data strips were cut into tiles of 100km x 100km. The products include backscatter images, coherence maps, texture images and the interpolated “GTOPO30” DEM (see Table 2.3). Sample images are presented in Wiesmann et al 2000a.

Table 2.3 *Description of the final JERS data products*

Backscatter images:	Backscatter coefficient σ^0 in short integer format. σ^0 = 1.e-06*SQR(value)
Coherence images:	Adaptive estimates of coherence in unsigned character format. coherence = value/255.0
Texture images:	The texture is obtained from sections of 5 range pixels x 15 azimuth pixels using $\lvert\log \langle\sigma^0\rangle - \langle\log \sigma^0\rangle\rvert$, where σ^0 is the backscatter coefficient. Images are stored in unsigned character format. Texture = 1.e-02*SQR(value)
DEM:	The interpolated global DEM is in short integer format. height [m] = value

The JERS data products have been successfully registered to ERS SAR images using the automatic registration software of Gamma RS. The JERS backscatter images have been used by the methodology team to develop an operational classification algorithm and within the forest map production. Almost unused so far is the coherence and texture information. However, 0 shows an extract of the JERS coherence mosaic. It shows that the JERS coherence has good potential for forest monitoring.

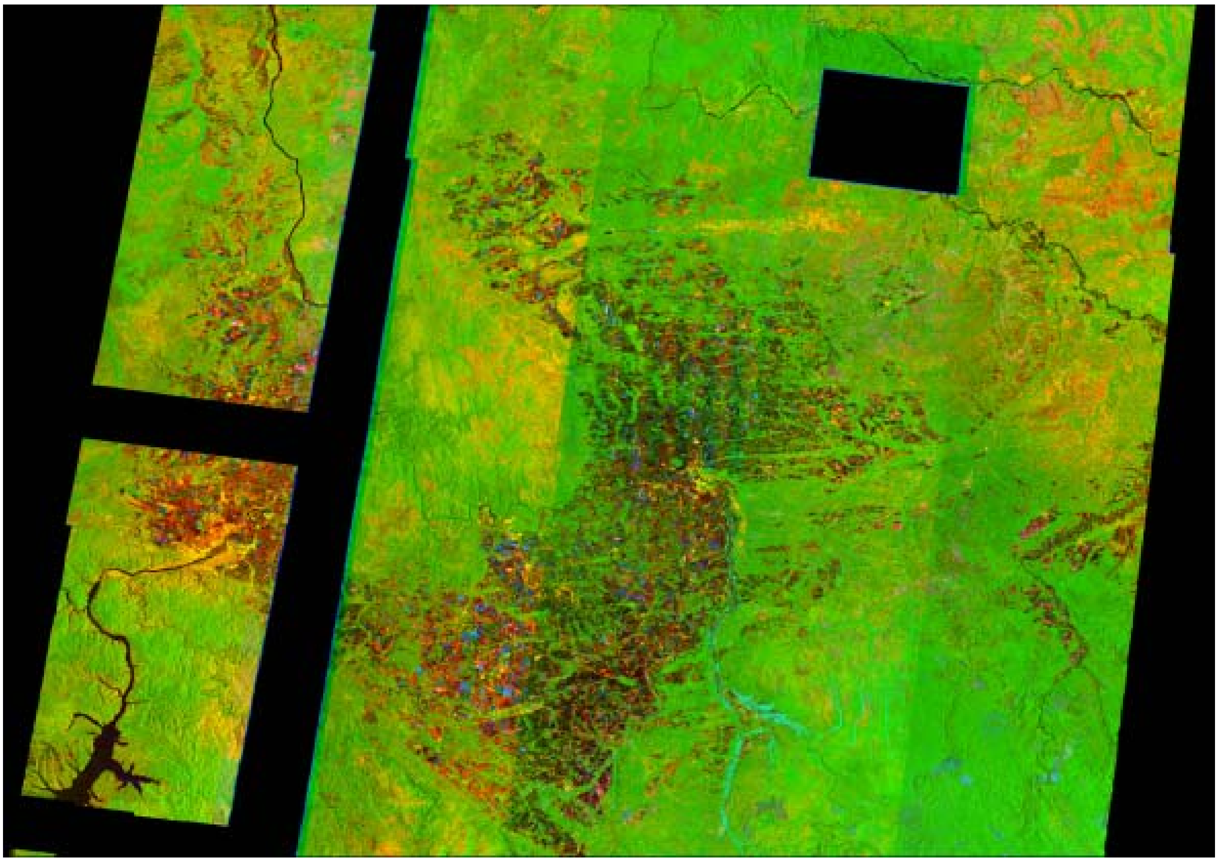

Fig. 2.10 *RGB composite figure of the JERS coherence (red), average JERS backscatter (green) and backscatter change (blue). The Figure shows an extract of the SIBERIA mosaic covering RSP 142 to 151 from 55.5 to 57 degrees north. Areas without double JERS coverage are masked out.*

2.2.2 Optical Sensors

Optical sensor data included three Landsat TM images and a NOAA AVHRR mosaic. Landsat TM data (from Landsat 7) were purchased for three test sites, Primorsky, Irbeisky, and Bolshe-Murtinsky (the Bolshe-Murtinsky scene has not been used in the analysis of AVHRR mosaic data due to fog). A Landsat scene covers an area of approximately 170 km by 170 km, and the resolution of the spectral bands used is 30 m. The Primorsky scene was acquired on 19 July 1999 and the Irbeisky scene on 8 July 1999. The Irbeisky scene was almost cloud free, but the Primorsky image had a partial cloud cover and also some smoke. The classification used bands 1 to 7 of the (enhanced) Thematic Mapper (TM), excluding the thermal band 6.

Table 2.4 *Landsat TM bands used in the classification*

Band	Wavelength
1	0.45 ... 0.52 µm, blue
2	0.52 ... 0.60 µm, green
3	0.63 ... 0.69 µm, red
4	0.76 ... 0.90 µm, near infrared
5	1.55 ... 1.75 µm "short-wave" infrared
7	2.08 ... 2.35 µm mid infrared

Before classification, the Landsat TM images were calibrated into reflectance values using the SMAC (Simplified Method for Atmospheric Correction) procedure (Rahman and Dedieu 1994). The atmospheric optical depth at 550nm was chosen experimentally separately for both images (Primorsky: 0.2, Irbeisky: 0.1). In both cases the water content was assumed to be 2.0 g/cm^2 and ozone content 0.350 cm-atm.

Table 2.5 *NOAA AVHRR bands used in mosaicking and classification.*

Band	Wavelength
1	0.58 ... 0.68 µm, visible
2	0.725 ... 1.10 µm, near infrared
3	3.55 ... 3.93 µm, middle infrared
4	10.5 ... 11.3 µm, thermal infrared
5	11.5 ... 12.5 µm, thermal infrared

NOAA AVHRR mosaics were prepared for the SIBERIA study area using archived data. Summers (May to September) 1997 through 1999 were scanned for cloud free data. Only data from NOAA-14 satellite were used, to exclude possible satellite-to-satellite calibration problems. Data from the first afternoon pass of the satellite were used to obtain approximately the same illumination conditions in all scenes used. All scenes input to the mosaicking process were first calibrated. The radiometric calibration of AVHRR thermal bands 3, 4, and 5 was based on the data included in the HRPT (High Resolution Picture Transmission) data stream (calibration using the on-board calibration target). Calibration of visible and near infrared band 1 and 2 utilised calibration coefficients provided by NOAA. Table 2.5 (Kidwell 1984) shows the spectral bands of the NOAA AVHRR sensor.

Atmospheric correction was applied to all scenes. The correction utilised the SMAC program as in the case of the Landsat TM images. From previous studies it is known that surface reflectance over mature coniferous forest vary between 1.5%-2.0% on the red channel 1 and between 15%-20% on the NIR channel (Kleman 1986). Several surface reflectance images were computed using different input values (0.10 ... 0.15 at 550 nm) for aerosol optical depth. Then reflectance values over mature forests were studied, and through experiment, the best value for aerosol optical depth was chosen. A BRDF (Bi-directional Reflectance Distribution Function) model was used to remove the distortions that are caused by different illumination conditions and viewing angles. The BRDF model was also used to normalise the scenes to correspond to a nadir view with a sun zenith angle of 45 degrees.

Image geo-coding was based on geometric information that was included in the raw (AVHRR) data file. The geo-coding was revised using GCPs (Ground Control Points) obtained by image correlation between individual AVHRR scenes. First trial mosaics were made per year. Careful study of the satellite data archive proved that a completely cloud-free mosaic was impossible for all three summers (1997, 1998, and 1999) studied. To produce a complete, cloud-free mosaic, the following mosaicking strategy was adopted:

- production of yearly mosaics always taking data from the scene that had the highest NDVI (Normalised Differential Vegetation Index)
- combination of the three yearly mosaics by computing a pixel-wise average of all mosaics that had data in the pixel.

The mosaicking strategy above has the advantages that it finds data in and around glaciers in mountainous areas and it produces a slightly less noisy image (due to the averaging) than an NDVI-maximising algorithm alone. 0 shows the mosaic for all three bands included in the mosaicking (mid-infrared or 3.7-µm band in red, near infrared in green and visible in blue). As the mid-infrared band is sensitive to the temperature of the target area, this band is not very suitable to quantitative analysis of forest types or forest stem volume. The temperature of the pixels included in the mosaic may have varied randomly within a range of +/- 10 degrees. In visual analysis this band can be used to differentiate between rock surfaces in the mountain areas (bluish colours) and the presumably bare soil dominated lowland areas (reddish colours).

The mosaic extends from the Krasnoyarsk region in the West to the Irkutsk region in the East. The South-western end of Lake Baikal can be seen in the lower right corner of 0. The large reservoir South of Krasnoyarsk can be seen as a dark feature close to the left edge of the figure. Rivers Yenisey and Angara are visible for the most part of their length in the mosaic. Major landscape units can be seen in the mosaic. Larger continuous coniferous forests have shades of dark green in 0 due to their low reflectance in visible and near infrared wavelengths. Zones containing more deciduous forests surround the coniferous forest areas. Deciduous forests have brighter green shades. This is due to the higher near infrared reflectance of deciduous trees. Areas dominated by various forms of agriculture have various reddish-yellowish tones. Agricultural areas also tend to have a higher pixel-to-pixel variance due to the higher dynamic variation of the reflectance within the growing season.

To study the synergy of SAR and optical data, the ERS coherence data were coregistered with Landsat TM images using ground control points measured visually from the images.

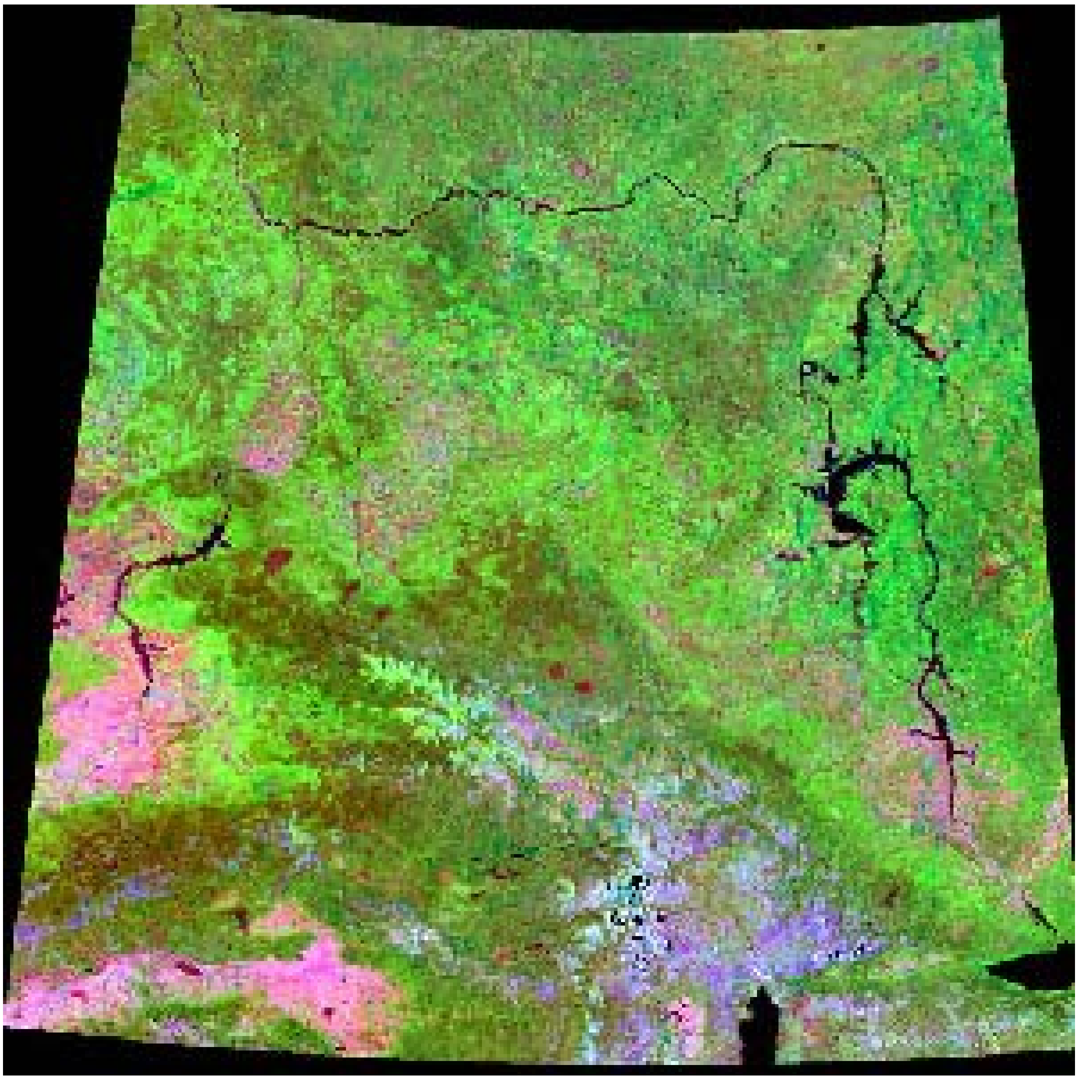

Fig. 2.11 *NOAA AVHRR mosaic. Red = visible, green = near infrared, and blue = mid infrared.*

2.3 Research Design

SIBERIA's scope is the operational production of a large forest database using images from SAR satellites. In a first phase, forest inventory data and a hierarchical classification requirement scheme was provided by the customers. At the same time, the extensive satellite data set was processed to a geo-coded, sometimes terrain-corrected, state and co-registered to be ready for the methodological work packages. This led into a complex analysis of the SAR measurements (intensity and coherence) as a function of forest stand characteristics. The key tasks of SIBERIA's scientific development is the investigation of the radar signal information content with respect to the customer requirements and the following development of a robust, but adaptive classification algorithm.

The research design involved two management structures: i) an iterative loop structure, where methodological progress is being checked in time intervals by the independent and critical customers; and ii) a matrix distribution of task responsibilities, which involves frequent interaction between team members. Furthermore, due to the importance of the scientific core analysis a dedicated methodology coordinator was responsible for these work packages.

The matrix structure is illustrated in Fig. 2.12. Three radar expert teams worked in parallel on assigned test sites. The respective team leads were responsible for following each of the indicated "horizontal" methodological work task. In addition, a responsible project team member was assigned to each horizontal task, thus coordinating, focusing, and summarizing the methodological progress. The customers were constantly involved in the validation loop.
This research design ensured by comparison of results between testsites and by evaluation of various techniques developed by the different research teams, that the best method or combination of methods were retained for application to the whole project area.

After an intensive period of algorithm comparisons, the customers and an internal independent methodology team member evaluated the map accuracy, using to the methodological team formerly unknown test sites. The customers even supplied "last-minute" ground checks for a special critical forest map assessment.

Short notes and weekly teleconferences supported the information exchange between team members. Computational issues (e.g. compatibility, property rights) were also supervised by a dedicated team member. After conclusion of the methodological development a publication list was generated in mutual agreement to ensure credit of this complex development to each of the project team members.

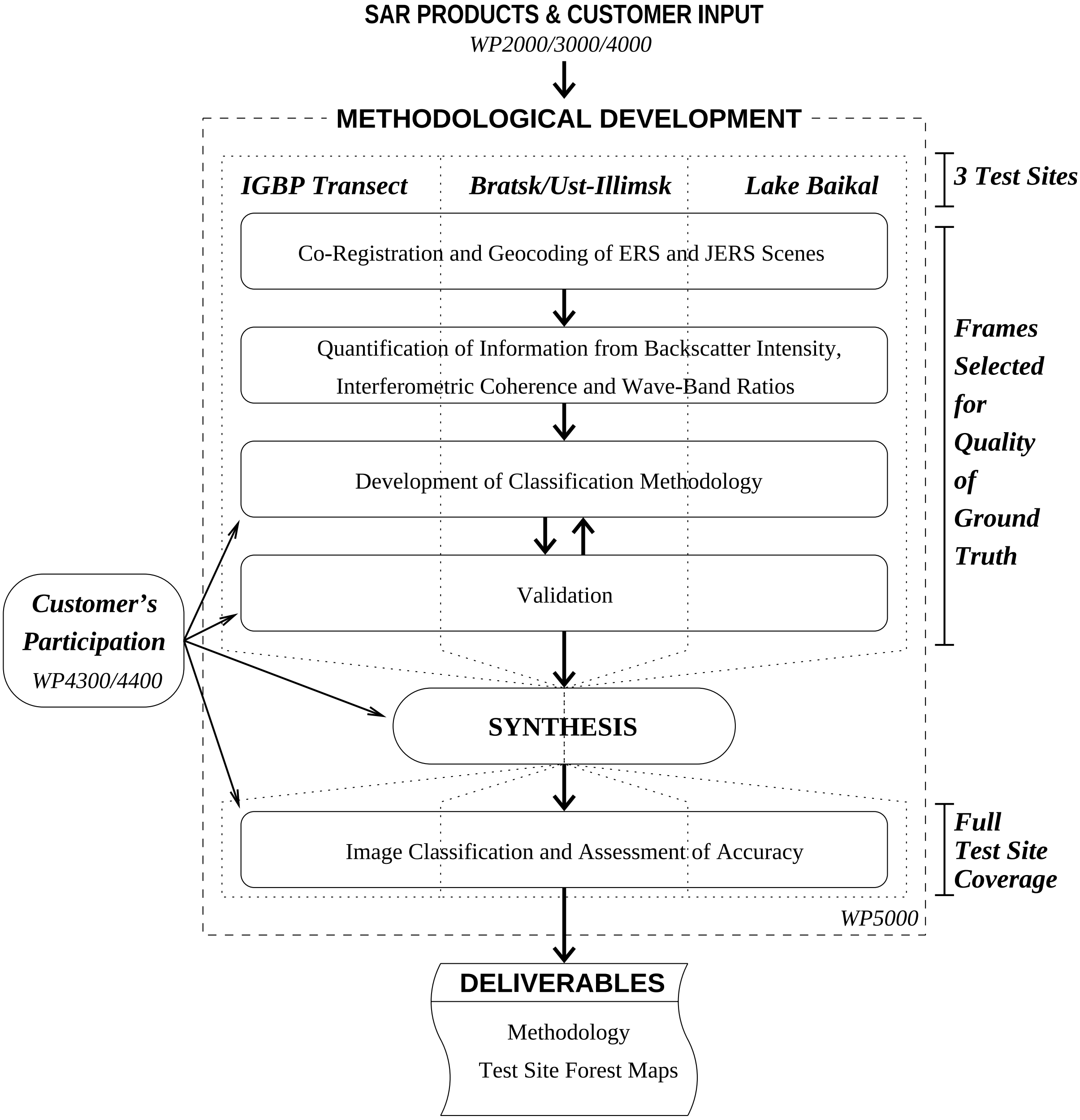

Fig. 2.12 *Flowchart for work package 5000.*

2.3.1 Classification Requirements

Current information requirements for any up-to-date forest inventory and monitoring systems stem from the transition of world forestry practices to the sustainable forest management paradigm (SFMP), which is formalized and evaluated through the implementation of national and international sets of criteria and indicators. Russian national criteria and indicators of sustainable forest management were officially approved by the Federal Forest Service of the Russian Federation in January 1998, and should be considered as framework targets. Current official data requirements on forests, including classifications, information themes, accuracy, etc., are defined by the manual for the forest inventory in Russia (FFS, 1995). There are significant differences between the existing and demanded approaches. The major changes caused by the transition to the SFMP include: 1) increased data demands with evident emphasis on ecological, in particular, biospheric services; 2) an equal priority on attributive and spatial information at all levels; and 3) increased completeness and continuity of information. Remote sensing applications are crucial in this process for Russia.

Major users of forest inventory data in Russia include: 1) at the local level (spatial scales from 1:1,000 to 1:50,000)–managers and professionals of state forest enterprises, environment protection authorities at the district level, and private firms of forest industry; 2) at the regional level (scales from 50,000 to 1,000,000)– regional bodies of state forest management and environmental protection, regional forest inventory and planning enterprises, regional offices of *Avialesookhrana* (the fire protection agency), regional governments, universities and NGOs, large industrial forest companies; 3) at the federal level (scales from 1:1 million to 1:10 million)–the Federal Forest Service of Russia, other federal ministries (Ministry of Natural Resources, Ministry of Extraordinary Situations, etc.), federal forest fire protection agency , universities, and NGOs; and 4) federal agencies responsible for the compliance of Russian-made international commitments (e.g. resulting from UNCED, Rio, 1992 or the Kyoto Protocol). Information requirements and interests of different user groups are to a significant degree different and not static (*cf.* de Gier, 1999; Malysheva *et al*., 2000).

Russia has a rather detailed and complicated forestland classification as well as a system of forest inventory and monitoring. About 69% of the entire Russian territory is comprised of the *Forest Fund (FF)* – all territories which are under state forest management. The FF is divided into *Forest Land (FL)* and *Non-Forest Land (NFL)*. The FL is represented by territories which are either covered by forests (so-called *Forested Areas*), or which are temporarily non-forested, but are designated for forest growth, e.g. burned areas, unregenerated harvested areas and grassy glades (*Unforested Areas – UFA)*. The NFL includes numerous land categories, which are either not designated for forest growth (e.g. water bodies, forest roads etc.), or are not suitable for forests (bogs, sandy lands, tundra, rocks etc.). Each primary inventory unit of NFL and UFA has a rather detailed description. Very detailed information is presented for each primary inventory unit (separate stand) of Forested Areas. The major information themes include:

- coordinates of a primary inventory unit (forest enterprise, forest district, forest compartment, number of primary inventory units), basic legislative categories (e.g. group of forests, protective categories, etc.) and its area;
- comprehensive quantitative description of a stand (including types of age and morphological structures, species composition, age, average diameter and height, relative stocking, site index, forest type, growing stock and its quality, amount of dead wood etc.);
- description of other parts of the ecosystem's vegetation (understory, undergrowth, green forest floor);
- site description (e.g. soil type, fertility, humidity, erosion etc.);
- other products from forest ecosystems; like fodder, medicinal plants etc.;
- forest health;
- elevation and slope;
- forest management operations during previous years and their quality;
- planned forest management operations.

The accuracy requirements prescribed by the current inventory and monitoring manual are rather high. For example, growing stock volume of each stand should be assessed within the standard errors of ± 15% (confidential probability 0.95) and systematic errors (bias) should be within limits of 1–3%.

Radar imagery alone is not able to completely satisfy the above requirements, but it can significantly contribute to an improved classification. Thus, in our attempts to develop a relevant classification we followed a holistic approach, aiming at achieving the best contribution to the complete system by using the advantages of radar sensors. The developed classification pursued two major objectives, connected to a significant extent: 1) to present available information needed for the development of a map of forest cover by using classes which are reliably identified by radar images; and 2) to generate a tool for updating existing forest inventory information. Both goals are of the same importance and priority.

All territories of the region considered had been inventoried by different types of inventories, but the inventories for a major (largely remote) part were completed 10 to 30 years ago. Forests of the region have a high level of natural disturbances and human transformations and consequently the current state of the forests for territories with obsolete information is unknown.

The classification used is presented in Fig. 2.13. The forest classes are linked to the forest inventory classes (which are currently more detailed and informative compared with those established by radar images). For the radar forest cover map, the growing stock volume per ha was selected as a target variable for the following reasons: 1) it is a directly measured indicator, which to some extent accumulates basic characteristics of forest ecosystems; 2) there are models which allow the calculation of total and fractional forest biomass (Nilsson *et al*., 2000) using growing stock as an important indicator; and 3) there is a developed system for updating the growing stock for a period of 10–50 years (Shvidenko *et al*., 1995).

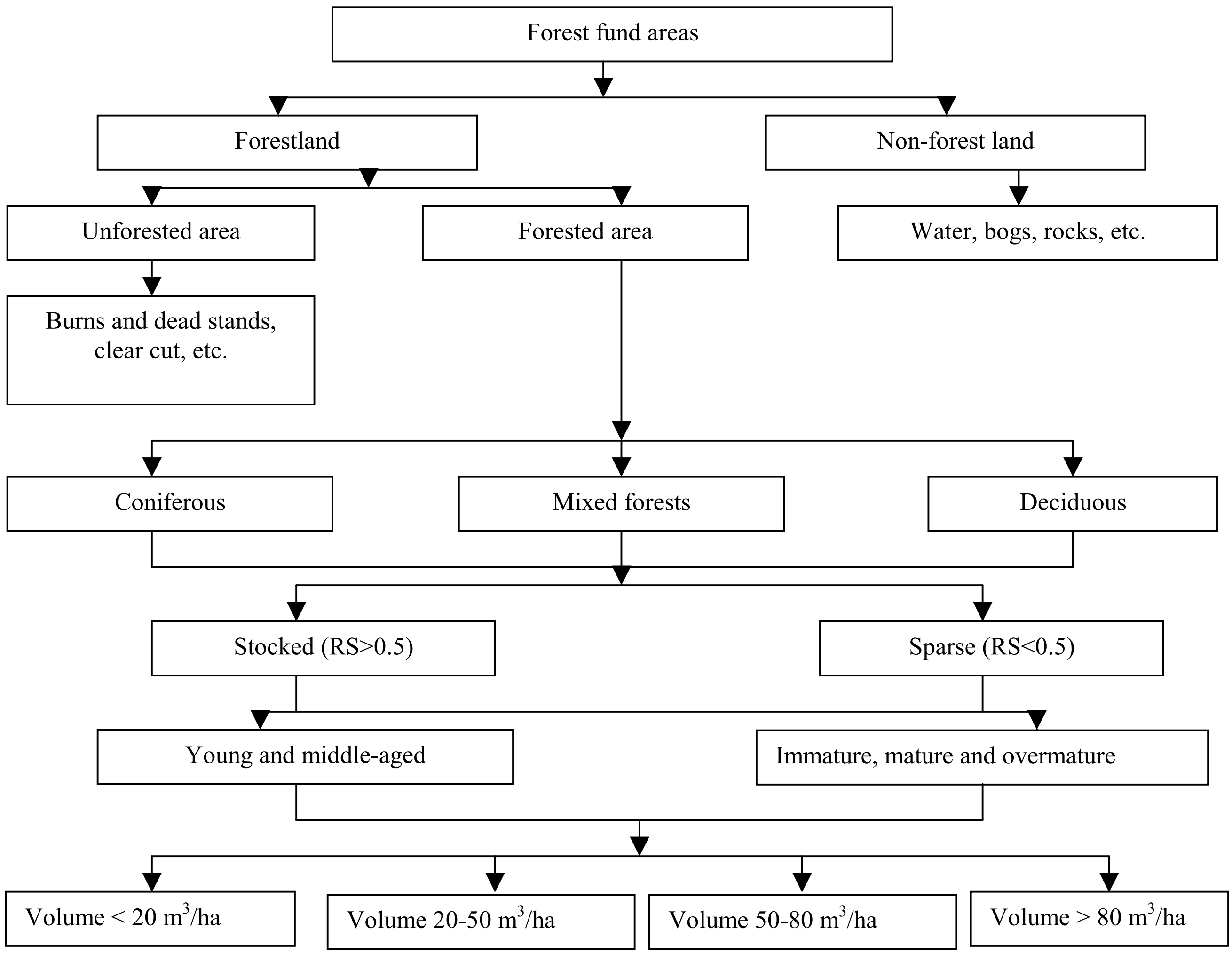

Fig. 2.13 *Forest Fund area classification used by this study.*

2.3.2 Methodological Development

Introduction:
The objectives of the methodological development in the SIBERIA project were:

To analyse the available radar data, with the help of ground data provided by Russian foresters, in order to

- identify the forest information provided by the radar data
- develop efficient and effective methods to extract that information and display it in map format.

The methods had to meet several conditions. They needed to be:

automatic because of the large amount of data to be handled (122 ERS scenes)
adaptive because of changes in image properties between scenes, caused by imaging geometry and environmental variations
consistent so that the assignment of information would not be scene-dependent and overlapping scenes would show no discontinuities
validated so that we could assign some degree of confidence to the results.

The essence of the methodology development is set out in Fig. 2.14 and the structure of this chapter essentially follows the flow indicated in this figure.

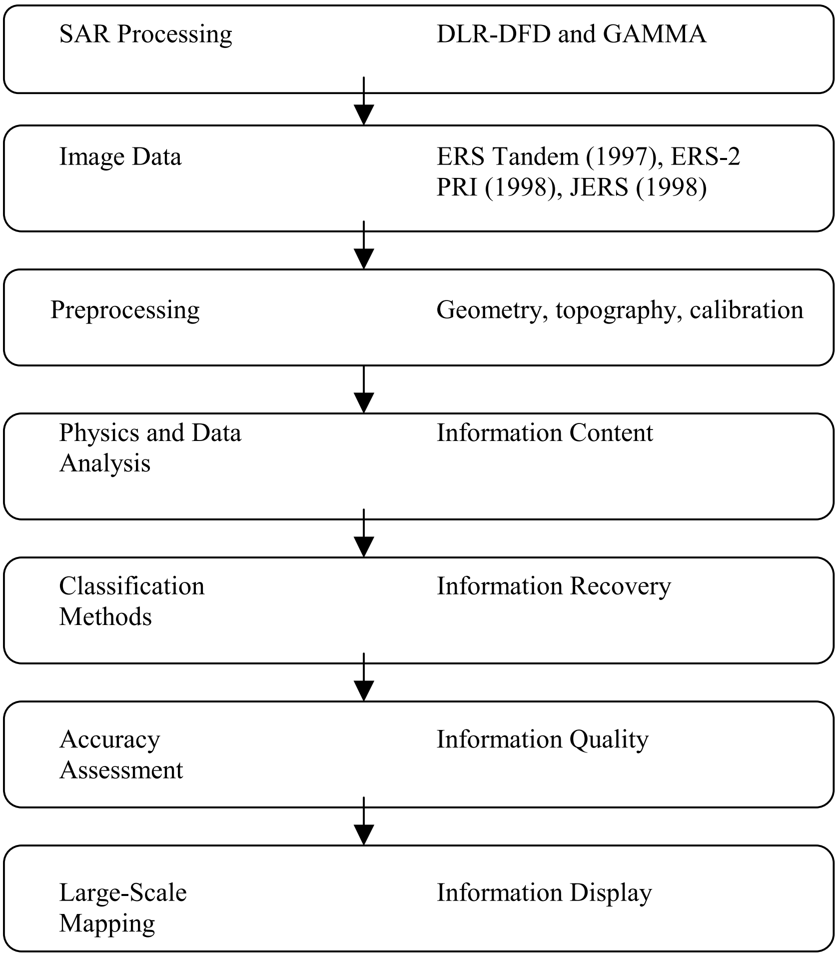

Fig. 2.14 *Conceptual flow in the methodological development*

There was no clear separation between the data supply and the work of the methodology team, since early analysis identified some data problems and indicated the data properties required (for example spatial resolution). The team were also heavily involved in evaluating the calibration methods for the ERS data.

A further important task carried out by the methodology team, which affected the interface between the data and the analysis, was to evaluate the impact of topography on the images. This affects both the data itself (for example its correction for local incidence angle and its geometrical qualities) and the information carried by the data.

Within the methodology development, responsibilities were assigned as follows:

- DLR: Geometry
- CESBIO: Information Content
- SCEOS: Pre-processing and Classification
- CEH: Accuracy Assessment
- UWS: Computational Issues
- Satellus: Map Production
- IIASA: Ground data

In practice, effective use of meetings, working notes, emails and teleconferences meant that the team as a whole was involved in most aspects of the development. This was one of the very successful and satisfying aspects of the SIBERIA project.

2.3.2.1 SAR Geometry

Due to the side looking geometry of SAR systems, topography causes considerable radiometric and geometric distortions in radar images. These distortions are different for the ERS and JERS satellites and have to be considered for classification purposes. Additionally the intensity images that were supplied to the methodology team were processed to different levels. While the JERS intensities were already calibrated, the intensities of the ERS had to be calibrated before performing the classification. The accuracy of the geometric terrain correction using the GTOPO30 DEM was of the order of a few hundred meters for both the JERS products and the ERS GEC products. To improve the registration, and for compatibility of the JERS and ERS images, fine registration between geocoded ERS (either GTC or GEC) and geocoded JERS data was necessary.

Over and above work defined in the proposal, the interferometric processing chain was modified to accommodate a third ERS data set acquired during the spring season 1998. This optimises the co-registration of the spring to the autumn 1997 tandem data and achieves pixel accuracy. The fitting of the spring data to the interferometrically derived DEM and the orthorectification of all data sets are performed in one step.

2.3.2.1.1 Radiometric Calibration of ERS and Strategy for Layover and Shadow Areas

The important quantity defining the information content of a SAR intensity image is the backscattering coefficient σ^0. To calculate σ^0 using the values of an intensity image the SAR sensor characteristics and the size of the illuminated surface area for each pixel must be taken into account. The size of the illuminated area depends on the inclination of the surface relative to the look direction of the sensor (actual incidence angle). If topographic information is available then the calculation of σ^0 corrected for the local topography is possible. Otherwise only an incidence angle for a flat area can be used. Additional problems caused by topography are layover and shadow (the extreme cases for the change of the size of the illuminated area of each pixel) for which the received data is unusable. It is desirable to deal with these problems within the calibration process.

The calibration program “calit“, developed by DLR-DFD, was adopted as standard software by the team. This program is designed to handle PRI and SLC products, and can calibrate geometrically corrected intensity images. “Calit” has the option to correct products to different levels of calibration. For the products used by the project the operations carried out include:

- replica pulse power correction,
- antenna pattern correction and
- range dependent incidence angle correction.

As well as the sensor specific radiometric corrections for SAR intensity images, “calit” is able to carry out radiometric correction using the local incidence angle. This angle is stored in an image file called the geocoded incidence angle mask (GIM), which can be generated from a digital elevation model (DEM), if available (see Fig. 2.15). After smoothing the InSAR DEM by 5x5 median filtering, the program “inci” also tests for layover, and writes the result in the GIM file.

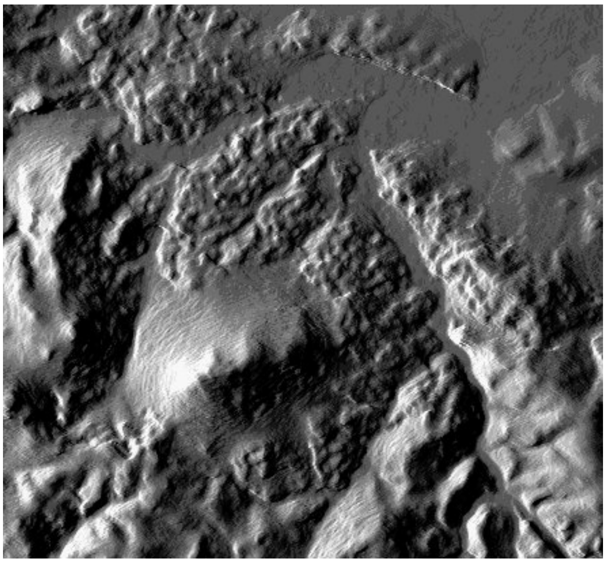

Fig. 2.15 *Geocoded Incidence angle mask (GIM).*

An InSAR DEM is much more sensitive to low local incidence angles than intensity images, since at very small local incidence angles the interferometric phase cannot be resolved by phase unwrapping procedures. This causes height errors in the DEM. Fig. 2.16 illustrates this for an effective baseline B_{eff} of 280 meters. Fig. 2.16 (a) shows the height difference Δh against the interferometric phase difference $\Delta\phi$. For $\Delta\phi \geq \pi$ (dotted line) the phase becomes ambiguous so that for a height difference between two adjacent pixels greater than or equal to 16.5 m, the InSAR DEM is not reliable. In Fig. 2.16 (b) the dependence of the local incidence angle θ_{loc} on the height difference between two adjacent pixels is shown for the case when the slope is oriented towards the sensor. It can be seen that a height difference of 16.5 m corresponds to a local incidence angle of approximately 9°. In practice, residual noise in the DEM led us to adopt a more conservative layover threshold of 8.6 m for the InSAR data.

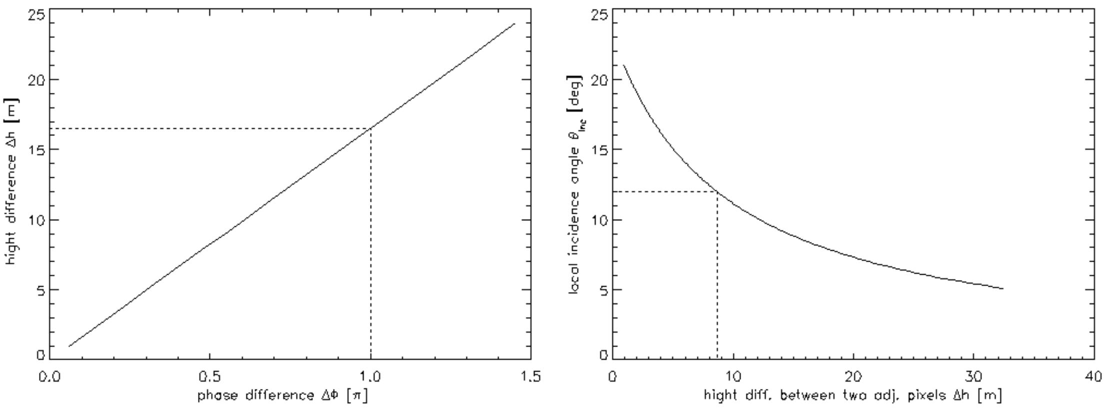

(a) *(b)*

Fig. 2.16 *(a) Height difference Δh vs. interferometric phase difference $\Delta\phi$ between two adjacent pixels for a baseline of 280 meters. For $\Delta\phi \geq \pi$ (dotted line) the phase becomes ambiguous, and cannot be resolved by phase unwrapping. (b) Local incidence angle θloc vs. height difference between two adjacent pixels. A value of 8.6 meters for Δh instead of 16.5 meters has been chosen to take the phase noise of the InSAR DEM into account.*

Because of the steep look angle of 23° for ERS, the occurrence of shadow is very unusual, and required no image operations.

Due to the lack of an accurate DEM it is not possible to correct the influence of the topography on JERS and ERS GEC products. As a result, areas of high relief were masked out, as discussed below. Due to time constraints in the project the InSAR DEMs could not be used to correct the JERS products. For this reason the ERS GTC frames also had to be masked.

2.3.2.1.2 Co-registration of ERS and JERS Images

Topographically induced geometric distortions are the main problem for the co-registration of JERS and ERS products. Two different dataset combinations for co-registration are relevant (see Balzter et al., in press):

1. *InSAR/GTOPO30:* The ERS GTC products are geocoded using the InSAR DEM and the JERS products are geocoded using the GTOPO30 DEM.
2. *GTOPO30/GTOPO30:* The ERS GEC and JERS products are both geocoded using the GTOPO30 DEM.

The ground offset for SAR images Δg can be estimated by (Schreier 1993):

$$\Delta g = \frac{h}{\tan\theta} \quad (1.)$$

where h is the elevation and θ is the look angle of the sensor. Using this equation it is possible to estimate the theoretically possible offset between the image products. Assuming an incidence angle of 23° for ERS and 35° for JERS, the offset for the InSAR/GTOPO30 case is:

$$\Delta g_{InSAR/GTOPO} = 2.3(h_{InSAR} - h_{true}) - 1.4(h_{GTOPO} - h_{true}) \quad (2.)$$

where h_{true} is the real elevation. Due to the smaller look angle of ERS, the offset is more sensitive to errors in the InSAR DEM.

The ground offset for the GTOPO30/GTOPO30 case is:

$$\Delta g_{GTOPO/GTOPO} = 0.9(h_{GTOPO} - h_{true}) \quad (3.)$$

so that the offset between the ERS GECs and the JERS images is roughly equal to the height error of the GTOPO30 DEM.

Using these equations, it is possible to estimate the standard deviations (StDev) of the ground offsets as a function of the standard deviation of the height errors of the DEMs. For an estimated StDev of 25 m for the InSAR DEM and 75 m for the GTOPO30 DEM, the StDevs of the ground offset are 120 m or 71 m respectively. Hence 95% of the offset values lie in the intervals ±240 m (or ±5 Pixels) and ±142 m (or ±3 Pixels) respectively. In general we can expect higher offsets for rugged terrain than for gently undulating areas. Therefore mountainous regions were masked out before co-registration.

The co-registration used software developed by GAMMA Remote Sensing. Its advantages are:

1. The process is very quick.
2. JERS can be co-registered to ERS GEC and GTC products.
3. Images with little overlap can be co-registered.
4. Output statistics are reported and can be saved.
5. The process can be automated.

Because of the large number of images that were processed in the project, points 1 and 5 are especially important. This software calculates an initial registration offset from the map offsets provided in the header files of the images and then refines it. Further analysis produces an offset field and a polynomial equation to perform the transformation. Bilinear resampling is then carried out from this equation.

2.3.2.1.3 Masking Procedure for Strong Topography

As mentioned above, masking of high relief areas was necessary for two reasons. Firstly, the ERS-GEC and the JERS images are not radiometrically terrain corrected. Secondly, the terrain-induced distortions can make the co-registration of JERS to ERS images impossible over mountainous regions. The method adopted is based on the GTOPO30 DEM, as follows:
1. Resample the GTOPO30 DEM to 50 x 50 m pixel spacing and generate a subset corresponding to the area of the respective ERS frame.

2. Calculate the geocoded incidence angle mask (GIM) based on the GTOPO30 DEM and the specific ERS acquisition geometry.
3. Calculate the standard deviation of the incidence angles for subsets of the GIM of a specific size, e.g. 10 x 10 pixels.
4. Apply a threshold to the standard deviation to mask out hilly terrain. The lower the threshold the stronger is the masking.

This masking method was shown to ensure the quality of the intensity images. Fig. 2.17 shows the mean absolute difference between radiometrically terrain corrected intensity images and intensity images that were only ellipsoid corrected as a function of the threshold value for masking. As can be seen, the stronger the masking (the lower the threshold) the smaller is the difference between the corrected and uncorrected images.

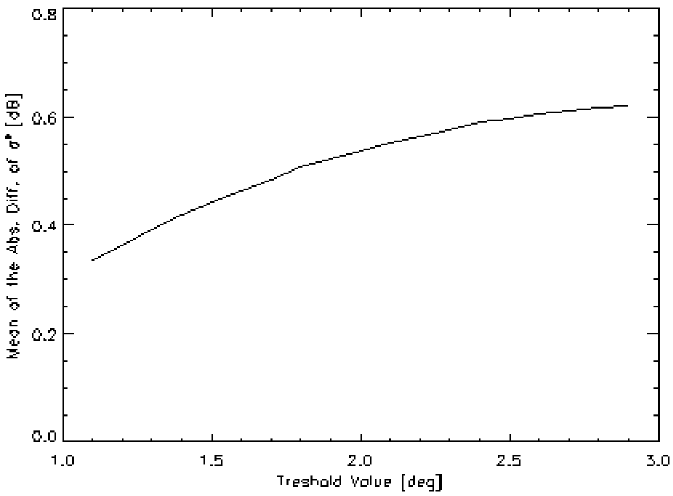

Fig. 2.17 *Dependence of the absolute difference between two intensity images, one radiometrically terrain corrected and one only radiometrically ellipsoid corrected, on the threshold value for masking. Lower threshold values represent stronger masking.*

A threshold of 1.4° and a window size of 20 x 20 pixels leads to the best results for masking (see Fig. 2.18).

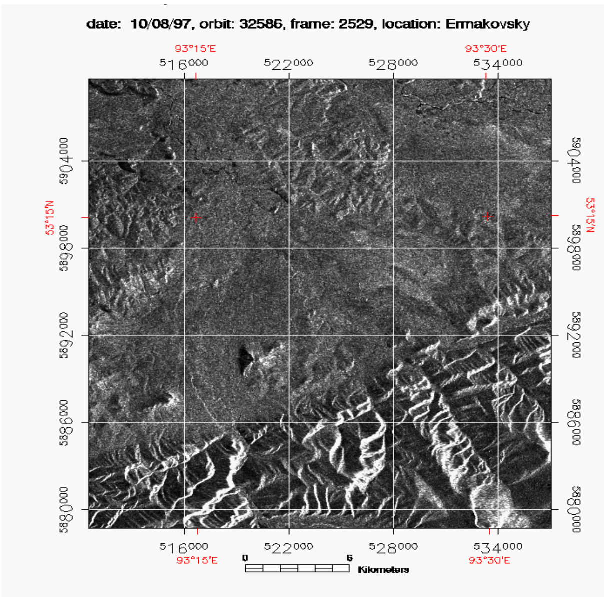

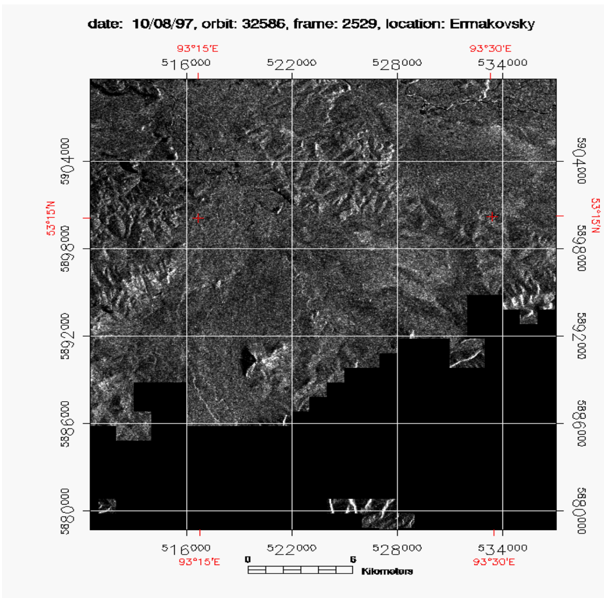

(a) *(b)*

Fig. 2.18 *Subset of an ERS backscatter image located in the Ermakovsky region in the south of the IGBP-Transect. a) Backscatter intensity image. b) Masked image. Acquisition date: 5.10.97.*

2.3.2.2 Information Content

2.3.2.2.1 Objective and Approach

The objective of this work package was to assess the information content of the available input SAR data with regards to the project user requirements. Carrying out such a study is essential in order to

1. determine the number and the labels of the map classes applicable to the large-scale SIBERIA SAR data,
2. to select the appropriate SAR measurements for the mapping task, and
3. to use these measurements in an optimal way within classification methods.

As a first step in identifying the information content of the available SAR measurements, i.e. ERS intensity and coherence, and JERS intensity, the underlying physical interactions defining SAR responses over forest are summarised. The list of forest attributes and land use/land cover classes defined by the SIBERIA forest information users were used as input, and their correspondence with the information which can be derived from the available SAR data examined. The result of this process is a selection of forest attribute and land cover types, which are 1) retrievable from the SAR data and 2), required by forest information users.

In a subsequent step, an extensive analysis of the different SAR measurements as a function of the relevant forest attributes provided by the forest database of over 39 forest enterprises is carried out. These experimental results are interpreted in terms of the underlying physical interactions and the various sources of frame-to-frame variability in the derived relationships highlighted.

2.3.2.2.2 Physical Background

ERS Intensity Response to Forest

For the ERS SAR (C-band, 23° incidence angle and VV polarisation), the backscattered intensity from a forest is quite stable, both in spatial and temporal extent, for stands with biomass levels above approximately 30 t/ha, or 40-50 m^3/ha of stem volume. The spatial and temporal variability of lower biomass stands is in general of the order of 0-3 dB and is due to variability in the understory characteristics (low vegetation, soil moisture and roughness) (Le Toan et al. 1992, Pulliainen et al. 1994, Quegan et al. 2000)

In terms of physical interaction mechanisms the backscatter signal can be depicted simply as a sum of scattering contributions from the canopy and from the ground, with the latter attenuated by the canopy layer. At C-band canopy scattering and attenuation is caused primarily by leaves, needles, twigs and small branches, which are characterised by their small size compared to the wavelength and also by their high number density. At a certain level of biomass the number density of the tree elements is high enough to cause two phenomena: a) the attenuation of the incoming wave by the canopy is sufficiently important to eliminate the soil contribution; b) the backscatter by the canopy itself is no longer dependent to the number of scatterers. This results in a saturation of the observed backscatter levels, which is well documented in numerous ERS-studies. The saturation level depends mainly on the size of the scatterers (deciduous forests usually have higher return compared to the coniferous forests) and can vary slightly between stands of different species composition. Environmental conditions, mainly rain or frost, also cause some variability of the saturation level. Overall, however, the variability of the mature forest response is relatively small, less than 2-3 dB (Le Toan and Floury 1998).

If the number density of the scattering elements is relatively small - corresponding to a low level of biomass - the ground return is non-negligible and can be dominant, depending on ground environmental conditions. If the underlying ground (without attenuation or at zero biomass) has higher backscatter than the forest saturation level (e.g. wet bare soil), a decreasing trend of the backscatter versus biomass curve is observed. If the ground backscatter is lower (for example very dry smooth soil or ground covered with low vegetation), an increasing trend is observed. In general, a decreasing trend is often observed for temperate forest plantations, and increasing trend can be found in natural boreal forests. As a consequence, the ERS backscatter coefficient is sensitive to biomass variation only over a small range of biomass levels, ranging from a ground response to an upper forest-dependent limit typically of the order of 30 t/ha (or 40-50 m^3/ha stem volume). Furthermore, this sensitivity depends on ground conditions and can have a temporal variation e.g. due to rain effects. Between-stand variability can be caused by different factors including species composition.

JERS Intensity Response to Forest

For the JERS L-band SAR, forest backscatter is also the result of the addition of canopy scattering and attenuated ground scattering. The canopy scattering and attenuation in this case mainly come from the branches, and their sizes and orientations are of importance in determining the backscatter levels. Since the latter parameters vary as a function of species, canopy scattering is expected to be more species dependent than in the case of C-band. The ground contribution is present until a high number of branches are reached. Overall there is an increasing trend of the backscatter coefficient as a function of biomass, since the ground contribution has in general lower backscatter than the canopy (smooth soil, or very small size underlying vegetation when compared to the L-band wavelength). JERS is also sensitive to aboveground biomass over a larger range of values than ERS. The sensitivity is of the order of 2-3 dB for a range of biomass of about 0-70 t/ha or 0-100 m^3/ha in stem volume. (Le Toan et al, 1992, Souyris et al, 1995, Luckman et al., 1997, Smith et al., 1998). The relationship between the JERS intensity and biomass, and also the saturation level, depend on the allometric relations between branch biomass and total biomass or stem volume. Thus for forest stands with differing species composition, the relationship between the backscatter signal and biomass can vary more between stands than in the case of ERS data.

ERS Tandem Coherence of Forests

An important parameter for forest studies is the interferometric coherence, which is defined as (Hagberg et al. 1995; Askne et al. 1997):

$$\gamma = |\gamma| e^{j\phi} = \frac{\langle s_1 s_2^* \rangle}{\sqrt{\langle s_1 s_1^* \rangle . \langle s_2 s_2^* \rangle}} \tag{4.}$$

where s_1 and s_2 denote the first and the second complex SAR images, here the two ERS-1 and ERS-2 images acquired with one day delay.

It is possible to factor the total coherence into different sources of decorrelation such that

$$\gamma = \gamma_{processing} \cdot \gamma_{geometry} \cdot \gamma_{volume} \cdot \gamma_{temporal} \tag{5.}$$

The decorrelation due to processing includes the effect of image registration and bias due to estimation of the coherence modulus. For instance if the registration is not perfect, the coherence is reduced, and the coherence loss is more important in terrain with relief. Also if the coherence is estimated using a small number of independent samples (i.e. small window size, the low coherence values (i.e. from 0 to 0.4) are biased towards higher values.

The decorrelation due to geometry concerns mainly the interferometric baseline. The coherence decreases with the baseline. This effect is in general corrected in interferometric processing software by "spectral shift filtering" to normalise the coherence based on the responses of stable surface.

The two remaining sources of decorrelation are related to the surface characteristics.

The volume decorrelation characterises the modification of the wave path inside the canopy between the two acquisitions, and to a lesser extent, the related changes in scattering mechanisms. This effect is caused by the change in incidence angle, and is very small at C-band compared to the temporal decorrelation (its relative importance increases at lower frequencies with more penetration and in single-pass interferometry).

The temporal decorrelation is caused by the movements of the scatterers between two acquisitions. At C-band the scatterers are needles, leaves, twigs and small branches, which are highly sensitive to wind effects. For different forest stands the coherence decreases with an increase in the proportion of the leaves, needles, small branches etc. in the stand. This means that indirectly the coherence decreases as a function of the biomass or stem volume. As the volume or biomass increases, the coherence drops and can reach the noise level. The shape of the decreasing function and the absolute levels of coherence as a function of biomass can be affected by the backscatter of the ground surface, which can vary e.g. as a function of rain induced soil moisture.

2.3.2.2.3 Data Analysis

Bearing in mind the above synthesis on what the available SAR data can provide, we now examine the correspondence between radar retrieved information and the class labels and forest attributes defined in the project forest database provided by Russian Forest Enterprises and compiled by IIASA.

Examination of the Land Use and Forest Attributes Defined in the Forest Databases

The land cover types included in the forest database only represent the surface types located within the boundaries of a forest enterprise. As a consequence

1. many land-use types present in SAR frames and outside the forest enterprises are not identified. This is the case for agricultural land, settlements, meadows etc.
2. the forest and non-forest classes found in the forest database are usually defined according to forest management criteria instead of actual land-use criteria. For instance a stand may be identified as a cedar stand (and economically valuable wood) even though cedar only constitutes 20% of the trees.

In the following, the land use/ land cover classes from databases are examined in terms of their equivalence to SAR classes:

1. Forest classes:

1101. Natural stand
1102. Unclosed natural forest
1104. Low productivity forest
1108. Forest plantation
1201. Unclosed forest plantation
1400. Sparse forest
1503. Burned Forest
1507. Stand marked for cutting
1509. Clear-cut area

Forest stands with increasing biomass or volume, corresponding respectively to increasing ERS& JERS intensity, and decreasing coherence

2. Non- forest classes:

2102. Agriculture, hay
2103. Agriculture, pasture

Areas with higher coherence and lower ERS&JERS intensity than the forest

2110. Stream
2308. Lake

Areas with low coherence and low JERS intensity, and variable ERS intensity

2507. Bogs

Areas with variable coherence and intensity depending on presence of water and vegetation density

2505 Exposed rock
2512. Talus
2540. Quarry or gravel pit

Areas with high coherence and variable intensity depending on roughness, non-relevant if small size

Forest attributes from the database

Each of the stands in the database is associated with the following attributes, which are defined by the SIBERIA project as follows:

Relative Stocking	A comparison of the stocking of a particular stand to the stocking achievable under perfect management condition. Local information, e.g. site quality and yield table are needed to understand the physical meaning of this attribute. Relative stocking cannot be related in a simple manner to basal area, percent cover or number density, as the label name may suggest.
Growing Stock Volume	In principle, stem volume for all living species in a stand. In practice, only trees with dbh ≥ 6 cm are considered.
Age	The age of the dominant species. However, dominant species do not dominate by number, but by its economic value. Cedar (*Pinus sibirica*) has the highest value, followed by pine (*Pinus sylvestris*), and deciduous species have the lowest value. When cedar trees are present in a stand, the stand age is the age of cedars, regardless of their percentage in the stand. Furthermore, age class (young, middle age, premature, mature, over mature) does not have the same scale for different species. Young and overmature classes are respectively 1-40 years and >140 years for pine, spruce, birch, larch; 1-80 years and >240 years for cedar and 1-20 years and >70 years for aspen and birch. If the stand age is 70, it is labelled a "young" stand if the dominant species is cedar, middle age if the dominant species is pine, spruce, fir and larch, or "overmature" if the dominant species are aspen or birch. The relationship between age and volume depends on species and site quality. However for forest stands with the same species composition, age class can reflect rough volume classes.
Composition	The proportion of a species in a stand, from 1 (10%) to 10 (100%).
Height	An estimate of the average tree height of the dominant species in the stand.
Diameter	The average tree diameter of the dominant species measured at breast height (dbh).

Among the above parameters only total growing stock volume is physically related to radar measurements through the relationships between stem volume-> stem biomass-> leaf, needle, branches biomass-> radar measurements. The other parameters are either dependent on non-physical concepts such as the dominant species (age, height, diameter), or on site quality (relative stocking) and therefore cannot be retrieved consistently using SAR data.

Analysis of the SAR Measurements as a Function of Growing Stock Volume

Growing stock volume is consequently the key parameter to be used in the analysis of the SAR measurements with regards to the SAR responses to forest classes. In the following, a summary of the experimental results, obtained at the 39 test sites for which forest databases were available, will be given.
The observed relationships between ERS intensity and coherence, and JERS intensity, as a function of the growing stock volume can be summarised as follows:

Under optimal conditions, the empirical relationships between ERS intensity and coherence, and JERS intensity, and growing stock volume established for the forest stands of an individual test site can be fitted using a monotonically increasing (ERS and JERS backscatter) or decreasing (ERS coherence) curve with standard regression procedures. However, sources of noise affecting these relationships are numerous. Overall, three categories can be identified.

The first category is related to the following forest and site characteristics:

- between-stand variability caused by species composition and horizontal distribution,
- environmental effects, mainly local rain.

The second category is the result of error sources in SAR measurements:

- calibration of the SAR intensity and variability of the ERS tandem coherence due to local weather conditions,
- error in estimating SAR intensity and coherence when the stand area is small,
- topographic effects, which cause distortions in the SAR intensity and loss of coherence,
- misregistration of the forest database and the SAR image.

The third category is related to error sources in the forest database:

- out-of-date forest databases, in particular due to clear cutting and fire,
- systematic errors in growing stock volume estimates, one of the causes being the exclusion of tree whose dbh is less than 6 cm, the other being the volume given in terrain with relief, which is given in horizontally projected unit area and not in actual area,
- random uncertainties due to methods of stand delineation and volume measurements.

Because of the above sources of error, the experimental data points (stand-based SAR measurements versus volume) can differ from one another for different test sites, different dates and different interferometric baselines. The most important influences affecting the SAR measurements vs. stand volume relationships are however:

- variations in ground and vegetation moisture due to rain, which cause slight differences in ERS and JERS intensity,
- tandem acquisition conditions in terms of interferometric baseline and change in weather conditions. The coherence decreases as a function of the baseline, and its dynamic range is reduced, e.g. rain or strong wind,
- errors in the interferometric processing, in particular in GEC data,
- overall underlying ground moisture condition, which affects the coherence over forests.

When using the experimental results for an inversion algorithm and for the accuracy assessment, it is important to bear in mind the different sources of variation in the data.

1. The scattering of data points around a mean curve (expressed in standard deviation) due to forest and site characteristics is intrinsic to the information content of the SAR measurements at a given site.
2. The frame-to-frame variation of the experimental observations due to environmental effects is intrinsic to the large-scale observation.
3. The data affected by error sources caused by measurements (data misregistration, uncorrected topographic effect, out-of-date forest database...) should be discarded.

ERS Intensity Versus Growing Stock Volume

Fig. 2.19 illustrates the relationship between the ERS backscatter coefficient as a function of growing stock volume when little experimental noise is present (no relief, good registration of SAR and forest data, more uniform forest stands, updated database).
The saturation level (-7 to -8 dB) in this case is associated with stand volumes greater than 70-80 m^3/ha. The "zero" volume areas have lower backscatter return than the forest saturation level. This could be an indication that the gaps in forest and the understory surfaces are covered by low vegetation, which has low return. The overall dynamic range in backscatter as a function of volume is about 2 dB for a volume range of 0-70 m^3/ha.

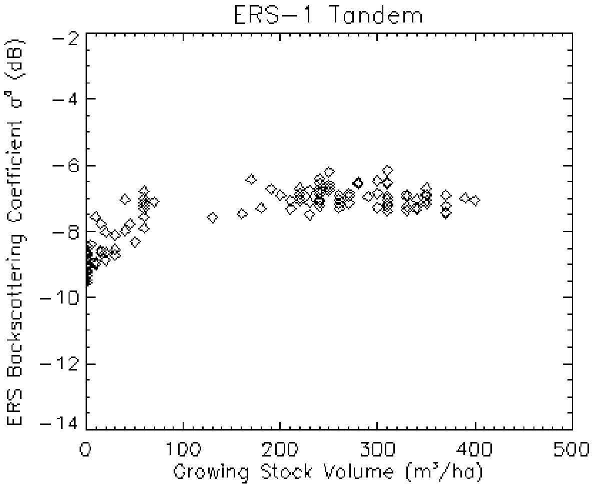

Fig. 2.19 Illustration of ERS intensity vs. growing stock volume relationship in a case where little experimental noise is present.

In many cases a small temporal change in the backscatter coefficient could be observed, e.g. between ERS fall tandem pairs or ERS autumn 97/spring 98 pairs. This is illustrated in Fig. 2.20. The amplitude of change is of about ±1 dB for the forest and ±2 dB for the low volume areas. Since the stability of ERS data is known to be of 0.2 dB on average, the primary cause for the observed temporal changes are environmental conditions (e.g. rain).

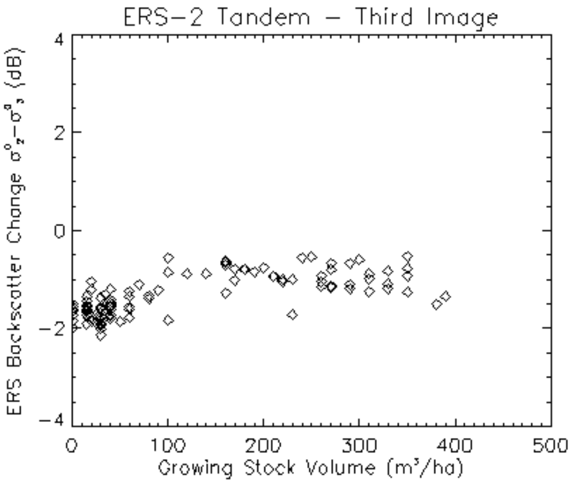

Fig. 2.20 *Illustration of temporal change (here between acquisition dates in autumn 97 and spring 98) in ERS backscatter as a function of growing stock volume.*

Examination of ERS backscatter coefficient versus growing stock volume established at all the test sites revealed that in general the noise observed in the experimental plots is much higher than in Fig. 2.19. This is illustrated by Fig. 2.21, in which the relationship of intensity with growing stock volume is obscured by topographic effects. Other sources of error may include misregistration of the GIS forest database and the radar image, and distortion of the radar backscatter coefficient as a function of the local incidence angle.

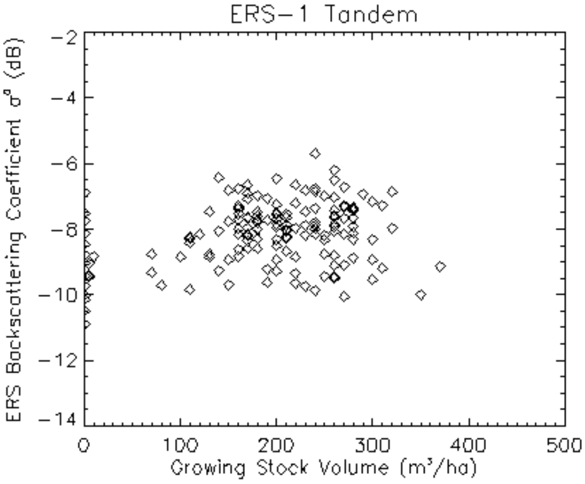

Fig. 2.21 Illustration of the influence of topography on the experimental ERS intensity vs. growing stock volume relationship.

JERS Intensity Versus Growing Stock Volume

In Fig. 2.22, a scatterplot of JERS intensity vs. growing stock volume shows the expected increasing trend with growing stock volume. The saturation level occurs at a higher total volume level (>100 m^3/ha) when compared to ERS data and is associated with a higher backscatter value (-5 dB to - 6.5 dB). The standard deviation around the mean curve is also higher, e.g. caused by the effect of species composition as previously discussed. However, the sensitivity to biomass is about 2.5-3.5 dB for the range of 0-100 m^3/ha growing stock volume.

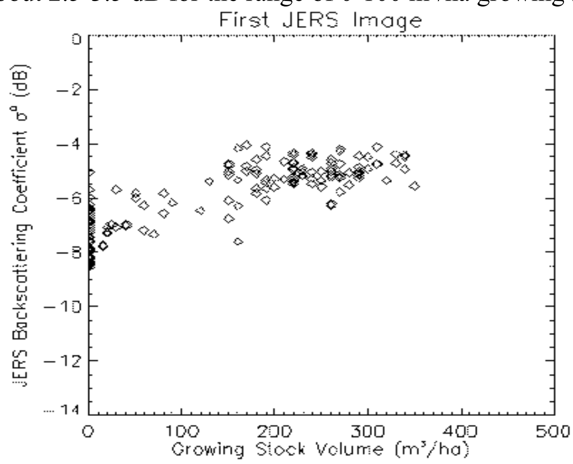

Fig. 2.22 Illustration of JERS backscatter as a function of growing stock volume.

Overall, the results of the analysis show that the experimental curves for JERS-1 have a higher between-frame variability than the ERS curves due to (1) less stability in JERS data and (2) to the effect of environmental conditions on low biomass areas. However, JERS has a higher dynamic range in backscatter as a function of stand volume than ERS.

Coherence Versus Growing Stock Volume

Fig. 2.23 shows various examples of the coherence versus growing stock volume. The examples include coherence estimated from polygons of more than 50 pixels and polygons containing 20 to 50 pixels, in order to observe the effect of the polygon size.

In general, the data points show the following characteristics:

1. a marked decreasing trend in coherence as function of growing stock volume due to a decreasing temporal correlation with increasing number of leaves, needles, twigs, small branches in the canopy
2. an important overall dynamic range as a function of stem volume, especially over the range of 0 to 100 m^3/ha. Above this threshold tandem coherence is relatively insensitive to stand volume. An illustration of high and low coherence classes is given in Fig. 2.24.

The relationships can be fitted by declining exponential functions, with the most steeply decreasing part being in the range of 0-100 to 130 m^3/ha, above which the coherence variation becomes insignificant.

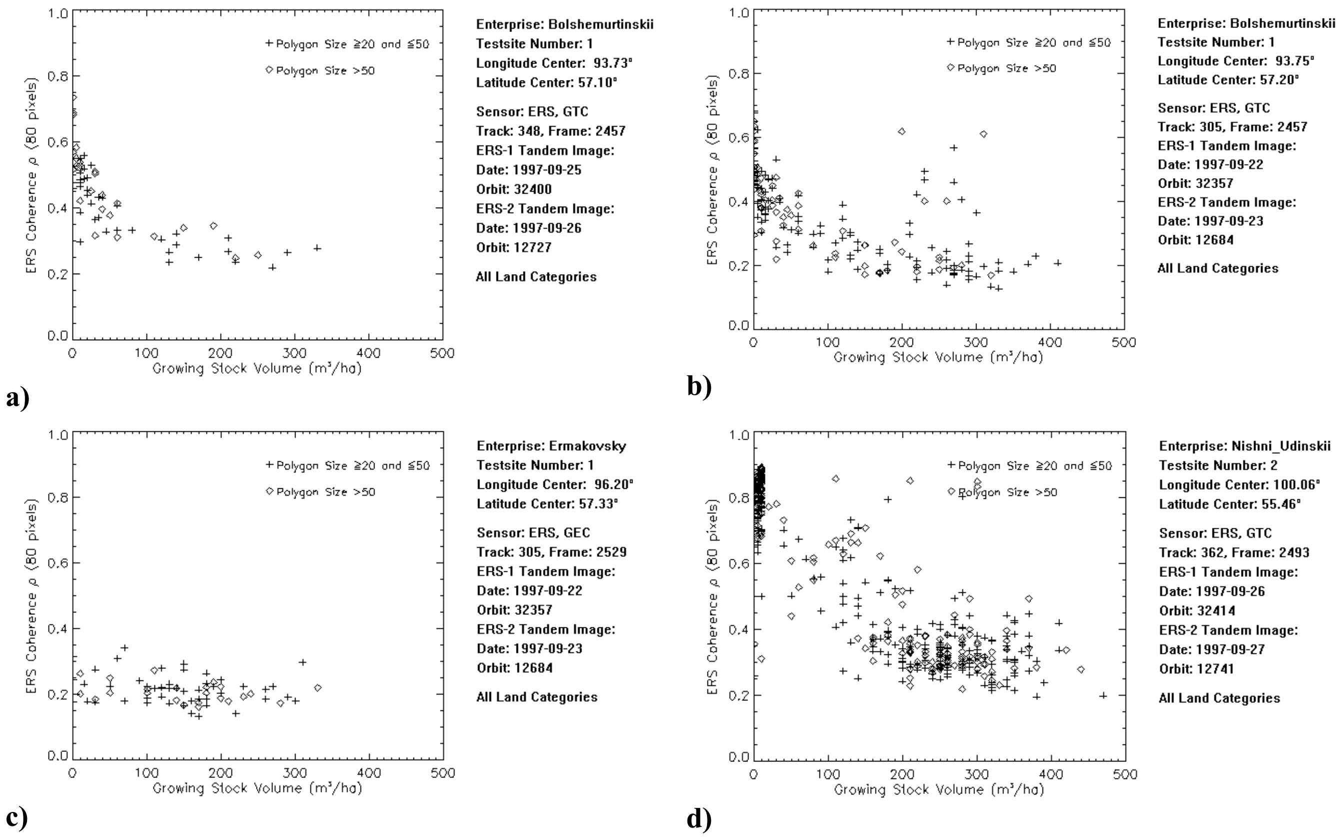

Fig. 2.23 Plots of tandem coherence vs. stand volume for different forest enterprise sites.

Fig. 2.24 Illustration of high coherence (left) and low coherence (right) forest stands associated with low and high stand volume levels respectively.

The above plots of coherence illustrate the fact that the data points for a given test site can present important scattering around the mean curve due to different causes:

- small polygon size; the figures show that polygons >50 pixels have a slightly reduced standard deviation. However, polygons of size >20 pixels were found a good trade-off to include a maximum number of stands in the analysis,
- out-of-date forest database, which results in outliers in data as illustrated in Fig. 2.23 b, where the high coherence of a number of data points may indicate recent clear-cutting or fire.
-effect of the topography, which results in a severe loss of coherence that is caused by misregistration of the forest database and the radar image (Fig. 2.23c).

At different test sites, different dynamic ranges in coherence can be observed (compare for instance Fig. 2.23a and Fig. 2.23d). Fig. 2.25 illustrates the average coherence values as a function of forest volume class computed on the basis of histograms from the 8 selected test sites. The examples exclude test sites with low coherence data apparently affected by measurement errors or caused by change in environmental conditions between the two tandem dates.

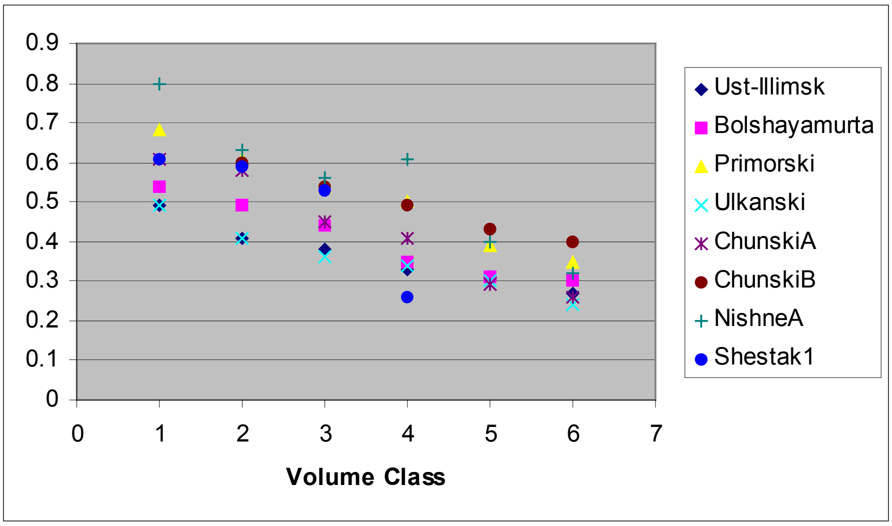

Fig. 2.25 *Average coherence values as a function of forest volume classes. The volume classes 1 to 6 correspond to volume ranges of 0-20, 20-50, 50-80, 80-130, 130-200 and >200 m^3/ha respectively.*

The observed differences are generally due to (1) baseline effects and (2) changes in environmental conditions between acquisitions dates. Since the ERS-1/ERS-2 interferometric baselines lie in a narrow range (100 to 200 m), their effect is relatively small. The change in environmental conditions prevailing at the acquisition time may explain the frame-to-frame variability in coherence.

To verify this hypothesis ERS intensity changes as an indicator of environmental changes between acquisitions are plotted against changes in coherence for 11 partially overlapping ERS image pairs (Fig. 2.26). The observations show that coherence increases with decreasing ERS intensity. While the observed relationship can be interpreted as being due to changes in soil moisture conditions the slope of the relationship is surprising. Previous work in temperate forests indicated that an increase in ERS intensity, corresponding to increasing soil moisture and an increased soil contribution to the total signal, resulted in higher coherence values (Le Toan and Floury, 1998). Here the contrary is observed. To fully understand the relationship between coherence and scene intensity, simulation by theoretical modelling is necessary. This could be an objective of further research work.

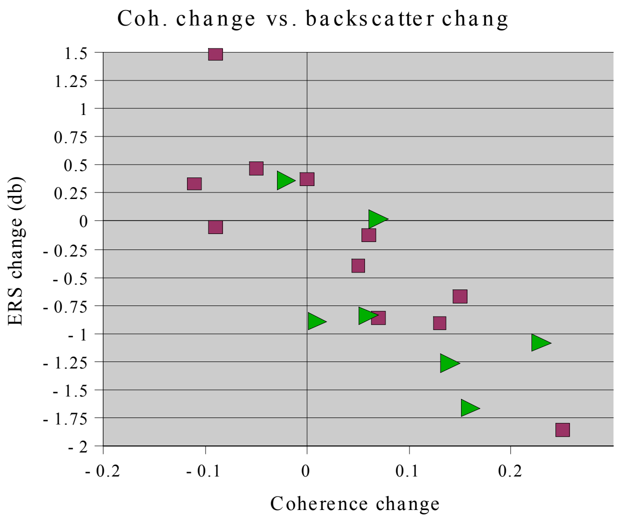

Fig. 2.26 Plots of change in ERS intensity vs. change in coherence for adjacent and overlapping frames. The data points in red represent the changes in mean value of ERS intensity and coherence, between one date and the other. The green triangles represent mean values of the overlapped parts of the images.

For the development of a generalised classification algorithm two approaches are possible. A first approach, adopted in the final classification algorithm, is to make use of image based histogram information to calculate the shifts in the experimental relationships for each frame. In this manner parameters of the SAR vs. stock volume regression are adapted dynamically within each frame to the range and shifts in coherence/intensity vs. growing stock volume relationships present within the frame. A second approach, which is still being explored, is to normalise the coherence curve vs. growing stock volume using ERS intensity.

2.3.2.2.4 Impact on Classification

Based on the examination of the information content of the available SAR data, key information for classification methods can be derived.

SAR Measurements to be Used

From the previous analysis it is clear that the tandem coherence provides most of the information about forest stand volume, whereas ERS and JERS intensity contribute to a lesser degree to the distinction of different biomass classes. However, by analysing a series of images surrounding the test sites, one result of the study was that JERS and to a lesser extent ERS can be used to separate some of the non-forest classes visible in many of the frames. An important result of the study is the selection of coherence and JERS data as classifying variables. Data with severe loss of coherence caused by strong relief and by drastic change in environmental conditions between the tandem acquisitions should not be included.
The advantage and inconvenient of the three types of SAR information in discriminating different land cover and forest volume classes can be cross compared and summarised in the following way:

ERS Tandem Coherence	higher contrast between forest/non forest, higher sensitivity to forest volume, confusion in water, dense forest loss of coherence at high relief frame to frame variation
JERS intensity	medium dynamic range, higher frame to frame variation good separability of forest and water surfaces good separability of agriculture fields less effect of relief (35°)
ERS intensity	small dynamic range, variable- response of water, variable response of open area, strong effect of relief (23°), indicator of environmental effect that can be used for normalising coherence

0 shows an example of ERS intensity, JERS intensity and ERS coherence images for a subsection of the Shestakovsky test site.

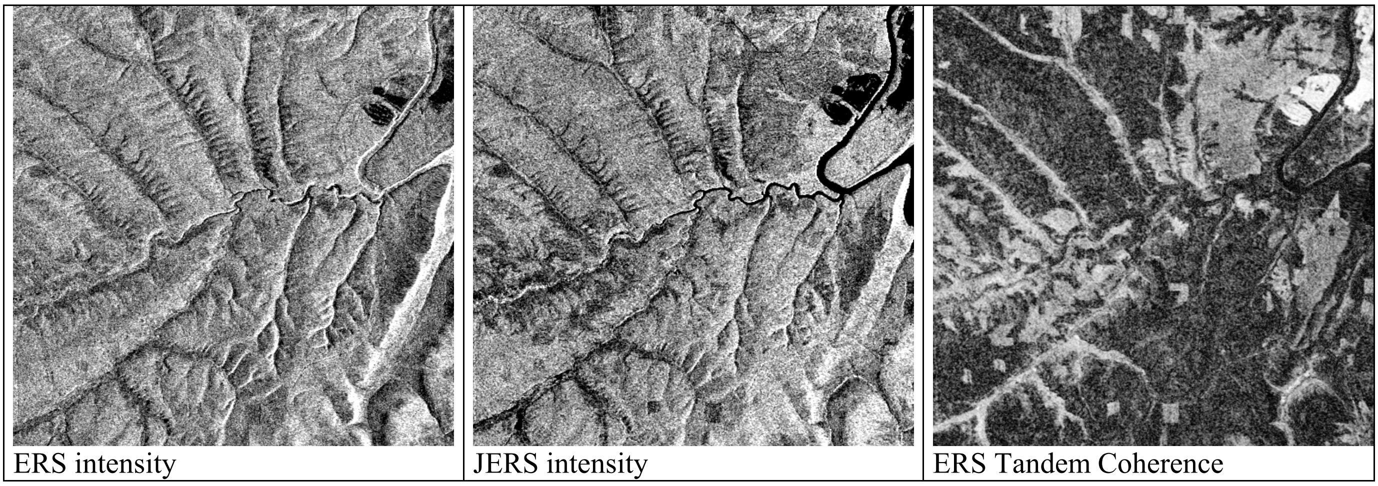

Fig. 2.27 *ERS and JERS intensity and ERS coherence images for the Shestakovsky test site (Frame 32600_2457). High / low biomass areas more visible in coherence image, water well distinguished in JERS image, less topographic effect in ERS image.*

Label and Number of Forest and Non-forest Classes

In order to derive a consistent set of classes, applicable to the classification of all frames, an intensive analysis of the frames where forest data were available was carried out. The analysis was done using both the quantitative information provided by the forest databases as well as visual interpretation of the non-forest land-use classes. The main results of our analysis are expressed in terms of ERS coherence and JERS intensity information, which provides the bulk of the information needed in the final classification scheme.
For non-forest classes the ERS coherence and JERS intensity of the main land-use classes are analysed. In general the non-forest classes were grouped into two classes depending on their radar signatures: 1) smooth surfaces, which include agricultural fields and bogs and are characterised by high coherence and JERS intensity and 2) inland water, which is characterised by low coherence and JERS intensity.
To obtain a more synthetic representation of the class signatures, two-dimensional scatterplots of JERS intensity and ERS coherence were generated for each frame. A typical result is given in Fig. 2.28(left). Examination of all such scatterplots gives rise to a general interpretation given in Fig. 2.28(right).

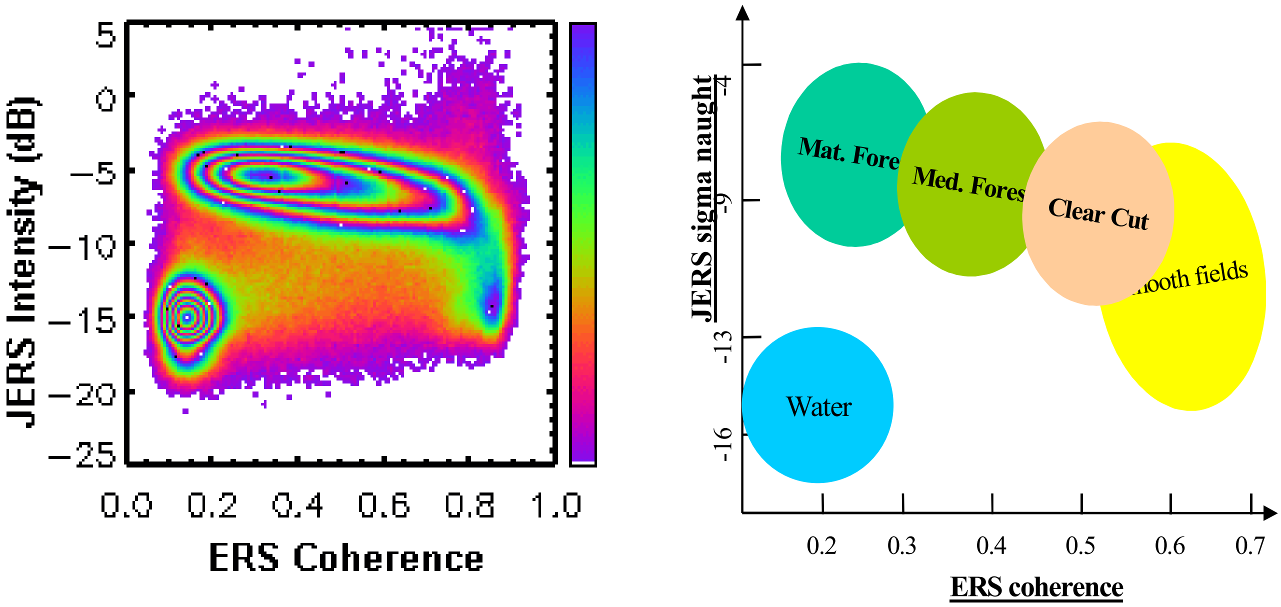

Fig. 2.28 Histogram of JERS intensity vs. ERS coherence (left) and interpretation of clusters (right).

There is a clear separation between water and the other categories and to a lesser extent between smooth fields and the various forest volume classes. Since the signatures of water and smooth areas proved to be relatively stable from frame to frame, statistical parameters of each class (mean and standard deviation) could be obtained through an analysis of a sufficient number of frames and used directly in the final maximum likelihood classification algorithm.
On the other hand the different forest volume classes occupy a continuous spectrum of coherence and JERS intensity values. The forest database provided values of growing stock volume which were regrouped in the data analysis in classes of 0-20, 20-50, 50-80, 80-130, 130-200 and >200 m^3/ha. Analysis of class separability based on assumption of Gaussian distributions characterised by mean values and standard deviation of coherence and JERS intensity suggests the following three classes: 0-20, 20-80, >80 m^3/ha; or four classes: 0-20, 20-50, 50-80 and >80 m^3/ha. In the second case, the accuracy of classification results for the two middle volume classes of 20-50, 50-80 m^3/ha is expected to be lower. The low volume class (0-20 m^3/ha) which represents clear-cut, burnt area or young regrowth in the forest is finally regrouped with open areas outside the forest such as bogs, meadows and hayfields, to form a class labelled "open area".
The following table summarises the SIBERIA classes:

Table 2.6 *Classes used by the SIBERIA project.*

SIBERIA classes	Land cover type
Water	River, lake, inland water
Smooth areas	Agricultural fields, river sand bar
Open areas	Bogs, meadows, hayfields, pasture, clear-cut, burnt forest, young regrowth
Forest 20-50 m^3/ha	Forest 20-50 m^3/ha
Forest 50-80 m^3/ha	Forest 50-80 m^3/ha
Forest >80 m^3/ha	Forest >80 m^3/ha

Statistics of non-forest classes used in SIBERIA classification are as follows:

Non- forest Class	*Coherence*	*Coherence StDev*	*JERS intensity*	*JERS intensity StDev*
Water	0.16	0.04	-17 dB	1.8 dB
Smooth fields	0.78	0.08	-14.5 dB	1.3 dB
Open areas	0.68	0.10	-7.8 dB	2.5 dB

For forest classes, statistics obtained from the analysis of selected test sites are as follows:

Forest Class	*Coherence*	*Coherence StDev*	*JERS intensity*	*JERS intensity StDev*
Forest 20-50 m^3/ha	0.52	0.08	-7.2 dB	1.4 dB
Forest 50-80 m^3/ha	0.42	0.06	-6.2 dB	1.5 dB
Forest >80 m^3/ha	0.30	0.06	-5.6 dB	1.3 dB

The above statistics can be used in the classification, e.g. maximum likelihood method. However, since coherence and JERS intensity values fluctuate from one frame to the next, the border effect in the classification could be important, in particular between forest classes of adjacent frames. A classification method must be chosen that is adapted to continuous growing stock volume classes without well-defined boundaries between classes and able to take into account the frame-to-frame fluctuations in the relationships between ERS coherence and JERS intensity data with growing stock volume.

2.3.2.3 Classification Procedure

After terrain correction and masking, the images were subject to the sequence of operations indicated in Fig. 2.29.

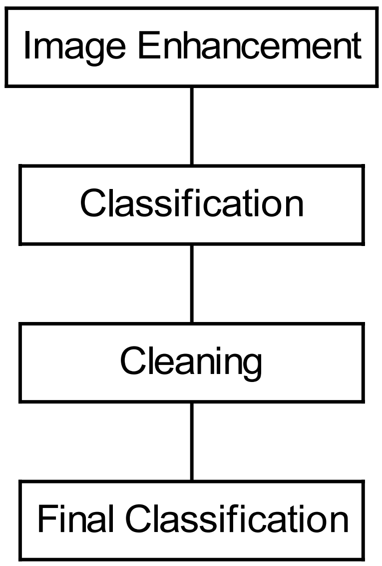

Fig. 2.29 *Sequence of image operations leading to classified image*

These operations are described in this section, following an introductory discussion of basic image properties that affect the processing. Note that Section 2.3.2.2 has indicated that most of the useful information in the SIBERIA radar dataset is carried by the ERS coherence (γ) and the JERS intensity ($\sigma°$). Hence the classification is based on just these two quantities, and the classification problem can be formulated as:
"How do we split up the $\gamma/\sigma°$ plane and assign the regions to physical classes of interest to (Russian) foresters?"

2.3.2.3.1 Image Properties

The images in the SIBERIA dataset were examined for three important image properties: texture, equivalent number of looks (ENL) and spatial correlation.

Texture

The presence of texture was investigated for two reasons:

- Textured data should be filtered using methods based on the *k*-distribution, whereas untextured data require filters developed for a Gamma distribution;
- Texture could be utilised as an aid to classification if it varies with the type of land cover.

The normalized log measure, defined as $T = \langle \ln I \rangle - \ln\langle I \rangle$, where *I* is intensity, provides a sensitive texture measure with better statistical properties than the more widely-used coefficient of variation (Oliver and Quegan, 1998). Fig. 2.30 shows images of *T*, estimated using a 5x5 window, for images of the Bratsk test site acquired by ERS on 23/9/97 and by JERS on 4/5/97. The following can be observed:

1. The texture images show little structure, except where edges cause significant contrast in the processing window;
2. At the steeper incidence angle of ERS, many of these 'texture' features are caused by topography;
3. The overall higher contrast of JERS causes more features and lines to be picked out. These do not correspond to stand information or land classes, but are almost all edge effects due to intensity changes between adjacent areas.

Hence, at the 50 m resolution of the images used in SIBERIA, the images are untextured, so that the data analysis methods can be based on a simple Gamma distribution for speckle.

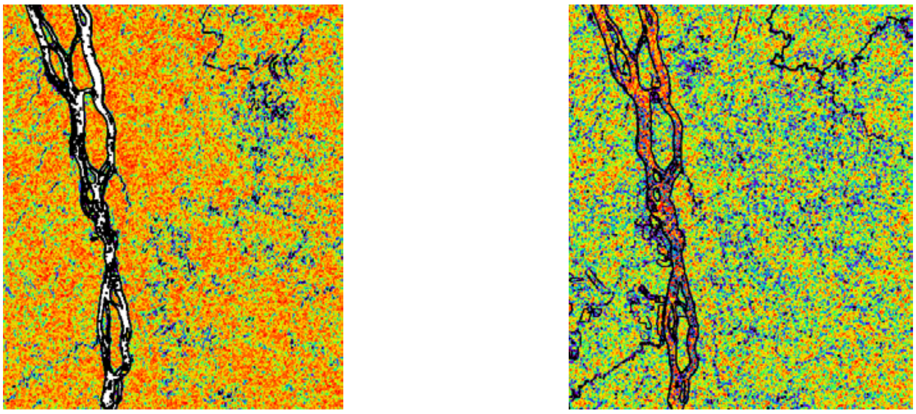

(a) (b)

Fig. 2.30 *Measurements of normalised log for (a) ERS and (b) JERS, estimated using a 5x5 window.*

Equivalent Number of Looks (ENL)

The ENL is defined as $\langle I \rangle^2 / \mathrm{var}(I)$, where $\langle I \rangle$ is the mean and var(*I*) is the variance of intensity. For Gamma distributed data, this is equal to the order of the distribution. It measures the spread of the data due to speckle, hence affects the classification accuracy. To determine its value in our original datasets, three visually homogeneous areas were selected from the ERS and JERS intensity images shown in Fig. 2.30. Table 2.7 shows the estimated values of $\langle I \rangle$ and var(*I*), denoted by $\hat{I}$ and *V*(*I*), for each area, with the corresponding estimates of ENL in the last column. Fits of the data to Gamma distributions indicate an ENL of around 15 for ERS and 6 for JERS. Such low values of ENL are inadequate for most classifications since they imply low accuracy in estimating backscatter. As a result, the ENL needs to be increased by filtering.

Table 2.7 *Estimated mean, variance and ENL from homogeneous areas in intensity images of ERS and JERS of the Bratsk test site.*

Data	Sample	Window size	$\hat{I}$	$V(I)$	ENL
ERS intensity of the Bratsk test site on 23/9/97	(a)	4080	0.1695	0.0018	15.74
	(b)	6229	0.1723	0.0022	13.63
	(c)	2285	0.1226	0.0012	13.06
JERS intensity of the Bratsk test site on 4/5/97	(a)	4080	0.4799	0.0037	6.18
	(b)	6229	0.4304	0.0445	4.17
	(c)	2285	0.3592	0.0301	4.28

Spatial Correlation

Spatial correlation reduces the number of independent samples in a window, and significantly affects many filters and analysis techniques, which often assume uncorrelated data. Estimated autocorrelations in the range and azimuth directions, denoted by ρ_r and ρ_a, are plotted as functions of lag in Fig. 2.31 for a mature forest stand in the Bratsk images. The different plots correspond to ERS intensity, JERS intensity and coherence images generated using both 80 and 20 pixel processing windows. The important points to note are:

- The ERS data are significantly correlated, with both ρ_r and ρ_a having values around 0.5 at lag 1 and 0.2 at lag 2;
- The JERS data are almost uncorrelated, with correlation coefficients less than 0.2 at all non-zero lags in both range and azimuth directions;
- For the coherence images, the correlation is not significant except at lag 1 in 80-pixel coherence, where ρ_r and ρ_a are both close to 0.5.

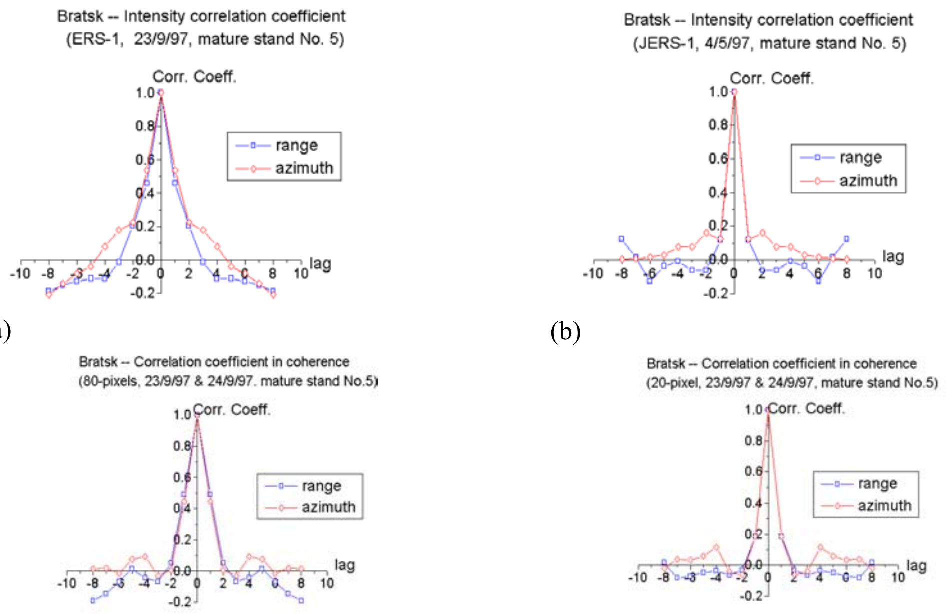

(c) (d)

Fig. 2.31 *Correlation coefficients calculated in the range and azimuth directions for a mature forest stand selected from the Bratsk images: (a) ERS intensity (b) JERS intensity (c) 80-pixel and (d) 20-pixel coherence.*

2.3.2.3.2 Multi-channel Filtering

The purpose of the filtering is to reduce the speckle in the images before attempting to classify them (Oliver and Quegan, 1998; Bruniquel and Lopes, 1997; Novak *et al.*, 1993). The filtering is achieved by linearly combining *M* intensity images from the same scene to produce *M* speckle-reduced images:

$$J_k(x,y) = \sum_{i=1}^{M} D_{ki}(x,y) I_i(x,y), \quad 1 \le k \le M \tag{6.}$$

where I_i, $i = 1,\ldots,M$, is the intensity value at position (x, y) in channel i out of M registered channels, and D_{ki} are weighting coefficients. These images will be unbiased and with minimum variance (hence minimum speckle) if (Quegan *et al.*, 2000[a])

$$\boldsymbol{D}_k^t = \sigma_k \frac{C^{-1}\boldsymbol{\sigma}}{\boldsymbol{\sigma}^t C^{-1}\boldsymbol{\sigma}} \tag{7.}$$

where $\boldsymbol{D}_k$ is the k^{th} row of the coefficient matrix, with ^{t} denoting transpose, C is the intensity covariance matrix, $C(i,j) = \langle (I_i - \sigma_i)(I_j - \sigma_j) \rangle$, and $\boldsymbol{\sigma} = (\sigma_1, \sigma_2, \ldots, \sigma_M)^t$ is the vector of mean intensities in the M images. The ENL of every J_k image is then given by (Quegan *et al.*, 2000[a])

$$\text{ENL} = \boldsymbol{\sigma}^t C^{-1} \boldsymbol{\sigma}. \tag{8.}$$

This filtering approach can be applied to the registered, mixed data types used in SIBERIA. Fig. 2.32 (a, b) show original ERS-2 and JERS images of the Bratsk area. The effect of filtering them in combination with one ERS Tandem pair and another JERS image from the 44-day repeat cycle, using a window size of 5 x 5 pixels, is shown as Fig. 2.32 (c, d). The improvement in quality is clear. Note also that the multi-channel filtering preserves resolution while reducing speckle. As a result, small features hard to distinguish in (a, b) are revealed in (c, d), for example, the short diagonal lines to the right of the river in the lower part of the image.

The degree of speckle reduction in the JERS image appears greater than in ERS. This is what we would expect from (Eq. 8), since the ENLs of the unfiltered images are around 15 for ERS and 6 for JERS, so that the gain in ENL is much greater for JERS. This is confirmed using ENLs measured from two visually homogeneous regions in the images. In Table 2.8, the ENLs measured on filtered images resulting from different input combinations are listed, with Experiment 4 corresponding to the results shown in Fig. 2.32. After filtering, all the images have similar, increased ENL; in Experiment 4, this is greater than 40. Experiment 3 corresponds to the actual SIBERIA data combination, suggesting increased ENLs of around 38.

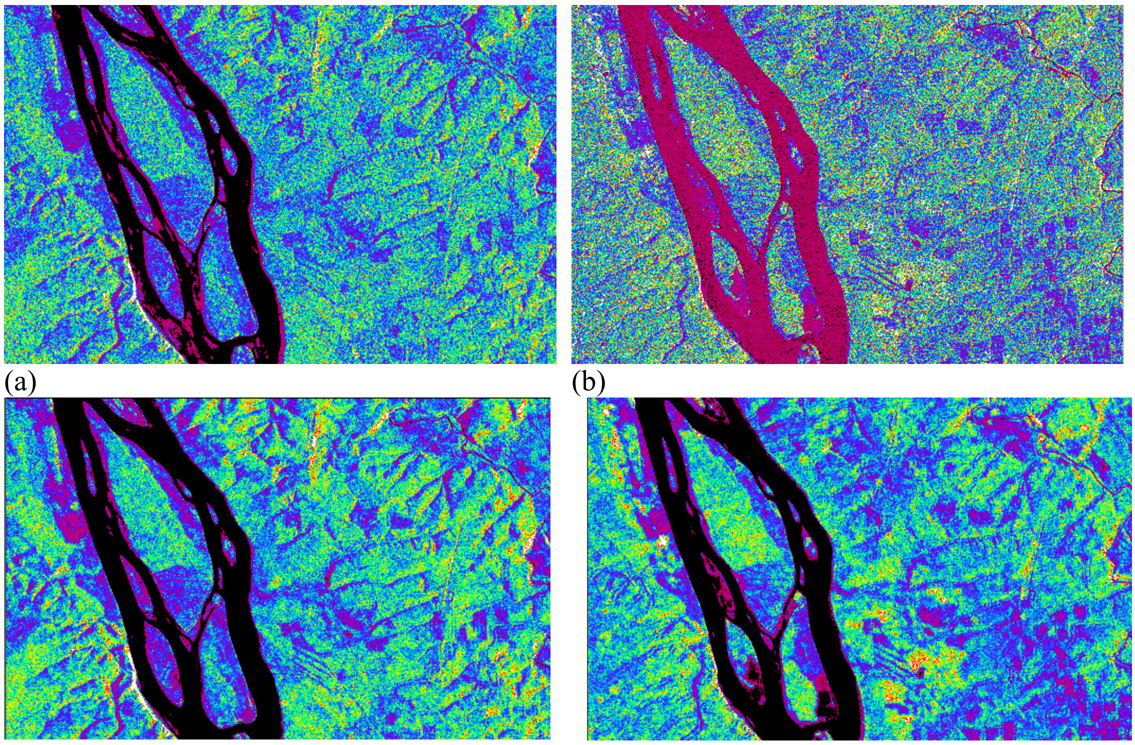

Fig. 2.32 *Bratsk: (a) original ERS-2 acquired on 24/9/97; (b) original JERS acquired on 4/5/97; (c) filtered version of (a); (d) filtered version of (b). Look-up Table = Pseudo-Colours.*

Table 2.8 *ENL measurements on filtered images using different combinations of inputs. All ENL values are rounded to integers. E1 = ERS-1, 23/9/97; E2a = ERS-2, 24/9/97; E2b = ERS-2, 27/5/98; J1 = JERS-1, 4/5/97; J2 = JERS-1, 31/7/97*

Exper. no.	Input images					Area no.	ENLs in filtered images				
	E1	E2a	E2b	J1	J2		E1	E2a	E2b	J1	J2
1	✓	✓				1	26	26			
						2	23	24			
2	✓	✓	✓			1	34	35	35		
						2	31	33	34		
3	✓	✓	✓	✓		1	37	38	37	39	
						2	36	38	39	41	
4	✓	✓	✓	✓	✓	1	39	40	40	41	38
						2	39	41	42	46	41
5		✓	✓	✓	✓	1		32	32	33	31
						2		36	36	38	35
6			✓	✓	✓	1			23	24	23
						2			25	26	24
7				✓	✓	1				11	11
						2				11	11

2.3.2.3.3 Classifications

Once the data were filtered (and the 80-pixel coherence data were 3×3 averaged), the dataset was ready for classification. As discussed in Section 2.3.2.2, classification is based only on coherence and JERS intensity, so that the problem is to assign regions in the γ / σ^0 plane to land cover classes. Fig. 2.33 also indicates that, in the γ / σ^0 plane, there are certain well-defined behaviours. Water exhibits low coherence and low backscatter, smooth surfaces have high coherence and low backscatter, and the vegetation classes are distributed in a cigar-shaped cluster with a weak negative slope (because σ^0 decreases as γ increases). This cigar-shaped cluster conceals characteristic relations between stock volume (or biomass) and both coherence and backscatter. In particular, coherence tends to decrease and JERS backscatter tends to increase as biomass increases. Hence, by partitioning this cluster we can attempt to extract the classes discussed earlier (Table 2.6).
Several different approaches were developed to try to solve this problem. Below we describe the main approaches that were assessed, before explaining the reasons for our final choice. Examples of the output from each approach are grouped together in Fig. 2.39.

Maximum Likelihood with Refined Class Statistics

This classification approach uses the results of data analysis in a maximum likelihood algorithm based on a multi-dimensional Gaussian model for the data. In this model, the likelihood that pixel $\mathbf{x}$ belongs to class c is given by

$$p\{\mathbf{x} \mid c\} = \frac{1}{(2\pi)^{K/2} |\mathbf{C}_c|^{1/2}} \exp\left(-\frac{1}{2} (\mathbf{x} - \boldsymbol{\mu}_c)^t \mathbf{C}_c^{-1} (\mathbf{x} - \boldsymbol{\mu}_c) \right) \tag{9.}$$

where $\mathbf{x}$ is a data vector, containing the values in the K input channels, ^{t} denotes transpose, $\boldsymbol{\mu}_c$ is the mean vector of class c, $\mathbf{C}_c$ is the covariance matrix of class c and $|\cdot|$ denotes determinant (Devijver and Kittler 1982). In our case K=2 since only coherence and JERS backscatter are used as inputs.

The means and standard deviations of the forest classes were defined from analysis of ERS coherence and JERS backscatter coefficient versus growing stock volume for all the frames. This followed a comprehensive assessment of the image and ground data. In particular, the whole of the forest database was examined in order to retain only those combined datasets that could be regarded as physically meaningful. Data with errors due to data registration, topographic effects, non-updated forest data, etc., were discarded. Non-forest classes were defined mainly by interpretation of the SAR images and examination of γ / σ^0 scatterplots.

Using these class statistics, the likelihood that a given pixel belongs to each class is computed and the pixel assigned to the most likely class. A posteriori probabilities and second-to-least probable classifications are also stored by the program and used subsequently within the ICP algorithm (see Section 2.3.2.3.4). After applying the classification algorithm on all the GTC and GEC scatterplots present on the Web, the statistics of the classes were plotted (see Fig. 2.33 for examples) and compared to the initial statistics. This comparison, in combination with physical reasoning, was used to refine the statistics of the classes, in particular the non-forest classes (water and open areas). Final class statistics are given in Table 2.9.

Table 2.9 *Mean and standard deviation of the ERS coherence and JERS backscatter coefficient of the 6 classes, used in the maximum likelihood algorithm.*

Class	$\langle \gamma \rangle$	St Dev (γ)	$\langle \sigma^o \rangle$	St Dev (σ^o)
1. Water	0.16	0.04	-17 dB	1.8 dB
2. Smooth fields	0.78	0.08	-14.5 dB	1.3 dB
3. Open areas	0.68	0.10	-7.8 dB	2.5 dB
4. Forest 20-50	0.52	0.08	-7.2 dB	1.4 dB
5. Forest 50-80	0.42	0.06	-6.2 dB	1.5 dB
6. Forest >80	0.3	0.06	-5.6 dB	1.3 dB

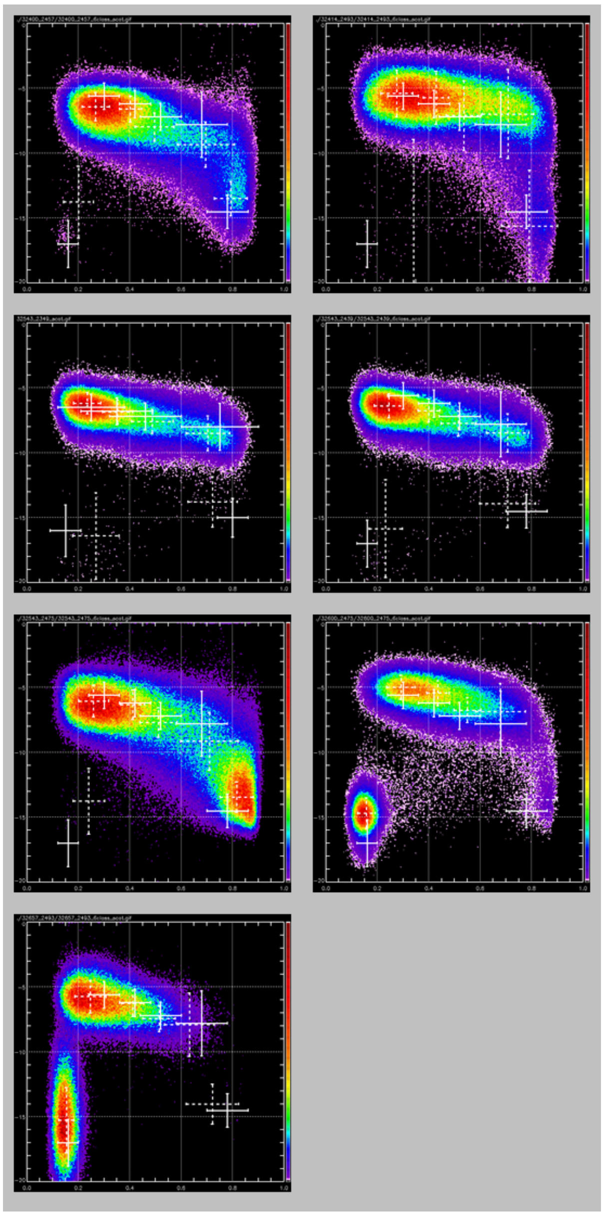

Fig. 2.33 *ERS coherence (horizontal axis) versus JERS backscatter coefficient (vertical axis) scatterplots for 7 different frames. Full crosses: mean and standard deviation of the classes used in ML classification. Dashed crosses: statistics of the 6 classes, after classification. This graph shows that when applying the same statistics to different data frames of SIBERIA, the results are acceptable in terms of accuracy. However, for adjacent frames with very different ERS coherence and JERS values, border effects may remain after classification.*

The Gaussian approximation to the class distributions was also qualitatively assessed, using histograms derived from the synthesis of polygons from the database for forest classes, and from manual selection of polygons for non-forest classes.

ISODATA Classification

An unsupervised, iterative approach to classification based on a version of the ISODATA algorithm (Quegan *et al*. 2000[b]) was developed and assessed. Given an initial classification, the class statistics (the $\mathbf{C}_c$ and $\boldsymbol{\mu}_c$ in Eq. 9) can be estimated and used to re-classify the pixels. This process is continued for a fixed number of iterations or until the proportion of pixels changing class falls below a user-specified threshold. As with ordinary maximum likelihood, this approach can be readily followed by the ICP algorithm (Section 2.3.2.3.4), which requires likelihood images as input (Balzter *et al*., 2000).

The ML approach assumes equal probability of all classes occurring, but unequal prior probabilities can be taken into account by using Bayes theorem to calculate the posterior probabilities:

$$p\{c \mid \mathbf{x}\} = \frac{p\{c\}p\{\mathbf{x} \mid c\}}{p\{\mathbf{x}\}} \tag{10.}$$

Here $p\{c\}$ is the prior probability of class *c*; $p\{\mathbf{x} \mid c\}$ is the likelihood and $p\{\mathbf{x}\}$ can be regarded as a normalising constant. The maximum a posteriori (MAP) algorithm assigns each pixel to the class with the largest posterior probability, in principle giving a better classification. It corresponds to ML if all the posterior probabilities are equal. However, the priors can be estimated from the data (as relative frequencies) once a classification has been carried out. This refinement is easily included in the iterative ISODATA algorithm: Each successive classification provides the priors needed for the next. Such an approach has been described in the context of polarimetric SAR data in Van Zyl and Burnette (1992). Notice also that this step can readily be used after an initial ML classification. This refinement helps to prevent diffuse clusters being eroded by more compact clusters during the iteration process.

Two methods were considered for providing the initial classification for ISODATA. In one, the γ / σ^0 plane was partitioned using simple rules based on the observed properties of scatterplots such as that shown in Fig. 2.33. In the second, the class centres and standard deviations specified in Table 2.9 were used to carry out an initial ML classification, ignoring correlation between channels. This is equivalent to simple maximum likelihood classification, ignoring correlation between channels.

Classification Based on Empirical Coherence and Backscatter Models

This algorithm concentrates on the structure in the cigar-shaped vegetation cluster (see Fig. 2.33). Scatterplots of the ERS coherence, γ, versus growing stock volume, *v,* were produced for all test sites. Typically, for test sites where the scatter is not too large, an approximately exponential relationship between γ and *v* is evident, as shown in Fig. 2.34. The data were therefore fitted by an exponential model of the form:

$$\gamma(v) = \gamma_\infty + (\gamma_0 - \gamma_\infty) \cdot e^{-\frac{v}{V_\gamma}} \tag{11.}$$

where γ_0 is the coherence at $v = 0$ m^3/ha (non-forest), γ_∞ is the coherence for asymptotic values of *v* (corresponding to dense forest) and V_γ is the characteristic *v* value where the exponential function has decreased by a factor e^{-1}. Deviations from this model were attributed to mainly to topographic effects, strong rainfall between the ERS tandem acquisitions, and errors in the forestry database.

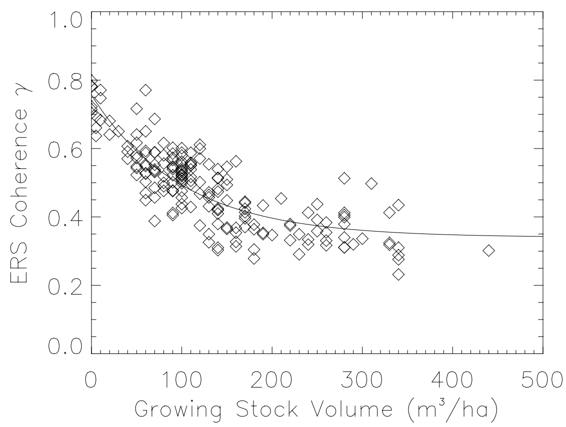

Fig. 2.34 *Observed and modelled relationship between ERS coherence and growing stock volume for Primorsky (102°E, 55.7°N).*

With a few exceptions, the estimated model parameters lie within the expected range. For example, V_γ was found to vary from about 40 to 250 m^3/ha, with a mean value of around 100 m^3/ha. However, the confidence intervals were large, indicating the need to reduce the number of degrees of freedom in the model. Since V_γ is much more stable than either γ_0 or γ_∞, it was set equal to its mean value. The confidence intervals of the estimated γ_0 and γ_∞

then decreased, while the standard deviation of the residuals remained more or less the same. Fig. 2.35 shows the estimated γ_0 and γ_∞ values. These vary over a large range, γ_∞ from about 0.2 to 0.5, and γ_0 from 0.2 to 0.8. It is likely that some of the unexpectedly high values of γ_∞ are caused by the age of the forest database (e.g. if the forest burnt between the inventory year and the ERS SAR acquisition). However, the strong influence of imaging characteristics and environmental conditions is clear. This variability must be accounted for if coherence is to be used consistently for estimating growing stock volume.

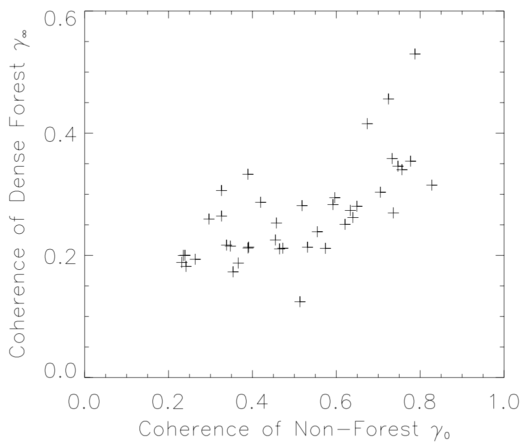

Fig. 2.35 *Coherence of non-forested areas versus coherence of dense forest.*

Mean JERS σ^0 values were also calculated and plotted against growing stock volume. Even though the scatter of σ^0 is large for all test sites, the analysis indicated the expected positive correlation between σ^0 and v for forests of biomass up to about 200 m^3/ha (Fig. 2.36). As with coherence, an exponential function is used to describe this relationship:

$$\sigma^0(v) = \sigma_\infty + (\sigma_0 - \sigma_\infty) \cdot e^{-\frac{v}{V_\sigma}} \tag{12.}$$

where σ_0 and σ_∞ are respectively the backscatter coefficients at v = 0 m^3/ha (non-forest) and for asymptotic values of v (dense forest), and V_σ is the value of v at which the exponential function has increased by e. Other authors have used different models (Luckman et al, 1997; Fransson and Israelsson, 1999) but overall they behave similar.

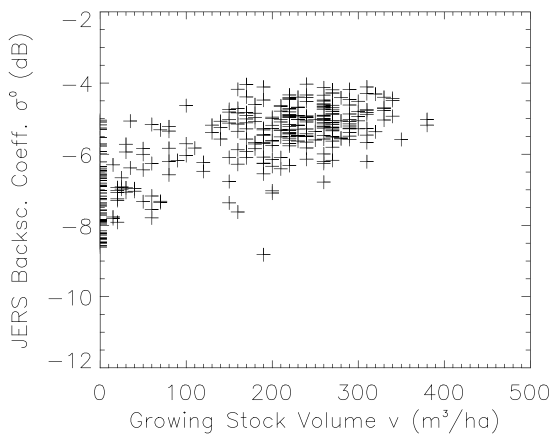

Fig. 2.36 *Scatterplot of JERS backscatter coefficient σ^0 versus growing stock volume for a test site located in the Irbeisky forest enterprise centred around 55.25°N, 96.08°E.*

The class centres of the selected forest classes can be determined from the models in Eq. 11 and Eq. 12 if the model parameters are known. For satellite scenes that cover one of the test sites, estimates of these parameters could be determined from the database, but for most scenes no reference data are available. Therefore it was necessary to identify image properties that allow the model parameters to be estimated in the absence of ground data.

Data analysis and simulations established that reasonable estimates of γ_∞ and σ_∞ can be derived from the coherence and backscatter coefficient histograms. The histogram parameters were denoted by γ_{75} and σ_{75} and represent those values where the distributions reach 75 % of their maximum value. In determining these estimates, the water class had to be removed from the data. The water mask is generated by classifying all pixels with σ^0 values lower than –12 dB as water. To find γ_0 we use the observation that γ_∞ and γ_0 are to some extent correlated. Hence γ_0 is estimated as

$$\gamma_0 = a_\gamma + b_\gamma \cdot \gamma_{75} \tag{13.}$$

leading to a regression curve for γ of the form

$$\gamma(v) = \gamma_{75} + \left(a_\gamma + (b_\gamma - 1)\gamma_{75}\right) \cdot e^{-\frac{v}{V_\gamma}} \tag{14.}$$

A similar expression was derived for JERS σ^0.

The parameters in these expressions were derived using all the data from the forest enterprises Bolshe-Murtinsky, Nizhne-Udinsky, Chunsky, Primorsky, and Ulkansky. Median γ and σ^0 values of the forest classes for these scenes are shown in Fig. 2.37 and Fig. 2.38.

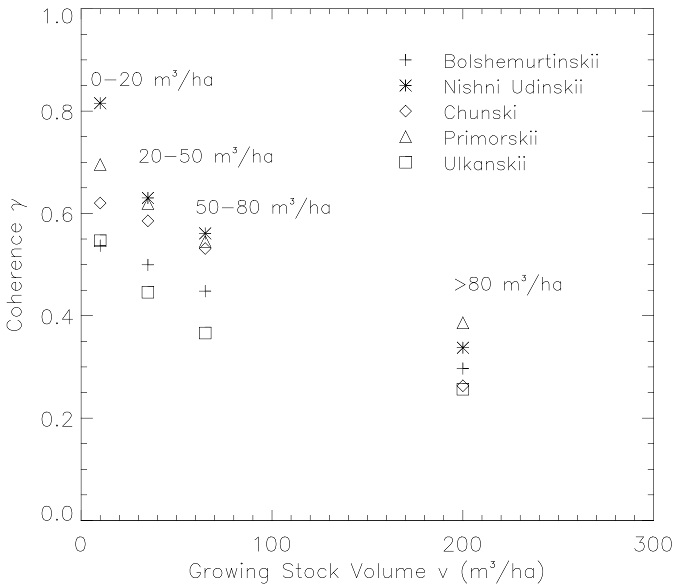

Fig. 2.37 *Median γ values of forest classes 0-20, 20-50, 50-80 and > 80 m^3/ha for five satellite scenes covering the forest enterprises Bolshe-Murtinsky, Nizhne-Udinsky, Chunsky, Primorsky, and Ulkansky. The γ values are plotted versus the mean growing stock volume of each forest class.*

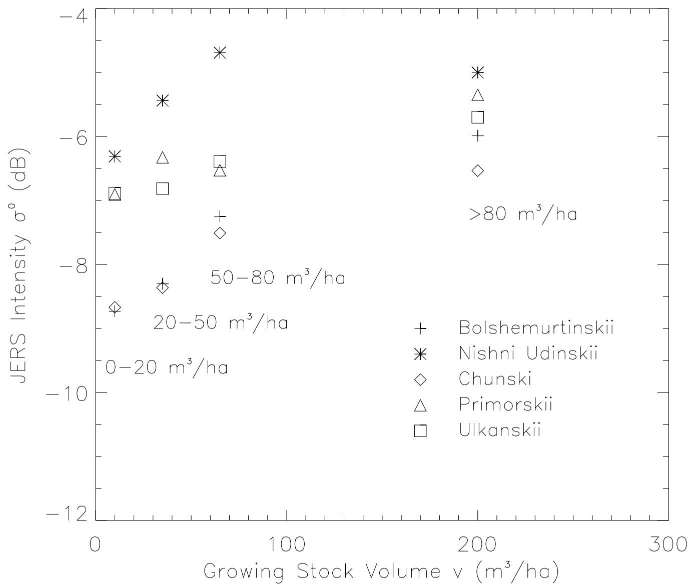

Fig. 2.38 *Median σ^0 values of forest classes 0-20, 20-50, 50-80 and > 80 m^3/ha for five satellite scenes covering the forest enterprises Bolshe-Murtinsky, Nizhne-Udinsky, Chunsky, Primorsky, and Ulkansky. The σ^0 values are plotted versus the mean growing stock volume of each forest class.*

Fitting led to the following results:

$$\gamma(v) = \gamma_{75} + \left(0.330 + 0.581 \cdot \gamma_{75}\right) \cdot e^{-\frac{v}{122.1}} \qquad (15.)$$

and

$$\sigma^0(v) = \sigma_{75} - 2.46 \cdot e^{-\frac{v}{107.34}} \qquad (16.)$$

These models were then used to determine class means for the defined ranges of biomass. In combination with standard deviations taken from Table 2.9, this allowed a Maximum Likelihood classification to be carried out. The classifications were then improved by applying the ICP algorithm.

Summary on Classification

Fig. 2.39 shows examples of the three classification algorithms, with the coherence model in (a), ISODATA MAP in (b) and ML in (c) (The black blocks indicate terrain masking). It can be seen that the classification based on the coherence model assigns more pixels to the classes “Forest 50-80 m^3/ha” and “Forest > 80 m^3/ha” than the other two approaches. The visual resemblance of (b) and (c) is the result of using the same class statistics in Table 2.9 However, there are more smooth surface pixels in (b) than in (c) (caused by the iteration process). The effect of applying ICP (see Section 2.3.2.3.4) to Fig. 2.39 (c) is given as Fig. 2.39 (d), which shows the improved visual quality of the classification.

The ISODATA approach provides an adaptive approach to learning the clusters in an image, and includes the ML and MAP methods as special cases. However, the iterative nature of this algorithm makes it less readily controlled than the single step decisions made in the other algorithms, and clusters could not be guaranteed to be stable. As a result, the adopted classification approach was based on the empirical coherence and backscatter models, combined with the analysis and methods developed to carry out maximum likelihood algorithm based on a full multi-dimensional Gaussian model for the data. The model-based approach allows us to adapt maximum likelihood to the properties of the scene, providing a classification method that can cope with variation between scenes was provided. The classifications were then improved by using the ICP algorithm.

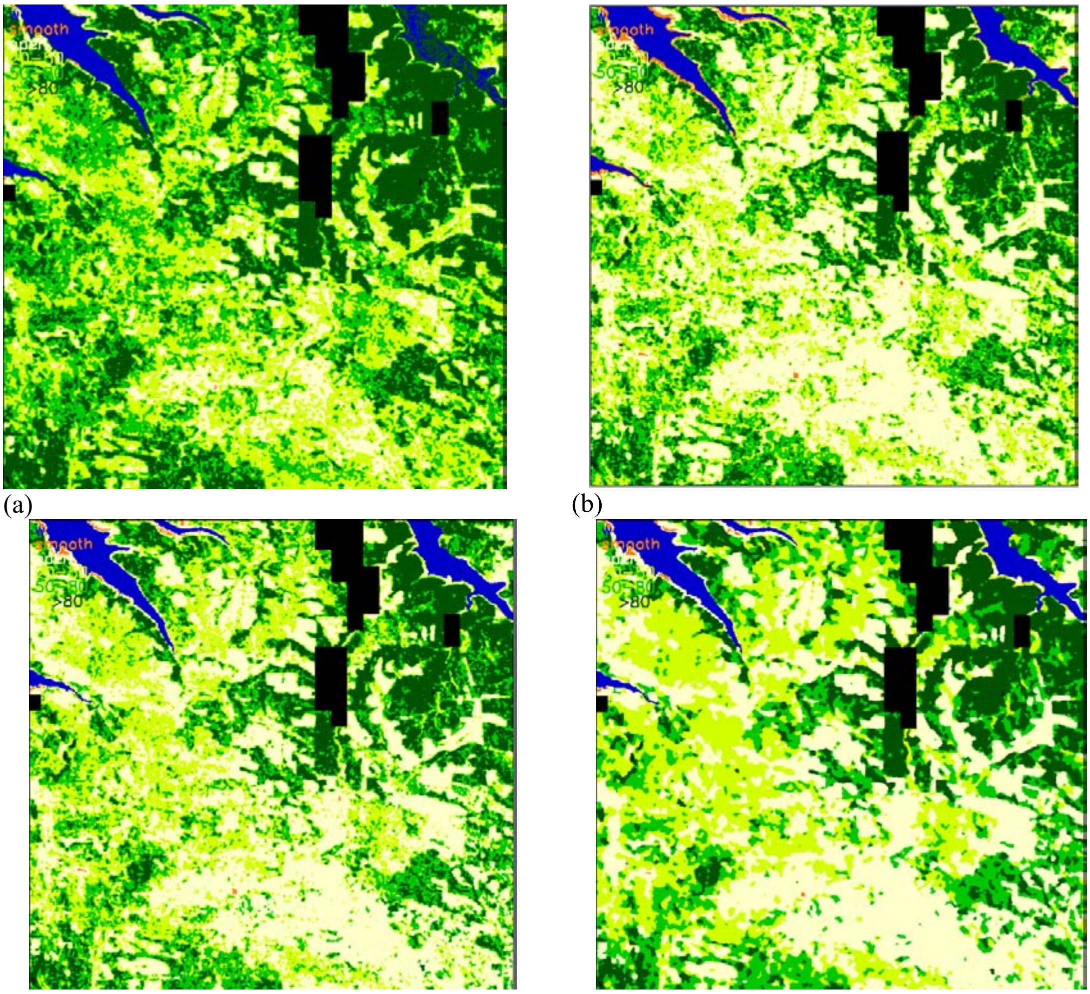

(a) (b) (c) (d)

Fig. 2.39 *Primorsky classifications generated using (a) coherence model, (b) ISODATA MAP, (c) ML and (d) the effect of applying ICP to (c), with high topography areas masked [from the SIBERIA web site].*

2.3.2.3.4 Iterated Contextual Probability Classifier (ICP)

In SAR intensity and coherence images, it is often possible to recognise polygonal shapes that are clearly anthropogenic (see Fig. 2.39). A human observer will always take into account the spatial context of the pixel. However, maximum likelihood classification considers pixels in isolation and makes no use of spatial information. As a result, the variation caused by speckle reduces the distinctness and separability of the forest classes. To incorporate this spatial context into the SIBERIA classification algorithm, we developed the Iterated Contextual Probability classifier (ICP).

This algorithm is based on Bayes theorem, as discussed in Section 2.3.2.4, but now in a spatial context. Given an initial classification (for example, that supplied by ML), the classification is iteratively improved by taking spatial information about the posterior probabilities of each pixel into account. For a window of size $n_\delta = w^2$ pixels, the posterior probabilities of a pixel belonging to a given class are calculated and used as prior probabilities in the next iteration. In addition, the weight of the spatial compared to the spectral information can be adjusted by raising the spatial probabilities to the power β:

$$p_n(c) = \left(\frac{\sum_\delta p_\delta(c|\mathbf{x})}{n_\delta} \right)^\beta \qquad (17.)$$

Here p_n is the prior probability of pixel *n* (where *n* indexes the pixel position) and δ indexes all the pixels in a neighbourhood (of size n_δ) of pixel *n*. The normalisation constant for the probabilities is determined by pixel-wise summation over all products for each class:

$$p(\mathbf{x}) = \sum_c p(\mathbf{x} \mid c) p(c) \tag{18.}$$

Adjustable parameters in this procedure are the window size, the contextual weight and the number of iterations. Parameter values giving good results in the SIBERIA project are $w = 3$, $\beta = 2$, and 3 to 10 iterations.

The performance of ICP was compared with the well-known Iterated Conditional Mode (ICM) algorithm (Besag, 1986). ICP showed a slightly better correspondence to the ground data than ICM at the Ust-Ilimsky test site (Fig. 2.40 left) as measured by the Kappa coefficient, κ, applied to the classification accuracies (see section 2.3.2.4). The computational demands of ICP are illustrated by Fig. 2.40 (right), which shows the mean square change (MSC) in the posterior probabilities, defined as

$$MSC = \frac{\sum_n \sum_k \left(p_{nk}(t) - p_{nk}(t-1)\right)^2}{NK} \tag{19.}$$

where $k = 1,..,K$ is the class, *t* is the iteration and *n* ranges over all the *N* pixels in the image. Most of the changes have occurred after 3 to 4 iterations, so that ICP is not computationally demanding and is applicable over large numbers of images. It was therefore used to improve the quality of the final classification.

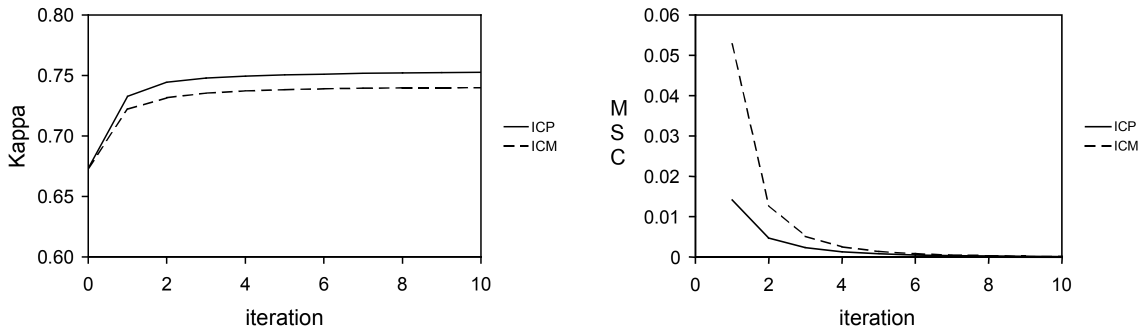

Fig. 2.40 *Left: Change of the weighted κ coefficient of agreement between classifications and ground data over the first ten iterations of ICP as compared to ICM. Iteration 0 is the Maximum Likelihood classification used to initialise both ICP and ICM. Right: Mean square change of a posteriori probabilities during the first ten iterations for ICP and ICM.*

2.3.2.4 Accuracy Assessment

Introduction

The purpose of accuracy assessment is to examine the reliability of a data product, since errors often have cost implications for the user. A frequently encountered problem in accuracy assessment is that the *accuracy* of the map cannot be determined because the reference data have (often unknown) errors. In this case only the *correspondence* of the map to the reference data can be quantified. A traditional accuracy assessment only compares area estimates of land cover types, but more recently the importance of a spatial accuracy assessment has been widely recognised (Lowell and Jaton 2000). This section deals with the definition of methods of accuracy assessment of the classification methodology, and the physical and statistical implications of the methods; the synthesis of the assessment of results on a training test site; an analysis of the implications for large scale mapping; and the development of methods for the accuracy assessment of the large-scale map.

Error Sources and Uncertainties

Some error sources involved in producing maps are related to the imaging process: orbital stability, radiometric accuracy of the sensor, calibration (Shimada 1999), signal-to-noise ratio, viewing geometry of the two SAR sensors for interferometry (mainly the baseline) or changing weather between acquisitions (Gens and Van Genderen 1996, Bamler and Hartl 1998). During image processing, more errors are added: co-registration errors, bias in estimated coherence values (Section 2.2.1.2), geometric differences between ERS-1/2 and JERS-1 in the geocoding, and topographic effects on the radiometry (Dowman 1992). The reference data from the Russian forest inventory is also not error-free. The Russian forest inventory manual requires 15% accuracy (with 95% confidence) for growing stock estimates based on aerial photography. GIS data are provided as rounded values in steps of 5 m^3/ha up to 20 m^3/ha, and in steps of 10 m^3/ha for greater values. But despite these accuracy figures, the total growing stock value of any particular forest stand is an uncertain quantity. Finally, the model for retrieving total growing stock from ERS coherence and JERS intensity (Section 2.3.2.3) introduces errors in the estimations, which increases for larger growing stock. As many as possible of these error sources have to be taken into account when assessing the accuracy of the map product.

Statistical Methods of Accuracy Assessment

In a review of accuracy assessments of land cover maps, Janssen and Van der Wel (1994) stress the importance of making the process of accuracy assessment transparent.
The most important effects on *geometric accuracy* are introduced during

- Co-registration of the complex ERS SAR images prior to interferometric processing (Section 2.2.1.2). Poor co-registration accuracy results in low coherence estimates.
- GIS vector registration to the ERS frame. The root mean square error was usually less than 1.5 pixels.
- Co-registration of JERS to ERS images (Section 2.3.2.1). The different viewing geometries of the two satellites and different DEMs used for geocoding (GTOPO30 and InSAR DEM) cause topography-dependent pixel displacements. The expected displacement in 95% of the image lies between 0 and 3 pixels, and is 1 or 2 pixels on average. A polygon erosion of 2 pixels at the polygon edges was implemented to reduce the resulting errors. The effects of co-registration errors and ground offsets on the estimation of the weighted kappa coefficient, $\kappa_{w,}$ were examined at three test sites and were found to be around 0.1.
- Terrain correction of ERS images to GEC/GTC products (Sections 2.2.1.2 and 2.3.2.1). As anticipated, the classification accuracy of GEC products was poorer than for GTC products.

The methods for assessing *classification accuracy* for different classification algorithms are essentially the same as described for map accuracy below. The coefficients of agreement provide a valuable summary statistic for the choice of the SIBERIA classification algorithm.

The basis for assessing *map accuracy* is the confusion matrix (Aronoff 1982, Foody 1992). It gives the correspondence of the classified map to the reference data (Table 2.10). The most intuitive statistic is the overall accuracy p_0, which is the percentage of correctly classified polygons:

$$p_0 = \frac{1}{N}\sum_{j=1}^{n} p_{jj} \tag{20.}$$

However, p_0 depends on the number of classes and chance agreement making it impossible to compare p_0 values from different classifications. To correct for chance agreement, p_e, different coefficients of agreement have been developed, based on the multinomial distribution (Nishii and Tanaka 1999). The range of values of these coefficients is -1 to 1, where 0 is pure chance agreement and 1 is perfect agreement. Negative values indicate a classification that is worse than chance.

Table 2.10 *Confusion or error matrix as used in the accuracy assessment.*

Remotely sensed data	Ground data			
	class 1	class j	class n	sum
class 1	p_{11}	p_{j1}	p_{n1}	$p_{\bullet 1} = \sum_{j=1}^{n} p_{j1}$
class k	p_{1k}	p_{jk}	p_{nk}	$p_{\bullet k} = \sum_{j=1}^{n} p_{jk}$
class n	p_{1n}	p_{jn}	p_{nn}	$p_{\bullet n} = \sum_{j=1}^{n} p_{jn}$
sum	$p_{1\bullet} = \sum_{k=1}^{n} p_{1k}$	$p_{j\bullet} = \sum_{k=1}^{n} p_{jk}$	$p_{n\bullet} = \sum_{k=1}^{n} p_{nk}$	$N = \sum_{j=1}^{n}\sum_{k=1}^{n} p_{jk}$

A priori coefficients like τ (Ma and Redmond 1995, Naesset 1996) use prior knowledge of the expected class frequencies to estimate the chance agreement between the classification and the ground data. Class frequencies are assumed equal if no prior knowledge exists. *A posteriori* coefficients of agreement like κ (Cohen 1960) estimate the chance agreement from the observed marginal distributions of the confusion matrix. κ can be calculated from the confusion matrix by

$$\kappa = \frac{p_0 - p_e}{1 - p_e} \tag{21.}$$

$$\text{with } p_0 = \frac{1}{N}\sum_{j=1}^{n} p_{jj} \text{ and } p_e = \frac{1}{N^2}\sum_{j=1}^{n}\sum_{k=1}^{n} p_{j\bullet} p_{\bullet k}$$

κ is only affected by whether a polygon falls within the correct class or not. For ranked classes, like the total growing stock classes considered here, a modified coefficient exists that is weighted by the seriousness of the classification error. The weighted κ_w coefficient in Eq. 22 (Cohen 1968, Balzter et al. 2000, Gonin et al. 2000) uses the entire information in the confusion matrix.

$$\kappa_w = \frac{\sum_{j=1}^{n}\sum_{k=1}^{n} w_{jk} p_{jk} - \sum_{j=1}^{n}\sum_{k=1}^{n} w_{jk} p_{j\bullet} p_{\bullet k}}{1 - \sum_{j=1}^{n}\sum_{k=1}^{n} w_{jk} p_{j\bullet} p_{\bullet k}} \tag{22.}$$

$$\text{where } w_{jk} = 1 - \frac{(j-k)^2}{(K-1)^2} \tag{23.}$$

For instance, classifying a pixel of class 20-50 m^3/ha in the ground data as 50-80 m^3/ha is less serious than classifying it as >80 m^3/ha. If many classification errors close to the main diagonal of the confusion matrix occur, κ is very low but κ_w indicates good agreement. If the weight matrix is the identity matrix $\kappa_w = \kappa$. If all w_{jk} are equal $\kappa_w = 0$, unless all $w_{jk} = 1$ in which case κ_w is not defined. κ_w has been applied to forest GIS data by Naesset (1996) and to a Landsat TM based forest classification by Foody et al. (1996).

The weighting addresses the problem of different severity of confusions of classes. However, the unknown accuracy of the total growing stock values in the Russian forest inventory is a different issue. The values are generated by manual air photo interpretation and have an associated uncertainty. A confidence interval as broad as ±20 m^3/ha is possible for some forest stands (Vaschuk, pers. comm.). To assess the effect of this uncertainty on the coefficient of agreement, the following uncertainty model was adopted:

$$\nu = \eta + \varepsilon \tag{24.}$$

The measured value ν of total growing stock of a polygon in the GIS is the sum of the (unknown) true growing stock η and a white noise process ε with zero mean and standard deviation σ_ε. In counting the cell frequencies in the confusion matrix, a polygon is considered to be correctly classified if its growing stock volume overlaps with the 95% confidence interval $\nu \pm 2\sigma_\varepsilon$. The effect of uncertainty on the unweighted and weighted coefficients of agreement was examined using the technique of accuracy assessment curves (Morisette and Khorram 2000).

Data processing Chain

A polygon in the Russian forest enterprise GIS databases is the basic unit of the accuracy assessment. All available polygons were included in the analysis. Some test sites were not usable because of high topography (e.g. Sayano), coherence anomalies (Hrebtovsky South) and the age of the forest inventory (e.g. Ust-Ilimsky 1991, Lake Baikal South 1984).

To assess the accuracy of a classified ERS frame, the following processing steps were carried out:

- Co-registration of the GIS vector database to the ERS frame using an automatic coarse registration and a fine registration with ground control points;
- Topographic masking (section 2.3.2.1) and polygon erosion by two pixels;
- Calculation of κ_w with a quadratic weighting function and noise process ε (Table 2.11).
-

Non-forest classes (water and smooth open areas) were excluded from the accuracy assessment because there were an insufficient number of polygons with these classes in the forest inventory database.

Table 2.11 *Weight matrix for calculation of κ_w for the four forest classes.*

	Ground data			
Remotely sensed data	<=20 [m^3/ha]	20-50 [m^3/ha]	50-80 [m^3/ha]	>80 [m^3/ha]
<=20	1.00	0.89	0.56	0.00
20-50	0.89	1.00	0.89	0.56
50-80	0.56	0.89	1.00	0.89
>80	0.00	0.56	0.89	1.00

Results

Some of the expected properties of the confusion matrix can already be inferred from the coherence model. Fig. 2.41 shows a scatterplot of coherence and total growing stock for test site Nizhne1 together with class boundaries determined from the coherence model. The distribution of growing stock values shows that many polygons of higher growing stock are classified as lower growing stock volume. This is caused by the large number of polygons >80 m^3/ha in the ground data, and implies high expected "errors of commission". The shape of the model also implies an increasing error for increasing growing stock. Not all these polygons are really classification errors. For selected test sites, we identified polygons thought to have been subject to land-cover changes since the acquisition of the aerial photographs used to form the forest inventory GIS. In all cases the Russian forest enterprises confirmed that management activities (thinning, cutting) had been carried out in the forest stands in question. Even in the protected forests at Lake Baikal South, the identified polygons were classified as lower growing stock volume because of sanitary cutting in the stands. The true accuracy of the classification may thus be expected to be higher than indicated by the errors of commission (or user's accuracies) and κ_w.

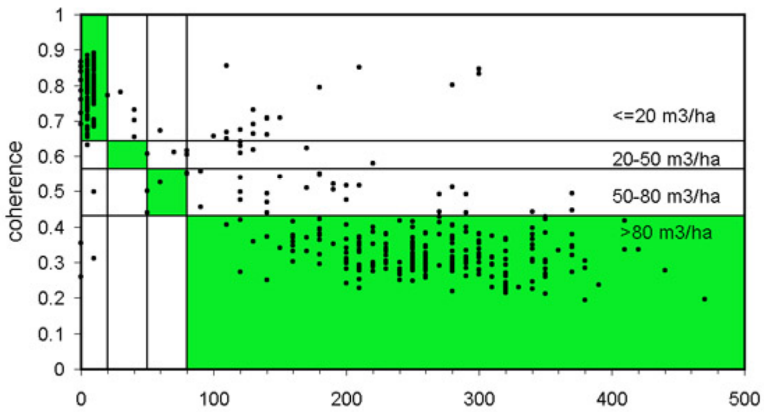

total growing stock in m^3/ha

Fig. 2.41 *Illustration of the errors involved in the classification for Nizhne1/Ukarsk (orbit 32414, frame 2493). Vertical lines show class boundaries, horizontal lines show coherence thresholds determined by the classifications algorithm. Green areas show correctly classified polygons for the growing stock classes. The use of JERS-1 intensity and the ICP algorithm slightly change the classification.*

Table 2.12 gives an overview of the ERS frames and GIS forest inventory data used to assess the accuracy of the map. κ_w in Table 2.12 was calculated without modelling the uncertainty in the ground data ($\sigma_\varepsilon = 0$) and reflects the degree of correspondence with the ground data rather than the accuracy of the map. The polygon counts of the confusion matrices of all test sites were added to get a pooled confusion matrix for the overall map (Table 2.13, $\kappa_w = 0.72$).

Table 2.12 *ERS frames and test sites used for accuracy assessment.*

ERS orbit	ERS frame	GEC/GTC	Baseline [m]	Test site	GIS update	κ_w
32357	2493	GEC	273.0	Mansky	1999	0.56
32400	2457	GTC	219.9	Bolshe-Murtinsky	1998	0.63
32414	2493	GTC	227.2	Nizhne 1 / Ukarsk	1997	0.88
32414	2511	GTC	233.0	Nizhne 2 / Porog	1997	0.62
32500	2403	GTC	224.6	Hrebtovsky	1996	0.46
32500	2493	GEC	247.7	Irbeisky 3	1996	small n
32543	2439	GEC	230.0	Chunsky 1	1998	0.74
32543	2493	GEC	244.3	Irbeisky 2	1993	0.33
32586	2439	GTC	187.4	Chunsky 2	1998	0.38
32600	2475	GTC	180.3	Primorsky	1996	0.68
32657	2493	GEC	169.7	Ulkansky 1	1998	0.49
32657	2493	GEC	169.7	Ulkansky 2	1998	0.47

Table 2.13 *Pooled confusion matrix for all test sites. Numbers are polygon counts.* $\kappa = 0.43$; $\kappa_w = 0.72$.

	Ground data					
Remotely sensed data	<=20 [m^3/ha]	20-50 [m^3/ha]	50-80 [m^3/ha]	>80 [m^3/ha]	total	user's acc.
<=20	589	104	21	136	850	69%
20-50	144	110	52	117	423	26%
50-80	135	237	297	1023	1692	18%
>80	31	96	223	5327	5677	94%
total	899	547	593	6603	8642	
prod. acc.	66%	20%	50%	81%		

Table 2.13 shows low user's accuracies (high errors of commission) for the intermediate growing stock classes 20-50 m^3/ha and 50-80 m^3/ha, as was expected from the high frequency of the class >80 m^3/ha in the ground data in Fig. 2.41.

To examine the likely effect of the uncertainty in the ground data on the coefficient of agreement, we recalculated κ and κ_w for varying σ_ε. The results are shown in Table 2.14 and Fig. 2.42. Higher uncertainty in the ground data results in a significant increase in both κ and κ_w. κ increases faster than κ_w, because of the built-in tolerance of κ_w to classifying a polygon as a neighbouring growing stock volume class. κ and κ_w tend towards a similar value for high uncertainty in the ground data (Table 2.14). For the statistically conservative accuracy figure from the Russian forest inventory manual, κ is in the range of 0.5 and κ_w above 0.7. Accepting a higher uncertainty in the ground data (up to 20 m^3/ha) gives less conservative κ values of around 0.7 and κ_w of 0.8

Table 2.14 *Effect of increasing standard deviation in the uncertainty model on two coefficients of agreement.*

σ_ε [m^3/ha]	κ	κ_w
0	0.431	0.717
1	0.476	0.724
5	0.520	0.736
10	0.621	0.755
20	0.721	0.797
30	0.800	0.849
40	0.847	0.893
50	0.883	0.917

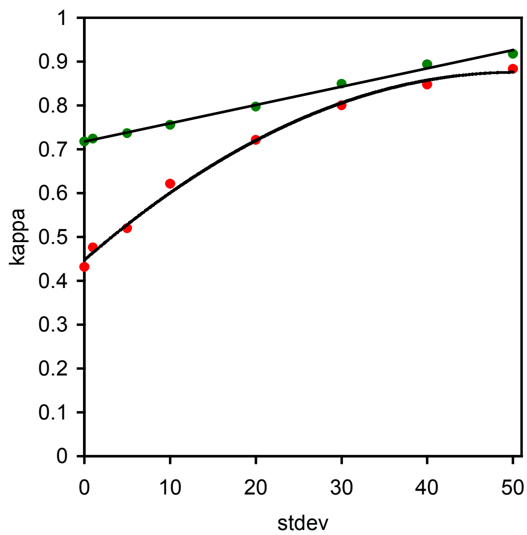

Fig. 2.42 *Accuracy assessment curves for the uncertainty model of the forest inventory data. Green: κ_w and fitted line, red: κ and fitted second-order polynomial. R^2>0.99 for both fitted trends.*

Conclusions

The results of the accuracy assessment show that a model for uncertainty in the ground data is required to understand the calculated accuracy statistics. The noise model introduced here explains the initial surprisingly low accuracy coefficients. Based on this model the "true" accuracy of the classified map is expected to be in the intervals $\kappa \in [0.5; 0.7]$ and $\kappa_w \in [0.7; 0.8]$. The κ_w coefficient was found to be more useful for describing the correspondence of ranked classes than the unweighted κ. The high errors of commission are explained by the histograms of total growing stock in the database and the definition of classes in the coherence model.

2.4 Synergy Between SAR and Optical Sensors

One of the tasks of SIBERIA project was to compare the results obtained with SAR data with those obtained with optical data, and to study the synergy of these data. The task was carried out by VTT, using Landsat TM and NOAA AVHRR data. Landsat TM images from three test sites Primorsky, Irbeisky and Bolshe-Murtinsky were available. Unfortunately it appeared that the purchased Landsat image of Bolshe-Murtinsky was unusable because of a layer of fog covering large proportion of its area .Sizes of the Landsat TM images were 170 km by 170 km and the pixel size was 30m by 30m. NOAA AVHRR mosaic was about 1000km by 1000km and pixel size was 1km by 1km.

The performed work can be divided into three parts. The first part was the variable estimation using the Landsat TM images. The second part was so called synergy estimation, where both Landsat TM data and ERS coherence data were used for estimation. The last part of the work was the NOAA AVHRR mosaic classification. The Landsat TM estimation results were used as reference data for the AVHRR mosaic classification. The classified AVHRR mosaic was then compared with the SAR classification of the same area by other partners of the SIBERIA project.

2.4.1 Pre-processing of Satellite and Ground Data

The remote sensing data consisted of Landsat TM, NOAA AVHRR and ERS coherence data. All six TM non-thermal channels were used. Atmospheric correction was performed for all Landsat TM images. NOAA AVHRR mosaics were prepared for the SIBERIA study area using onboard-recorded data, that were downloaded from the NOAA archives. For the synergy study ERS coherence data from Primorsky test site were loaded from the project ftp site. The coherence data were rectified to the same coordinate system with the Landsat TM images using ground control points, which were measured from Landsat TM and ERS images.

The ground data were received in MapInfo Interchange (MIF) format and they were converted to reference images using an in-house developed software. The reference images contained the ground-truth values of variables in raster format. Eight variables were selected for estimation from the Russian forest database that was used as ground data. The variables were growing stock volume and percentages of pine, spruce, fir, larch, cedar, birch and aspen. These eight variables were regarded as the most interesting ones in the database and for them also reasonable estimation results could be expected. The pixel size and the coordinate system of the reference images were set to the same as for Landsat TM images. For both test sites three different reference images were created. The reference image containing all polygons was meant for achieving the best possible ground data for AVHRR mosaic classification. Training and test images were created for evaluation purposes. Training images contained 2/3 of the polygons and test images contained 1/3 of them. The polygons that were obvious outliers were eliminated. This was done by comparing the ground data growing stock volume values and polygons' average reflectances of visible red and near infrared channels. To avoid problems caused by boundary pixels, morphological erosion was performed for the polygons.

2.4.2 Estimation Method

Eight variables were selected for estimation from the Russian forest database that was used as ground data. The variables were growing stock volume and percentages of pine, spruce, fir, larch, cedar, birch and aspen. These eight variables were regarded as the most interesting variables in the database in terms of information requirements and in terms of feasibility of the estimatation using optical data.
A VTT in-house developed method was used for variable value estimation. The method has originally been developed for change detection (Häme *et al.* 1998). First, homogeneous 2 by 2 pixel groups were selected from an image. The criterion for the homogeneity was the standard deviation vector magnitude of the pixel groups' reflectance values compared to the standard deviation of the whole image. The standard deviation vector was

computed for all the spectral channels. The selected homogeneous pixel groups were clustered to predetermined number (k) of spectral classes using the k-means algorithm. The pixels representing water were masked out using an interactively determined threshold for the near-infrared channel.

Mean vector (μ_c) and covariance matrix (C_c) between spectral channels were computed for every spectral class that were obtained through clustering. Based on these statistics, probability distributions $p(x \mid c)$ were estimated:

$$p(x \mid c) = \frac{1}{2\pi \mid C_c \mid^{1/2}} e^{\frac{1}{2}(x-\mu_c)^t C_c^{-1}(x-\mu_c)} \tag{25.}$$

The dimension of the distribution was the number of channels used in the clustering. The estimated distribution gave the probability $p(x \mid c)$ of a reflectance vector x to belong to a spectral class c. The class membership probabilities were computed for observations that were involved in clustering. The observations whose probability of belonging to the spectral class was smaller than a set threshold α were rejected. Since the a priori probabilities of the spectral classes were assumed to be equal, the class membership probabilities for the observations were obtained using the formula:

$$p(c \mid x) = \frac{p(x \mid c)}{\sum_{c=c_1}^{c_k} p(x \mid c)} \tag{26.}$$

The target variable values for the clustering observations were sampled from the ground-truth images. Using the sample, the means (μ_{g_c}) of the ground variables were computed for the spectral classes (Häme et al. 2000). If the spectral class had very few clustering observations in the region of a ground-truth image, it was removed. The estimation was possible to do after the removal of a class, since when the class membership probabilities were computed for each pixel, the a priori probabilities were always scaled so that their sum over all spectral classes was equal to1. In the final stage of the process, a variable estimate was computed for every pixel in the image. The estimate $y(x)$ was computed as follows:

$$y(x) = \sum_{c=1}^{K} p(c \mid x)\mu_{g_c} \tag{27.}$$

2.4.3 Evaluation Measure

Separate ground truth images were created for training and testing. Area-weighted root mean square error (RMSE) was used to evaluate the estimation results in the test set. The RMSE was computed as follows:

$$RMSE = \sqrt{\frac{\sum_{i=1}^{N_s} A_i(\bar{y}_i - q_i)^2}{\sum_{i=1}^{N_s} A_i}} \tag{28.}$$

where A_i is the area of stand i in pixels, q_i is the ground-truth value for the stand, $\bar{y}_i$ is the average estimated value of stand i and N_s is the number of the analysed stands in the image.

2.4.4 Estimation Using Optical Data

The estimation method that was described above was applied to the two atmospherically corrected Landsat TM images. After analysis, 35 spectral classes were retained for the TM data. The threshold for near-infrared reflectance value in water masking was set in both cases to 12.4%. Observations, whose probabilities of belonging to any spectral class were less than 0.1, were rejected from the sampling from the ground-truth image.

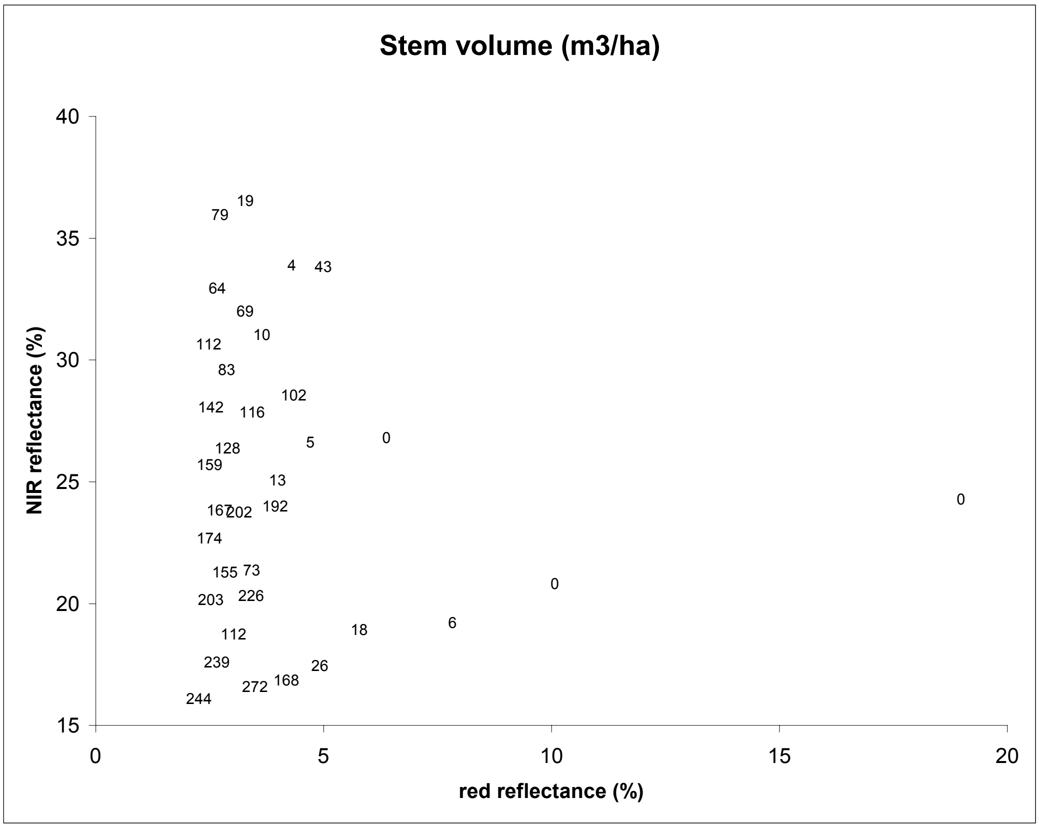

Fig. 2.43 *Location of the 35 spectral classes in spectral space. The numbers within the figure indicate the average growing stock volume computed from the ground data. Landsat TM data, Primorsky site.*

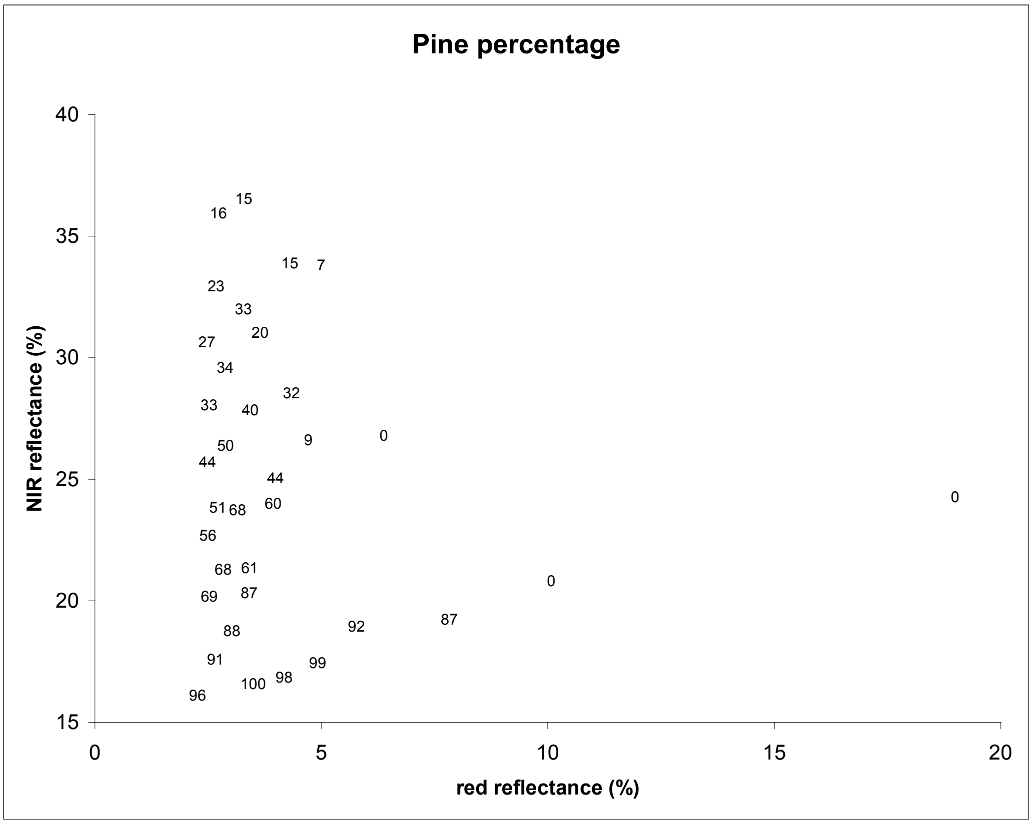

Fig. 2.44 *Location of the spectral classes in spectral space and their average pine percentages computed from the ground data. Landsat TM data, Primorsky site.*

Ground-data values were computed for growing stock volume and percentages of tree species. If some spectral class had only few ground samples, their sensibility was considered. If some spectral class did not have any observations in ground sampling or if it could be clearly seen that the computed values were contradictory, the spectral class was removed. On the other hand, if some spectral class did not have any ground samples but if its visible red and near-infrared (NIR) reflectances were high it could be assumed that the growing stock volume value of that spectral class was zero.

It can be seen in Fig. 2.43 and Fig. 2.44 that high growing stock volume values occur when both red and NIR reflectance values are low. The same is true for the pine percentage. Typically coniferous forests have fairly low red and NIR reflectance whereas low red reflectance values and high NIR values are associated with broad-leaved forest.

After computing the ground data values for the spectral classes, the target variable values were estimated for the whole TM images. The computation of the ground data values and estimation of the target variables were performed two times, using the training set only and using all ground data.

The test results are shown in Table 2.15 and Fig. 2.45. The estimation procedure tended to overestimate lower volumes and underestimate high volumes resulting in an average underestimation.

Table 2.15 *Ground data means, estimated means and RMSE. Landsat TM.*

Test site	Primorsky			Irbeisky		
Variable	ground mean	est. mean	RMSE	ground mean	est. mean	RMSE
Growing stock vol (m^3/ha)	146	132	86	179	139	60
Pine (%)	29	35	22	1	0	3
Spruce (%)	5	3	13	3	4	8
Fir (%)	5	2	10	22	16	27
Larch (%)	9	7	12	1	0	5
Cedar (%)	2	1	4	40	26	30
Birch (%)	33	31	20	21	23	29
Aspen (%)	15	16	15	4	6	11

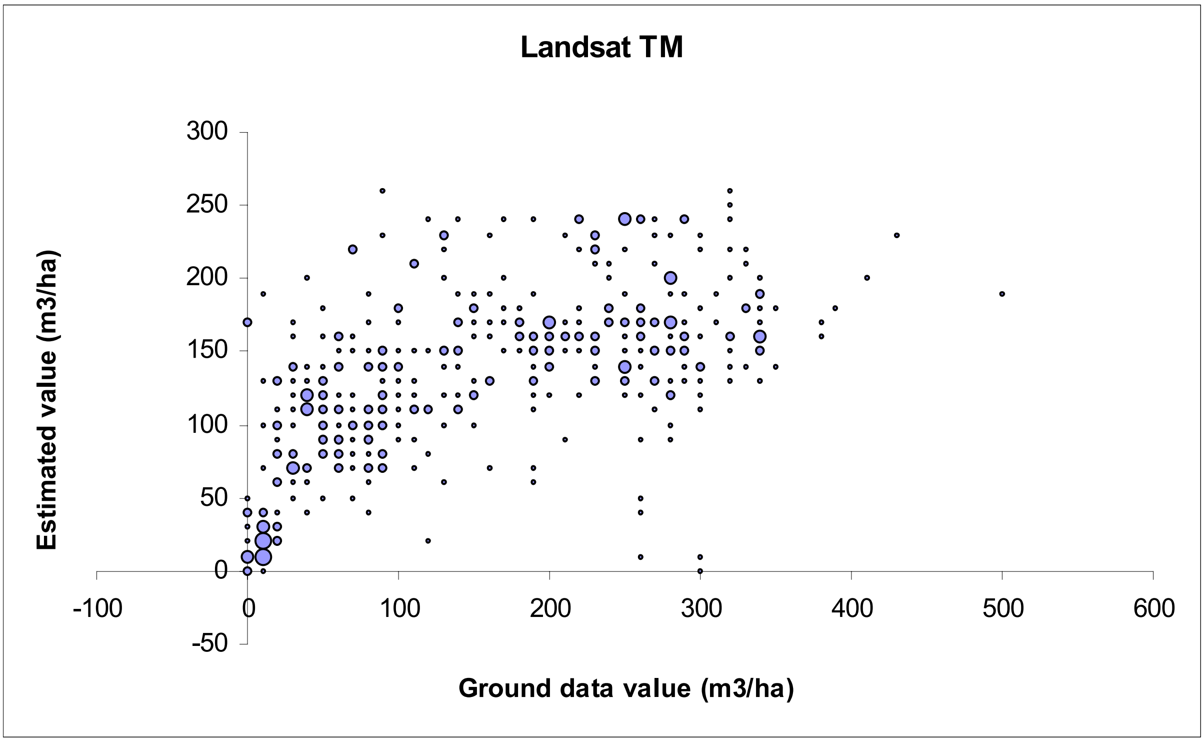

Fig. 2.45 *Average estimated growing stock volume and the volume in ground data of Primorsky test site for 442 test polygons. The bubble size describes the number of samples having same values.*

2.4.5 Estimation Using Optical and SAR Coherence Data

To study the synergy of optical and SAR data, a variation of the method described in the section 2.4.2 was applied. The Primorsky test site was selected for testing because both Landsat TM and SAR data were available from there. The Irbeisky test site could not be used for comparison because the Irbeisky site had so many missing pixels (either due to topography masking or missing data) in the SAR classification. The difference to the earlier procedure was that clustering was done hierarchically. For first clustering only the Landsat TM channels were used. The resulting clusters were then further clustered to secondary clusters using ERS coherence data. The number of preliminary clusters was reduced to 20 and the number of secondary clusters was set to 3, which gave 60 clusters in total. Also a higher number for primary clusters was tested, but then quite many clusters had too few observations to estimate the probability distributions reliably.

The estimation procedure was performed for all the variables (growing stock volume and percentages of the different tree species) using the formed 60 clusters. The synergy results were tested in the same way as the optical estimation results (Table 2.16, Fig. 2.46).

Table 2.16 *Ground data means, estimated means and RMSE. Optical and SAR data, Primorsky site. The corresponding optical evaluation results are in parentheses.*

Variable	ground mean	Est. mean	RMSE
Growing stock vol (m^3/ha)	146	131 (132)	75 (86)
Pine (%)	29	35 (35)	25 (22)
Spruce (%)	5	3 (3)	13 (13)
Fir (%)	5	2 (2)	10 (10)
Larch (%)	9	6 (7)	13 (12)
Cedar (%)	2	0 (1)	5 (4)
Birch (%)	33	31 (31)	22 (20)
Aspen (%)	15	15 (16)	14 (15)

It can be seen from Table 2.16 that the growing stock volume RMSE has decreased by 11 m^3/ha whereas the percentage errors in tree species have slightly increased. The estimated mean of volume has not changed in the synergy estimation. Comparison of Fig. 2.45 and Fig. 2.46 indicates that the estimation of the volumes below 100 m^3/ha has improved after the inclusion of coherence data.

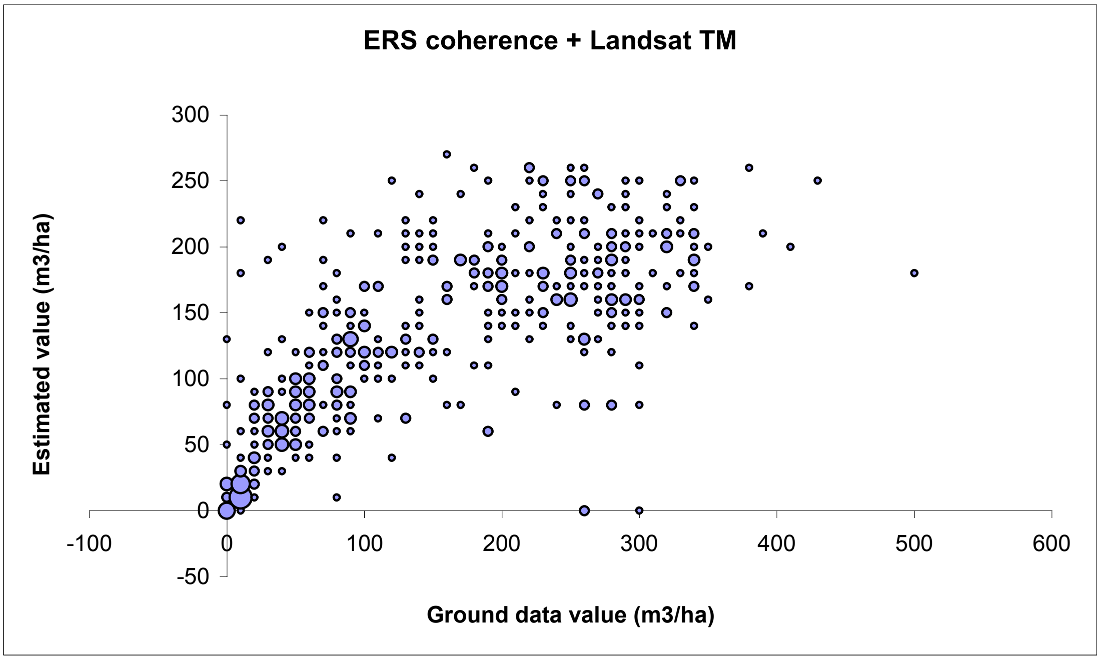

Fig. 2.46 *Average estimated growing stock volume and the volume in ground data of Primorsky test site for 442 test polygons. The bubble size describes the number of samples that have same values.*

2.4.6 AVHRR Mosaic Classification

The principal estimation method was applied to the AVHRR mosaic, which had been made for the study area. However, the estimation procedure was hierarchical in the spatial sense, since the TM-image-based estimates represented the ground data. A direct application of the ground data would not have been possible due to coarse resolution of the AVHRR. Only the first two channels of AVHRR (red and near infrared) were used. The mosaic was clustered to 35 spectral classes and after that the ground data values were computed from the classified TM images. The water-masking threshold was interactively set to 8% in this case but all other clustering parameters were set the same as for Landsat TM image clustering. The continuous volume estimates were converted to 6 information classes for the map output. The final classes were water, open and growing stock volume classes 20-50m^3/ha, 51-80 m^3/ha, 81-130 m^3/ha, and >130 m^3/ha (Fig. 2.47).

It seems that there are too many pixels assigned to water class in the classified mosaic, which reflects some problems in water masking. The problems were mainly caused by mountain shadows in coniferous forest areas. Water extraction using NDVI was also tested but it did not improve the results compared to the exclusive use of the near-infrared channel.

The continuous volume estimates were computed only for forested area. For the obvious non-forest area, an "open" class was defined. In the final result the "open" class comes directly from the unsupervised clustering.

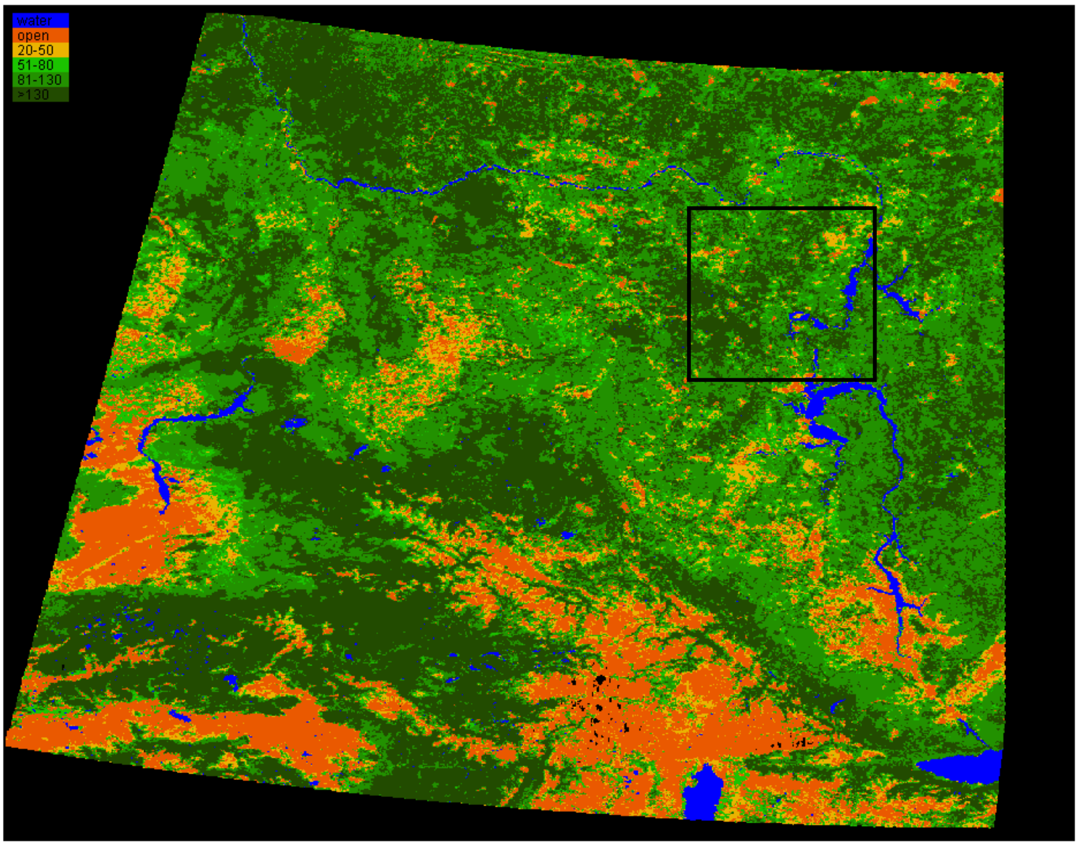

Fig. 2.47 *The classified AVHRR mosaic. Size of the mosaic is 1000 km by 1000 km and the pixel size is 1 km by 1 km. Classes are described in the upper left corner of the figure. The black rectangle marks the area where SAR and AVHRR classifications were compared (Fig. 2.48).*

2.4.7 Comparison of SAR and Optical Classifications

Visual comparison of the AVHRR and SAR classifications (made by the SIBERIA team) indicates that the classifications agree in great lines reasonably well (Fig. 2.48). The AVHRR classification is less detailed, which can be expected since the resolution of AVHRR is 1.21 km^2 at best (at image nadir) and worsens to almost 11 km^2 at the swath edges. However in this study 300 pixels were excluded at swath edges; only pixels smaller than 5 km^2 were used in the mosaic. There seems to be a slight difference in average growing stock volume levels between the AVHRR classification and the SAR classification. AVHRR usually indicates a higher growing stock volume class than SAR.

The RMSEs were not computed for the AVHRR mosaic estimates, because the resolution of the AVHRR data was so coarse compared to the ground data. The AVHRR mosaic classification was compared with the SAR classification in the region marked as a black rectangle in Fig. 2.47. The comparison was made using the pixel size of SAR classification 50m by 50m. The classes 'open' and 'smooth' of SAR classification were combined to one class (open). To make the comparison possible, the maximum volume class was set to >80 m^3/ha also in the AVHRR estimate, although the original estimation result had as high volumes as 190 m^3/ha. Table 2.17 presents the confusion matrix that was computed from the two classifications. Kappa value was not computed, since neither of the classifications could be regarded as ground truth.

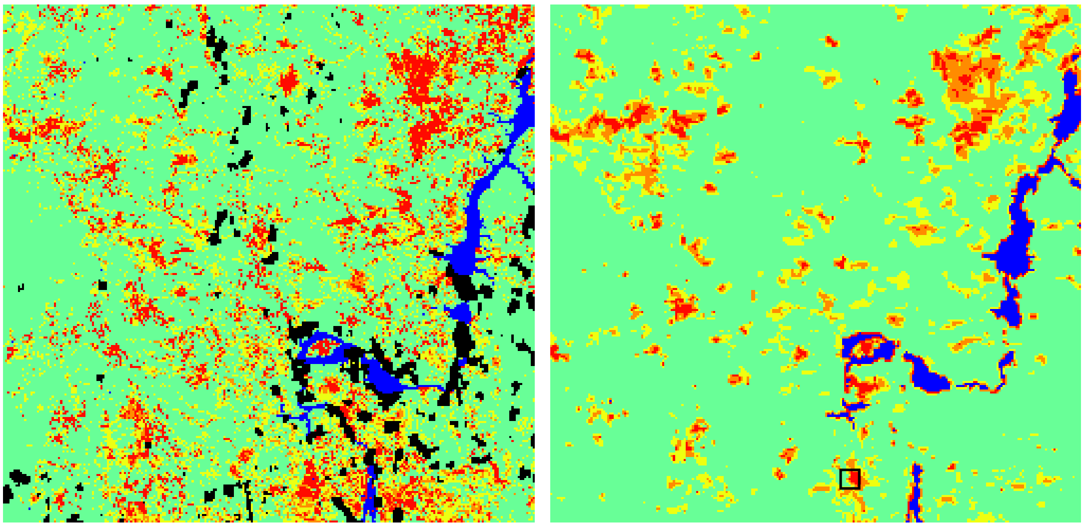

Fig. 2.48 *Example of SAR and AVHRR classification. The SAR classification made by the SIBERIA team (pixel size 50m by 50m) is on the left and the AVHRR classification (pixel size 1km by 1km) on the right. Classes are blue=water, red=open, orange=20-50 m^3/ha, yellow=51-80 m^3/ha, green=>80m^3/ha. Black colour means masked SAR pixels. The area size is approximately 200 km by 200km.*

Table 2.17 *Confusion matrix between SAR and AVHRR classification. The values indicate numbers of 50m by 50m pixels. In parentheses is shown the proportion of all test set pixels.*

		AVHRR					
		water	**open**	**20-50 m^3/ha**	**50-80 m^3/ha**	**>80 m^3/ha**	**total**
SAR	**water**	264958 (1.8 %)	19754 (0.1 %)	17972 (0.1 %)	23701 (0.2 %)	41165 (0.3 %)	367550 (2.5 %)
	open	8405 (0.1 %)	167424 (1.2 %)	236791 (1.6 %)	330722 (2.2 %)	731369 (4.9 %)	1474711 (9.9 %)
	20-50 m^3/ha	2015 (0.0 %)	37220 (0.3 %)	43533 (0.3 %)	110504 (0.7 %)	426396 (2.9 %)	619668 (4.2 %)
	50-80 m^3/ha	10980 (0.1 %)	99129 (0.7 %)	103821 (0.7 %)	323432 (2.2 %)	2028073 (13.6 %)	2565435 (17.2 %)
	>80 m^3/ha	46482 (0.3 %)	171350 (1.2 %)	192442 (1.3 %)	690100 (4.6 %)	8798774 (59.0 %)	9899148 (66.3 %)
	total	332840 (2.2 %)	494877 (3.3 %)	594559 (4.0 %)	1478459 (10.0 %)	12025777 (80.6 %)	14926512 (100.0 %)

On average 64.3% of all pixels were classified in the same way in both classifications. The majority of the pixels with the same classification belonged to the class >80 m^3/ha. Water was classified quite similarly. The SAR classification had more open areas than the AVHRR classification. The proportion of class 20-50 m^3/ha was similar in the two classifications, but they did not match well at the pixel level. In 26.6% of all the pixels the AVHRR classification indicated higher growing stock volume value than the SAR classification whereas in 9.3 % of all the pixels the situation is reverse. The confusion matrix supported the visual impression that the AVHRR classification gave considerably higher growing stock volume estimates than the SAR classification.

Fig. 2.49 illustrates the difference between classifications. The image is a detail of Fig. 2.48 in which its location is marked with a black rectangle. Fig. 2.50 shows the same region in the Primorsky Landsat TM image. As it can be seen in Fig. 2.49, the classifications differ significantly at the detailed level. The AVHRR mosaic classification is of course less detailed than the other classifications but also the SAR classification differs from the Landsat TM-based classifications greatly.

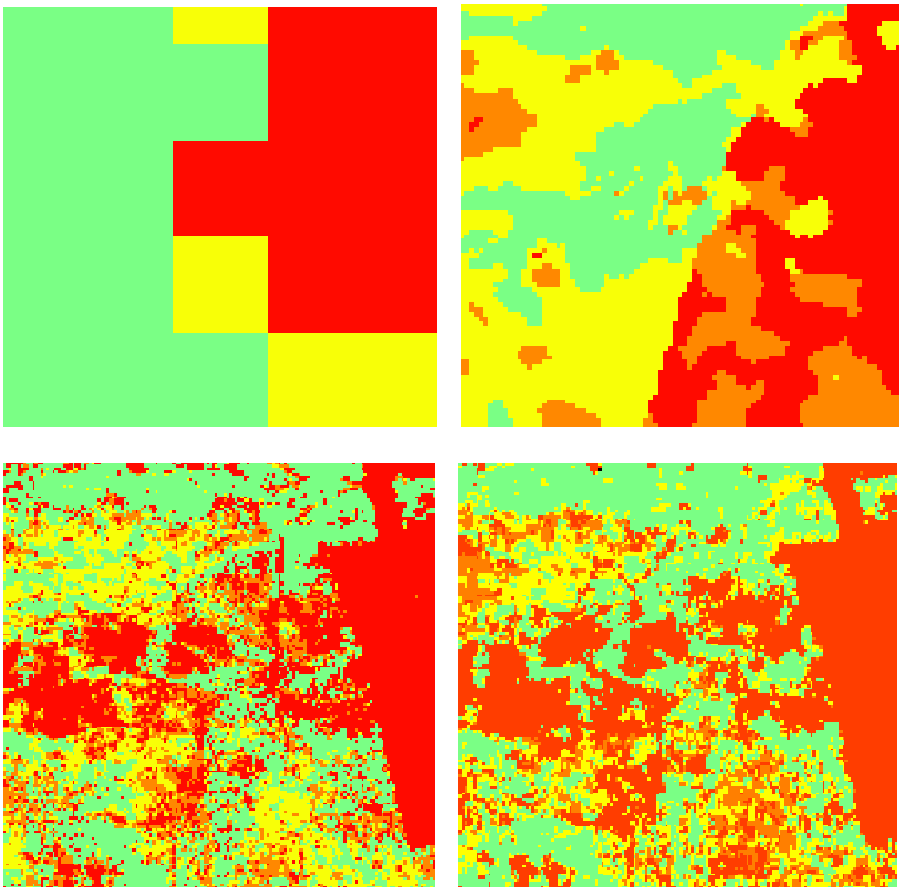

Fig. 2.49 *Examples of different classifications of the same area. The upper left image represents the AVHRR mosaic (pixel size 1km by 1km), the upper right the SAR classification (50m by 50m), the lower left image is Landsat TM result (30m by 30m) and the lower right is the synergy Landsat-SAR classification (30m by 30m). Classes are blue=water, red=open, orange=20-50 m^3/ha, yellow=51-80 m^3/ha, green=>80 m^3/ha. Area size is about 4.5 km by 4.5 km.*

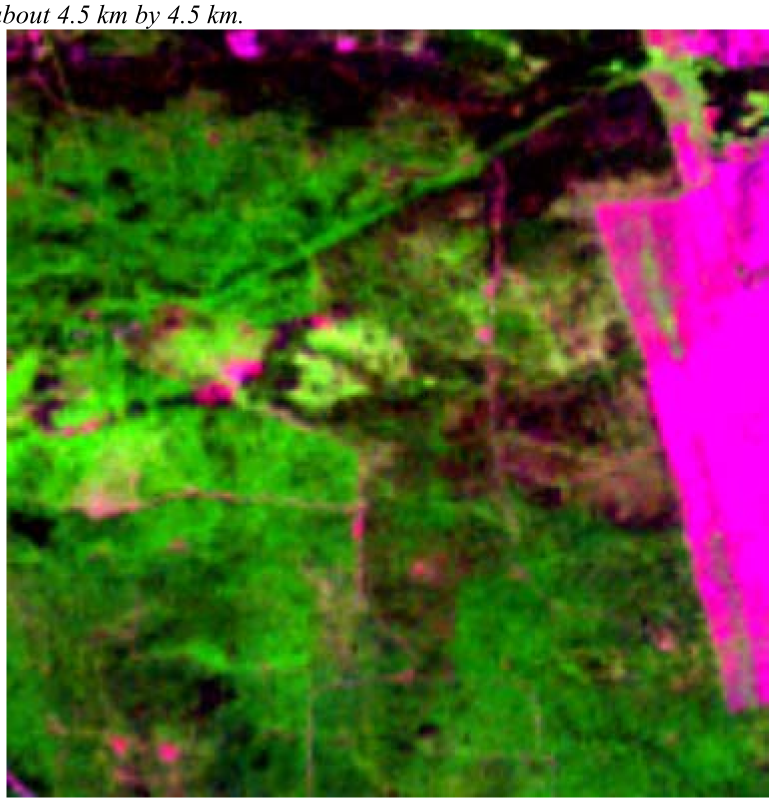

Fig. 2.50 *The same region as in Fig. 2.49 in Landsat TM image. Red=channel 7, Green=channel 4 and Blue=channel 3.*

2.4.8 Discussion

The mapping results obtained with SAR (ERS coherence and JERS), Landsat TM and NOAA AVHRR data are at different scales, and consequently, when the results are compared, there is a need to take the scale differences into account. Similarly, there are differences in data availability, data costs, operationality (operator intervention) and robustness of the processing chain.

The data sources can be compared in terms of their information content with respect to the forest variables. ERS coherence is sensitive to forest biomass or stem volume and saturates at about 100 m^3/ha. The coherence data are best used to map biomass classes up to this volume. JERS data can discriminate in an unsupervised manner water surfaces and smooth fields. Optical data are sensitive to tree species, and are related to the growing stock volume through the absorption of visible light by needles and leaves. Optical data saturate at a level slightly above 100 m^3/ha. The relationship with volume can be affected by factors such as soil reflectance, tree density and proportion of shadows.

The combined use of optical and SAR data could improve species and growing stock volume mapping. This requires use of an appropriate technique (e.g. the stratification of an optical classification with SAR coherence) that does not make unrealistic assumptions on the form of the joint distribution between SAR and optical variables.

The differences between the optical and SAR classification results were remarkable. Comparison of the AVHRR mosaic classification and the SAR classification of the SIBERIA team showed that the AVHRR classification usually indicated higher growing stock volume than the SAR classification. The TM estimates served as ground data for the AVHRR image-based estimation, which means transferring of the errors in TM classifications to AVHRR classifications. An additional reason contributing to the differences between AVHRR and SAR classifications at pixel level is possible geometric shifts between the data sets.

The two TM images covered approximately seven percent of the area of the AVHRR mosaic. Although their area proportion may be adequate for reference data, they were only from two locations, which may lower the accuracy of the AVHRR estimation.

The accuracy of the Russian forest database data was not known. Visual comparison of Landsat TM images and ground data showed in Primorsky site obvious clear-cuts that were not included in the database. Furthermore, comparison of the spectral values and ground data suggested that the growing stock volume of the broad-leaved tree forest might have been underestimated in the database.

2.5 Map Production

2.5.1 Image Preprocessing

The aim was to produce both maps of the mosaic of classified multi-frequency image frames and maps of the images themselves as represented by an RGB colour-composite made up of ERS tandem coherence, JERS backscatter, and ERS backscatter. This section deals with the co-registration of the multiple datasets and mosaicking of the classified and pre-processed images.

2.5.1.1 JERS Geometric Correction and Co-registration to ERS Data

ERS and JERS satellite tracks do not coincide because of differing orbits, look angles, and swath-widths. Hence a method of registering these two datasets was necessary to produce the multi-frequency composite. Since all other data was already co-registered to the ERS frame system, it was decided also to co-register the JERS data to the same ERS frames on a frame-by-frame basis. The JERS data was processed and calibrated as described in Wiesmann et al. (1999) and Shimada (1996) on a track-by-track basis, rather than as standard frames. Since each track is narrower in width than the standard ERS frame (75 km compared to 100 km), most ERS frames coincided with sections of two JERS tracks and a few needed three neighbouring tracks to give full frame overlap.

The JERS tracks were already projected, by Gamma RS, into the UTM reference scheme using the GTOPO30 DEM with a pixel size of 50m. Co-registration of the re-projected JERS imagery to the geocoded ERS data was achieved by automatically finding ground control points through cross-correlation of image patches followed by a low-order polynomial transformation. Despite the different geometry's of ERS and JERS, and the different radar wavelengths used, this automatic method worked satisfactorily in all but a small minority of cases, thereby greatly reducing the amount of user input to the procedure and maximising the geometric accuracy of the match. Commercial software from Gamma RS was used to make the registration of the JERS to the ERS data. The algorithms were so versatile that over 95% of the 122 image frames were co-registered automatically without any intervention.

2.5.1.2 JERS Radiometric Matching Between Satellite Tracks

The look-angle of JERS varies by a few degrees across its swath and the effect, particularly in forested areas, is to make the near-range brighter than the far-range, even after appropriate scattering-area calibration (van Zyl, 1993; van Zyl et al., 1993). Thus, although cross-correlation between JERS and ERS data was very successful in geometrically matching the scenes, where the far-range of one track was abutted to the near-range of another track within one ERS reference frame, the step in image brightness became very apparent (although radiometrically well within the expected calibration accuracy of JERS (Shimada, 1996)). This effect was compensated for by linearly transforming the backscatter intensity of the image with lesser coverage of the frame such that the tenth and ninetieth percentiles of the histograms (within the overlap areas only) were matched to those of the image with the greater frame coverage. A similar procedure was adopted for those ERS frames encompassing 3 JERS tracks and the effect was a seamless mosaicking of JERS data within the ERS reference frame system.

This technique was achieved entirely automatically and, as well as enhancing the interpretability of the images, improved the subsequent automatic classification of the multi-frequency composite.

2.5.1.3 ERS and JERS Radiometric Matching Between Frames

At this stage in the processing, the complete image database consisted of 122 frames defined by the standard ERS reference system but comprising registered tandem coherence and fully calibrated JERS and ERS-1 backscatter images. Only where all these data sources were present were the pixels within the frame passed on to the next step in the processing chain (otherwise the data was labelled as missing). These multi-band data frames were used as input to the forest classification procedure (section 2.3.2.3) and were also used to create the tandem-coherence/JERS-backscatter/ERS-backscatter RGB mosaic.

Despite the fact that the data were calibrated to the best standards available, there remained quite noticeable differences in the radiometric properties between frames for each of the three image sources. These features were attributed to two factors:

1. Variability in the backscattering characteristics of the forest between the times of acquisition arising from meteorological or seasonal changes.

2. Calibration differences within the tolerances of each instrument.

No simple compensation factor could account for the first factor, even if sufficient meteorological data had been available. However, the second factor was compensated by using the following procedure:

Choose a reference (master) frame to match each other frame to (track 319, frame 2457 was chosen for its diversity of land-cover). Then for each image (tandem coherence, JERS backscatter and ERS backscatter) for each remaining frame (121 slaves):

1. Find those parts of each image that correspond to forest by using the classified image frames.

2. Construct histograms for only those parts of the image corresponding to forest in both the master and slave image to ensure that only similar features are used to determine the match between images.

3. Linearly transform the backscatter intensity of the slave image such that the tenth and ninetieth percentiles of the forest histogram match the corresponding percentiles of the forest histogram of the master image.

This technique worked well on both the backscatter intensity (in linear σ^0 units, i.e. not in dB) and the coherence images, despite the very different statistical properties of these two data sources (Tough et al., 1995). By choosing to match the percentiles, rather than the full range of data values, particularly high values did not adversely affect the match.

Matching only the pixels believed to contain forest ensured that the match was largely independent of the highly variable proportions of different land covers within each frame. However, in mountainous regions, where the image classifier was considered unreliable because of radiometric slope effects (van Zyl, 1993) and reduced confidence in geometric fidelity (Kwok et al., 1994) and in those frames which contained a relatively small percentage (< 10%) of forest cover, slightly different approaches were required. In both cases, the histogram match was made on all pixels in the images, apart from those believed to be from water bodies (which have highly variable backscatter characteristics) and again the tenth and ninetieth percentiles were used. Where forest pixels covered less than 10% of the scene but the area was not mountainous, the same master image was used and the greater range of land covers within the matched histograms was found to allow an adequate match. In mountainous cases, a different master image was chosen (track 348, frame 2547) which before radiometric transformation seemed to match the characteristics of the first master image but which better represented the kind of radiometric properties generally found in mountainous parts of the region.

2.5.1.4 ERS and JERS Across-Frame Radiometric Balancing

Even after histogram matching across all 122 frames of 3-band data, there remained a clear decrease in brightness from near to far range in the ERS and JERS backscatter images, arising from the dependence on look angle of scattering mechanisms within the forest. This systematic effect should not be considered as an error since it contains information about the scattering processes and the properties of the canopy (Fransson and Israelsson, 1999). However, without compensation it would have yielded stripes within the RGB composite mosaic so, a method was sought to compensate for it.

The brightness ramp for ERS and JERS backscatter images was found to be approximately linear for forest. Unfortunately, after transforming to a ground reference system, the across-track direction no longer corresponded to the across-image direction. However, by determining the original satellite track heading, and determining the geometric transformations that had been performed on each image, the equivalent across-track angle was found for each image frame and the gradient of the across-track ramp in the ERS and JERS (forest only) backscatter was measured from a few sample images.

To compensate for the across-track ramp, the angle of the track to the frame orientation was determined for each image frame and a linear radiometric transformation applied to cancel out this ramp in the across-track direction. Since the transformation was based only on forest pixels, this procedure did not improve the look of the non-forest areas that normally exhibit a different relationship between backscatter and across-track position. However, as the final mosaic was mainly of forest, and intended for the use of foresters, this was not considered to be a drawback. The same compensation gradient was used in each frame. The gradient used was equivalent to ± 0.55 dB for ERS across the whole image and ± 1.12 dB for JERS.

2.5.2 Creation of the Mosaics

At the final stage, all images were held as floating-point (32-bit) data (i.e. a very large volume of data). The RGB mosaics needed only three bands of byte (8-bit) data for presentation purposes so the last stage in the process prior to mosaicking was the radiometric enhancement and byte-scaling of each frame of the three bands of data. This reduced the volume of data by a factor of four.

To best present the dynamic range of the JERS and ERS backscatter images, they were first converted to dB and then scaled between minimum and maximum values chosen to encompass the majority of distribution of values (while also being rounded to the nearest dB). For JERS the scaling was between -10 dB and -4 dB and for ERS, the limits were -10 dB and -6 dB. The coherence images were enhanced with a linear function and minimum and maximum values of 0.15 and 0.85, again chosen to optimally represent the available data within the 0-255 output dynamic range.

The enhanced images were mosaicked together in one process for each band using map reference data (UTM47 corner coordinates) derived from the ERS geocoding stage. The data order was chosen by track and by frame such that GTC data always overwrote GEC data where there was an overlap, so as to preserve the data with the best geometric and radiometric fidelity. Mosaics of the classified frames were created in a similar way but only for one band of data.

2.5.3 Mosaic Division

The geographic area for the output mosaics was chosen to encompass all 122 frames of data and have UTM boundary coordinates in round numbers of 100,000 m. This gave a mosaic of 1,500 km by 1,300 km (30,000 by 26,000 pixels of 50m) with top left coordinates (UTM zone 47) or -200 (Easting), 6,900,000 (Northing). The mosaics were divided into map sheets of 100 km by 100 km (2,000 by 2,000 pixels) for printing, making 15 by 13 maps or 195 in all. Many of these maps (62) covered only boundary areas where no data was present so they were discarded. It was decided to print only those maps with greater than 20% of their area including image data and this reduced the number to 111 for the RGB mosaic. As a result of masking areas out of the classified images because of high topography, the number of maps of classified images with greater than 20% data coverage was 96.

2.5.4 Map Design and Printing

The map sheets were named according to a labelling scheme where the upper left map sheet was named A01, the next map sheet in the same line A02, etc. The digital map sheets were delivered in ERDAS .img format geo-referenced to UTM zone 47 WGS 84.

The Radar Image Maps and the classified Forest Cover Maps were also presented in analogue form as printed colour maps on a scale of 1:200 000. For the analogue products a map design was agreed and a legend produced. The Radar Image Maps were presented as false colour RGB maps where ERS tandem coherence was presented in red, JERS-1 intensity in green and ERS-1 intensity in blue.

The classified data was presented as Forest Cover Maps where the different land cover types were represented in different colours and the growing stock volume classes in different shades of green.

The analogue maps included the following information
- UTM and Geographic coordinates with geographic grid lines in the map
- Map title
- Project logotype
- Map name: Name of Geographic site and Map index number ex: Irkutsky K11
- Scale bar and scale (1:200 000)
- Projection information (UTM zone 47 WGS 84)
- Acknowledgement
- Map index map
- Legend (Forest Cover Map)
- Band combination information (Radar Image Map)

The map sheets were finally converted to postscript format and 4 copies of each map sheet was printed on an ink jet plotter at 720 dpi.

2.6 Computational Issues

A significant number of computational issues had to be resolved in the SIBERIA project, including site-specific hardware and software compatibility, protection of intellectual property rights and implementation of the processing chain to convert uncalibrated imagery to geocoded classification maps and mosaics of multi-sensor data.

2.6.1 Institutional compatibility

In the early stages of the project enquiries were made regarding the computational facilities (both hardware and software components) at each institution so that standards for software packages in image processing, word processing and statistical analysis could be agreed. The results of these enquiries were as follows:
- All institutions had access to high-powered SUN workstations and/or INTEL PC networks running SOLARIS and/or LINUX operating systems.
- Most institutions had all the necessary support hardware and backup devices, e.g. large disk space, sufficient memory, backup tape writers, CD re-writers etc.

- All institutions had the necessary 'c' programming language compilers.
- Several institutions had an IDL (Interactive Data Language) license.
- The choice of commercial image processing software (e.g. ERDAS Imagine; ENVI; PCI; GAMMA RS ISP, DIFF & LAT tools etc.) varied between different institutions.
- Various word processing facilities were available at each institute.

From these observations a number of recommendations were made regarding the implementation of algorithms. An example of these recommendations would be that, if possible, the solution to the problem would be developed in the 'c' programming language, as all institutions would be able to implement the code. In addition it was agreed that all documentation was to be produced in Microsoft Word97 or Adobe PDF format.

2.6.2 Intellectual Property Rights (IPR)

Since many programs and algorithms, some of which were developed in-house by institutions prior to the project, were potentially to be transferred to commercial partners in the project, it was considered vital to protect copyright for these ideas. This issue was investigated by seeking advice from experts at the University of Wales, Swansea and attending a course on intellectual copyrights and protection. The outcome of these investigations was a number of recommendations:
- Compiled binaries should be delivered to commercial partners in preference to source code, and only with prior consent of the issuing partner.
- Source code was only to be given to commercial companies with prior consent if no other avenue was available.
- All computer code, on being run, should display copyright information (author, institution, project, date).
- Implementation of some programs was limited by copyright to the lifetime of the SIBERIA project.
- Gamma RS kindly authorised the use of their software to enable many of the processing steps to be undertaken at UWS. Although a license is granted at this institution, the GAMMA RS programs were dedicated to solving the projects computational issues, therefore additional programs were developed at no additional expense.

2.6.3 Processing Chain

Different parts of the processing chain were developed at different institutions and hence took slightly different approaches to implementation, often utilising different programming languages. However, one of the positive aspects of the SIBERIA project was that colleagues at several institutions contributed to writing programs and algorithms that have made a success of the whole project. Full acknowledgement and copyright is given in the programs to the various people and institutions that have contributed. Satellus were originally tasked to develop the operational implementation of the processing chain to produce the multi-sensor (RGB) composite and the classified output maps. However, later in the project it became clear that computational issues could be solved more easily if this processing chain was implemented at UWS. Some transfer of funds was arranged to make this possible.
The final processing chain was implemented in 'c' and 'IDL' and coordinated by the use of 'c-shells'. Stages of the chain include calibration, co-registration of ERS and JERS products, topographic masking, edge masking (for consistency between ERS and JERS coverage), multi-image filtering (Quegan *et al.*, 2000), production of scatter plots (for interpretation), classification (various algorithms tested), histogram matching, reprojection to UTM zone 47, image enhancement for multi-sensor RGB composite, mosaicking. Several key components of the processing chain were only achievable by using programs developed by GAMMA RS. For the registration and mosaicking tasks the computation issues team (UWS) made recommendations that Satellus obtain the necessary software from GAMMA RS, upon which a commercial contract was arranged. The processing chain was made fully automated and this was only made possible by the efficient, adaptable and robust nature of the programs developed by ourselves and colleagues in partner institutions, with particular recognition given to the important and positive role played by Gamma RS.

2.6.4 Processing and disk burdens

The input data to the SIBERIA project comprised 122 frames of autumn ERS1, autumn ERS2 and spring ERS2 data plus 26 part-tracks of JERS data, some including 44-day repeat-pass coverage. The volume of the raw data was around 150 Gbytes and probably reached 200 Gbytes after processing to SLC images and combined for interferometry. This data burden was handled by several project partners.

The RGB mosaic only required one ERS coverage, one tandem coherence coverage and one JERS coverage and the data was assimilated into the mosaic processing sequence as multi-look geocoded images. Once co-registration of the ERS and JERS data was complete, the data volume was:

122 (frames) x 3 (bands) x 4 (bytes per pixel) x ~2,400 (pixels) x ~2,400 (lines) = ~8.4 Gbytes.

The output mosaics have a geographical span of 1500 km (East-West) x 1300 km (North-South) which, at a pixel-size of 50 m, equates to 30,000 pixels x 26,000 lines. Thus the data volume for the output mosaic is:

3 (bands) x 1 (byte per pixel) x 30,000 (pixels) x 26,000 lines = ~2.3 Gbytes

All processing for the mosaicking part of the analysis (co-registration, filtering, classification and image pre-processing) was achieved using 400 MHz Pentium II PCs running the Linux operating system. Almost all processes ran autonomously for nearly all frames and the full processing sequence including all the processes described (not including reading data from CD or tape) took around 1 week of processing time to complete.

3 List of Deliverables

Three types of progress monitoring tools have been defined for SIBERIA:
1. meetings, followed by external progress reports and comments to the EC;
2. internal deliverables (working notes, methodological tools, data products) and internal milestones (conclusion of a work package, which is essential for the project's progress);
3. external deliverables for third parties.

Meetings have been crucial evaluation points in SIBERIA´s management. The status of deliverables was observed during the meetings and described in the respective progress reports, which were produced in the month following the meetings. This chapter starts with a short summary of the major meeting decisions, followed by the list of deliverables as contained in the Technical Annex.

3.1 Meetings

3.1.1 Kick-off Meeting

The kick-off meeting was hosted by IIASA and was held in Laxenburg, 10-11 August, 1998. All partners of the consortium and two representatives from the EC (DG 12D, JRC-CEO), Martin Krynitz for the scientific questions and Katleen Engelbosch for financial issues, participated in the meeting. From the Russian customer side Dr. Rozhkov from the V. V. Dokuchjaev Soil Institute, Dr. Skudin from the East Siberian State Forest Inventory and Planning Institute, Dr. Sokolov from the V. N. Sukachev Institute of Forest of the Russian Acadamy of Sciences, and Dr. Vachtchouk from the Irkutsk Forestry Board were able to attend.

Besides presentations of all partners and discussions on technical points the meeting included:
1. a **Radar Short Course** (WP 1400) on radar remote sensing and digital image processing techniques for the customers, to supply them with the necessary background for the lay-out of their classification requirements.
2. a **Presentation of Customer Requirements** (WP 4100 and 4400) that included a description of the current Russian inventory system, the forest data base, and potential problems in the future.

The presented material and hand-outs were collected and printed as a workshop report. Copies were distributed to all partners, the Russian customers, and the EC.

3.1.2 First Progress Meeting

The first progress meeting was hosted by CESBIO and was held in Toulouse, 14-15 December, 1998. The following major team decisions were made:
1. The methodology hand-over is **postponed**, due to bad data situation. The work plan faces a three month delay.
2. Team **cannot longer wait** for processing solution on availability of JERS-1 data acquired during spring 1998 in Ulaanbaatar. Gamma will start to order JERS archived data of ground-truth sites.
3. Gamma's JERS-Products: full resolution products for ground-truth sites, other project area 50m-products.
4. 20-look coherence maps will also be included in analysis, in addition to 64-look map.

5. Team agrees on motto: **quality over quantity**! IIASA prefers good test area results rather than large-area map of lesser quality. Consequence for DLR-DFD: GTC processing emphasized - takes time!
6. IIASA performs geo-coding of GIS vector data to UTM coordinates.
7. Based on the analysis at CESBIO and followed by checks at DLR of the ERS interferometric products, **major improvements** were undertaken in the algorithms for the interferometric processing chain. The DLR-DFD interferometric processor is now adequately adopted to SIBERIA's special requirements.
8. **Additional Methodology Meeting** in March/April in Swansea, UK.

The **1st Progress Report** was delivered to the Commission containing the work accomplished during the first six months.

3.1.3 (Additional) Second Progress Meeting

The 2nd Progress Meeting had been additionally scheduled due to severe delays of the JERS-1 data delivery and the connected delay of our work schedule. The meeting was hosted by UWS and was held on April 19-20, 1999. The following decisions and conclusions were made:

1. For ERS scenes with 50% DEM-possibility, DLR-DFD should produce both a GEC **and** a GTC.
2. JERS calibration coefficients should be "**frozen**" to guarantee uniform calibration for all JERS imagery.
3. A rough geometric correction should be applied to ERS and JERS GECs using a 30 arc-seconds global DEM (**GTOPO30**).
4. Until JERS data are available, apply "**Minimum Map Approach**" for ERS data only: not more than 2-3 non/forest classes, one forest class, water, agriculture and man-made classes can be identified.
5. Goldstein's phase filter is now used in DFD's InSAR Processing Chain.
6. Disclaimer in Contract with Gamma and SSC for **software code** developed within SIBERIA.

3.1.4 Siberia Excursion

From May 30 to June 12, 1999 a large part of the SIBERIA team participated in a field trip to Siberia which had been planned by IIASA and its Russian partners. The objective of the excursion was to get hands-on experience about Russian forests to aid the interpretation of the radar imagery and to learn more about the Russian forest inventory system. Several test sites in the regions around Krasnoyarsk and Irkutsk were visited. At these sites Russian foresters explained the local forest characteristics and the GIS and remote sensing maps were compared to the actual conditions. A detailed documentation of the excursion can be found in Appendix B. Following the excursion, the **2nd Progress Report** for the second six months was delivered to the EC.

3.1.5 Third Progress Meeting

In December 1999, the 3rd Progress Meeting took place as scheduled at the location of Satellus in Kiruna, Sweden. The planned hand-over period of the forest classification algorithm from the Methodology Team to the map producing company Satellus, however, had to be postponed due to the **severe delays** of the JERS-1 products. The meeting still took place to discuss the several **pre-processing steps** (calibration, co-registration, filtering) and the overall final **map lay-out** (projections, map projection, paper quality, frame, legend, etc.). The **3rd Progress Report** was delivered to the Commission containing the period August 1999 until January 2000.

3.1.6 (Additional) Fourth Progress Meeting

Due to the 3-month delay of the methodological development an additional Meth-Team meeting was scheduled for March 10 and 11, 2000 at the site of Partner 7, NERC, Monkswood/UK. The meeting was oriented towards a decision upon the **final classification methodology**. Issues were: histogram comparisons, testsite comparisons of the competing classification algorithms, software implications for algorithm hand-over. A decision was made, but had to be dismissed later due to improving results from the empirical model approach.

3.1.7 (Additional) Fifth Progress Meeting

On July 14-15, 2000 the Meth-Team met for a last interim meeting at IIASA together with the Russian customers. Based on the accuracy assessments for all classification scenarios, the question arose on how many forest classes to distinguish since this number also changes the overall accuracy (**less classes – better accuracy**). The team agreed finally on **seven** classes. Further map layout refinement followed (raster lines, Russian names, logos, acknowledgements).

3.1.8 Final Meeting

From 26 to 27 October 2000, SIBERIA's final project meeting took place at the location of the German Aerospace Center (DLR) in Oberpfaffenhofen, Bavaria. All project partners, including three Russian partners, were able to join. The European Commission had sent the responsible Scientific Officer Martin Sharman. The respective ESA representative for the ERS Announcement of Opportunity, Henri Laur, was also present. 25 non-project participant came from the industry, universities, research institutions and a film company. The sessions were organised in a logical way, from the data processing description to the presentation of the final classified maps, including the rationale for the applied classification methods. The Work Packages were presented by the responsible team leads. The final words came from the EC and ESA representatives and the Russian customers. The false-color mosaic was displayed in the original scale (1:200.000) in the lobby. The meeting commenced with an internal team session in which it was decided to continue the cooperation and develop SIBERIA's results to a larger area and a new challenging task: adoption into climate models. The new project name: SIBERIA-II.

3.2 Internal Deliverables

SIBERIA's internal deliverables (compare Table 2.18) consisted of working notes to specific technical topics, methodological tools (such as algorithms), data products (i.e. forest database), and internal milestones (conclusion of essential work packages). In addition to the Project Deliverables, monthly progress reports have been sent to the Methodology Coordinator at SCEOS from each Methodology Team member. The status was then summarized and discussed during the monthly teleconferences. In a later phase with rapid changes, teleconferences were performed weekly and the progress reports were dropped.

Internal Milestones 2 and 3 and later 7 and 8, as well as the major milestone (MM1) "Methodology Synthesis" had severe delays due to tremendous logistical problems in establishing a processing procedure at NASDA for the special recording format of the repeat-pass JERS-1 data acquisitions at the DLR Mobile Receiving Station Ulaanbaatar during summer 1998. Due to the outstanding support of Dr. Klaus Reiniger/DLR-DFD and Dr. Masanobu Shimada/NASDA this only complete repeat-pass JERS-1 coverage of Siberia was later synchronised at DFD and processed at Dr. Shimada's new processor at NASDA. The Swiss partner Gamma also proved to be extremely flexible and supportive in adopting software and processing an immense amount of data in a short time.

Due to delays in the methodological development, the map production (and therefore also its assessment) was severely delayed (Deliverables 29 and 30, Internal Milestone 7. Unexpected smart software solutions were found by UWS' post-doc, Dr. Kevin Tansey, and the originally assigned large time period for the application of the classifier could be drastically reduced. After this very late, but very positive development, the project was again on schedule.

Milestone 8 suffered from not sufficient availability of optical data. In addition, the team member also had to wait until the radar-based forest map was produced for comparison. This milestone was only concluded at the final meeting.

Table 2.18 *List of SIBERIA's internal deliverables, responsible work packages and due dates.*

Item	#	Title	Work Packages	Due
Techn. Deliver-able	*1*	2-monthly Processing Prioritisation	1150	T0-T19
	2	Classification Requirements I	4100	Kick-off
	3	Test Site Locations	4200	Kick-off
	4	Co-Registration Procedure I	5010	Kick-off
	5	Computational Issues I	5050, 5150, 5250, 5350	Kick-off
	6	Reference Data I (Assessment)	4300, 5040	Kick-off
	7	Contrib. Customer Workshop	5010-5050	Kick-off
	8	Co-Registration Procedure II	5010	T3
	9	Computational Issues II	5050, 5150, 5250, 5350	T3
	10	Filtering Requirem. & Method.	5030	T3
	11	Processing Status I	2100-2200, 3100-3200	T5/6
	12	Classification Requirements II	4100	T5/6
	13	Reference Data II	4300	T5/6
	14	Co-Registration Procedure III	5010	T5/6
	15	Quantification of Image Info I	5020, 5120, 5220, 5320	T5/6
	16	Classification Methodology I	5030, 5130, 5230, 5330, 4200, 4300	T5/6
	17	Accuracy Assessment Methods I	5040, 5140, 5240, 5340, 4200, 4300	T5/6
	20	Computational Issues III	5010-5050, 5150, 5250, 5350	T5/6
	21	Computational Issues IV	5010-5050, 5150, 5250, 5350	T11/12
	22	Quantification of Image Info II	5020, 5120, 5220, 5320	T11/12
	23	Processing Status II	2100-2300, 3100-3300	T11/12
	24	Reference Data III	4300, 4400	T11/12
	25	Accuracy Assessment II	4500, 5040	T11/12
	26	Classif. Methodology II (Draft for MM1: Method. Synthesis)	5020, 5030, 5130, 5230, 5330, 5400	T11
	27	Processing Status III	2300, 3300, 3400	T17/18
	28	Accuracy Assessment III	4500, 5040, 5140, 5240, 5340	T17/18
	29	Map Status	6100	***Delay***
	30	Sampling Scheme for Map Assessm.	6300	***Delay***
Mile-stones	1	Forest Data Base Structure Defined	4100, 4400	T11/12
	2	Co-Registration Strategy	5010	***Delay***
	3	Quantification of Image Info Defined	5020	***Delay***
	4	Interferometric Proc. Concluded	2100, 3100, 3200	T14
	5	Reference Data Manual	4300	T14
	6	DEM Generation Concluded	2200, 3300	T17/18
	7	Classification Meth. Revised	4400, 5000	***Delay***
	8	Synergy SAR + Landsat	5510	***Delay***
	9	Terrain Correction Concluded	2300, 3300	T21
	10	Synergy AVHRR + SAR	5520	T23
	11	Map Classification Concluded	5160, 5160, 5360, 6100	T23
	12	Map Mosaicing Concluded	6200	T23
	13	Cost Efficiency Evaluated	7100	T22
	14	Data Archiving Concluded	2400, 3400	T24
	15	GIS Map Implementation	7200	T24
Major Mile-stones	**1**	Methodology Synthesis	5000, 5130, 5230, 5330, 5400	***Delay***
	2	Map Assessment	4500, 5140, 5240, 5340, 6400	T0 + 22

3.3 External Deliverables

External deliverables were SIBERIA's Progress Reports to the Commission, since they were also distributed to the interested scientific community. For example, the project team considered the 2nd **Progress Report** as a summary of major developments in the field of forest radar remote sensing and send out 34 copies to interested parties around the world, resulting in intensified contacts and feedback.

Table 2.19 *List of External Deliverables.*

Deliverable #	Title	Work Packages	Due Date
Radar Short Course	Customer Support	1400	Kick-Off
31	Customer Requirements Doc	4100	Kick-Off
34	EWSE Advertisement	1300	T1
35	EWSE Update I	7300	T12
36	Public Info	7400	T12

In connection with the kick-off meeting, a Radar Short Course was organized to inform the customers about possibilities and limitations of radar remote sensing. Also during kick-off the Customer Requirement Document was discussed. The EWSE Webpage was being updated with material from the SIBERIA progress reports. Links were installed to the two project webpages: SIBERIA Project Page at UWS (http://sunset.swan.ac.uk/siberia– this page is currently protected by a password), SIBERIA Ground Truth Page at IIASA (http://www.iiasa.ac.at/Research/FOR/siberia/index.html).

Public information activities:

- meetings and discussions with World Expo Representatives – unfortunately without result because of costs,
- participation in the IGOS/GOFC activities,
- SIBERIA leaflet distribution through ESA's Earth Observation Quarterly (notice: although information was sent, this leaflet contains no information about the funding agencies to our large regret).

4 Comparison of Initially Planned Activities and Work Actually Accomplished

4.1 Encountered Problems

Three main problems have been encountered in the **first six months** of the SIBERIA project:

1. The **change of the consortium** has caused a delay in the finalisation of contractual matters, and consequently has created administrative and financial problems for most partners.
2. **Late availability of topographic maps**: For the production of DEMs from ERS tandem pairs, and consequently for the generation of GTC products, reference topographic maps are needed. Unfortunately, maps of sufficient quality have been difficult to obtain. Thanks to IIASA's good connections, maps for the entire study area were delivered in January directly from Russia. Despite the fact that the maps are colour copies of the originals which can result in large displacements, it was decided to use these maps as base for the DEM and GTC production because the late availability of data has already created problems for the methodology team.
3. **Ordering of JERS SAR Scenes**: Despite considerable effort, it has not been possible to obtain JERS SAR scenes from 1998, acquired at the DLR mobile receiving station in Mongolia. Because the methodological team has an urgent need for JERS data over the main test areas, historical JERS scenes from the NASDA archives have been ordered as backup solution. The first interferometric JERS scenes are expected to become available to the methodological team in the middle of February.

The problems created a delay of approximately three months. An additional Methodology Team Meeting had been decided to take place at UWS on April 19-20, 1999 to continue the discussions about the methodological Work Packages, started during the Toulouse Meeting.

The main problems that have been encountered in the **second six months** of the SIBERIA project are:

4. The improvement of the ERS SAR processing chain has **taken somewhat longer** as expected but the resulting operational products are now of high quality.

Same as 3. Only a small number of JERS SAR data from the NASDA archive have been available for methodological development. **Unexpected problems** caused a further delay: e.g. break-down of DLR's MDA tape recorder, loss of tape recorder in the mail, damage of tape record after final delivery, further

program changes to NASDA's processor.
5. Problems with the understanding of the **relevance and irrelevance** of the various attributes of the extensive ground-truth database. Thanks to the excellent communication with IIASA and their Russian collaborators and the intensive discussions during the Siberia excursion a good understanding was obtained.

The main problems that have been encountered in the **third six months** of the SIBERIA project were:
Same as 3. The central database is **still incomplete** as not all JERS data have arrived or been processed. However, analysis based on existing data suggests that rule-based classification using single threshold schemes will not be able to correctly classify all test sites in this project. Instead, a data-based unsupervised approach, ISODATA, which will be linked to physical class interpretation appears a more productive and pragmatic approach.
6. The unsupervised improved ISODATA algorithm seems capable of generating very sensible results at the Bratsk test site. The immediate task to be carried out is to **test this algorithm on various test sites**. If the results can be explained using physical interpretations, a final classification approach (i.e. the *alpha-classifier*) for the Siberia project can be considered to be established.

During the **last six months** the team had to face the following problems:
7. Step-by-step improvement of competing algorithms made **postponement** of classifier decision repeatedly necessary.
8. Map design possibilities seemed to be **limited** by the software.
9. Accuracy assessment results drove the decision making process, but was **dependent** on characteristics of the used test site, number of classes, age of ground-truth.
10. **Late hand-over** of methodology (or data) for map production to Satellus started to become a worrying timing problem.

The major problem of the **post-project phase**: a severe delay of the final report. The coordinator had changed organizations and was 1) occupied with new duties, 2) disturbed by problems with the Russian Federal Security Bureau, 3) her available personal was only limited for this task, and 4) became occupied by initiating the successful follow-on project SIBERIA-II and through its contract negotiations.

4.2 Solutions

Due to shared responsibilities throughout the methodological development phase, all team members identified their work with the overall goal: the optimal adaptive classification algorithm. The above named problems could all be solved due to a common project philosophy of constructive criticism shared by all members

1. Change of consortium: several partners hired personnel later than planned, some financial problems were buffered by the understanding of the individual administrations.
2. Late topographic maps: a logistic problem only one part in an overall problem of late data delivery.
3. JERS-order: a logistic problem with many unlucky coincidences – eventually the solution came through personal engagement.
4. ERS-processing chain: more time needed than expected. Outcome though: better quality than expected. Again personal dedication was the key to the solution.
5. Ground-truth relevance: disappointing discovery that only one parameter could be used from the forest inventories to interpret the radar data. However, communication was very intense between remote sensing and forest team – both sides learned tremendously about each other's disciplines.
6. Algorithm testing: limited test sites due to delayed built-up of database (due to processing problems, points 3 and 4). No solution, but more thorough investigation of available test sites. Sharing of data between team members. Deeper discussions about algorithm development.
7. Postponement of classifier decision : a very competitive time for the Meth-Team members, but therefore successful! An optimal solution was found: the classifier was built up step-wise, combining the best algorithms from each partner's procedure.
8. Limited software: exchange of ideas and experiences between partners solved this problem.
9. Accuracy assessment driving the number of classes: some decisions had to be made by the coordinator even if the majority of the team voted for the "safer", smaller number of classes (i.e. higher accuracies). Here, the coordinator's whish for the variant with the maximum possible number of classes had to be accepted.
10. Late hand-over: this put a lot of pressure on Satellus, SIBERIA's map producer. With the help of smart software solutions using the Gamma software, time could be gained and the last maps were directly delivered to the final project meeting in Bavaria.

5 Management and Co-ordination Aspects

5.1 Change of Consortium, Personnel

The project started officially August 1, 1998. Unfortunately, one industrial partner of the original consortium, Infocarto, was not able to sign their contracts with the EC, which did not allow the finalisation of contractual matters between the consortium and the EC. Since a solution to this problem was not in sight even four months after the start of the project, it was decided to search for a new partner. Three potential partners were identified, and after consultations with all partners from the consortium, SSC Satellitbild was chosen.

Despite the delay in the finalisation of contractual matters, all partners were able to approve the recruitment of new staff or to assign permanent staff members to SIBERIA before the signature of the contract. After the first project year, changes had taken place at NERC and VTT. At NERC, new staff replaced a retired team lead. At VTT, responsibilities were transferred to new personnel due to the leaving of the respective team lead.

Six months before the project end, the coordinator changed organizations. This caused a number of formal problems, and was also a sensitive issue for the transferring organization. Related management problems are mentioned in Chapter 4.1.

5.2 Communication and Web Sites

Communication within the team and with the customers, IIASA and its Russian partners, was excellent. Progress monitoring, sharing of methodological tools, and data transfer was secured by following means:

1. Regular e-mail contact between all partners. E-mail distribution lists for the entire SIBERIA team and the methodological development group exist.
2. Monthly progress reports of the methodological team. The individual monthly partner reports are collected by SCEOS who write and distribute a summary monthly report.
3. FTP Servers at UWS, DLR-DFD, and IIASA.
4. Regular phone calls and, in the last six months of the project, weekly teleconferences.
5. Regular publication of working notes on specific topics were distributed via e-mail and integrated at the UWS web page.
6. The web pages established by IIASA and UWS (http://sunset.swan.ac.uk/siberia/, and http://www.iiasa.ac.at/Research/FOR/siberia/index.html) have proven to be very useful for the project. The initially planned web page at DLR was not implemented - instead contributions from DLR-HF were integrated at the UWS web page. The site serves to inform the public and promote the research being undertaken on the project. Encouraging feedback, on how informative the site is, has been received from colleagues in institutions not linked to SIBERIA. The web site serves also as a catalogue of image data, for the distribution of documents and meta-data and for charting the progress of all aspects of the project. The web site at http://pipeline.swan.ac.uk/siberia/ contains the following information:

- **Home Page** - lists funding, general objectives, geographical location (a map) and partner institution information.
- **What's New** - lists all the new and important project developments and recently acquired images.
- **E-mail Listing** – lists full SIBERIA group and methodology sub-group e-mail addresses
- **ERS/JERS Coverage** – lists all ERS and JERS images that have been processed. From here thumbnail and low-resolution images can be viewed. Provision is made for searching the SIBERIA project region by geographical location via point and click images.
- **Field Data** – lists important field data information and links to the IIASA web site.
- **Working Notes** – lists SIBERIA technical notes, results, EU reports and conference papers. The notes can be downloaded in either html or pdf format.
- **ERS/JERS Status** – lists the ERS and JERS satellite orbit information over the SIBERIA area.
- **Weather Data** – lists weather data for climate stations in the region.
- **Database Plots** – lists the plots of image information against forest parameters.

6 Results and Conclusions

"The main objective of the CEO Environment and Climate Programme is the generation of information for dedicated customers using Earth Observation data sources and techniques. In line with this objective, the SIBERIA project aims to produce an extensive forest map of a geographical region for which only limited information is currently available but for which detailed information is of immense scientific, environmental and commercial interest, both to specific customers and to the general population……The forest map will be derived primarily from state-of-the-art satellite data and remote sensing techniques…….The primary objective of the project is to support the development of sustainable management policies and regimes at the strategic and operative levels in order to manage the Russian forest resources in an efficient and ecological way…"(SIBERIA Proposal, Chapter 1, October 1997).

The objectives of SIBERIA are twofold: support of sustainable development and advancement of Earth Observation (EO) technologies. This chapter takes reference therefore to the proposal's first chapter on objectives and evaluates SIBERIA's results from these two perspectives.

6.1 Independent Product Quality Validation by SIBERIA´s Customers

The quality of the final product – the Forest Cover Map of East Siberia – has been checked against different independent sources including data from recent forest inventories, air photography and remote sensing data from other satellites. The indicators checked included the accuracy of the classes used in the map (six classes), consistency of polygons' boundaries, and shape and size of identified polygons. In addition, analysis of physical peculiarities of masked areas was provided.

6.1.1 Methods and materials

Two approaches were used for the validation: GIS tools and manual comparisons. The validation was provided for 10 areas or sheets of the map. The territories selected for the validation had to meet the following requirements: 1) they should include major types of vegetation (in particular, forests), the most distributed types of both landscapes and land cover mosaics, and major types of disturbances (forest fires and logging); 2) as a rule, they should not coincide with test areas which were used by the SIBERIA Project for the development of methodologies; 3) control data used should be as recent as possible and reliability of them should be known; and 4) the amount of data (by area or by number of points compared) should be large enough for statistical analysis (more than 400 for expert comparisons and more than 10^4 for the GIS approach).

For each examined territory, a relevant number of points were selected in a systematic fashion (using a square or rectangular grid) [In this context, "a point" represents an area of about 1 ha (4 pixels), if the evaluation was performed manually by professionals, and 1 pixel for the computer evaluation]. Corresponding "map" and "actual" classes were identified for each point, and frequency matrices were used for the succeeding statistical analysis (i.e., regularities of frequency distributions, measures of similarity).

GIS-based methods for spatial comparisons and validations were provided for a number of polygons, for which air photography and imagery from *RESURS* (scanner *MSU-E*, resolution about 80 m) were available and were transformed into comparable projections.

6.1.2 Results

The following conclusions can be made from the evaluations.

1. Visual comparisons of overlapping areas, size and shape of polygons that have clearly defined boundaries and low (up to 25–30 t dry matter per hectare) amounts of aboveground phytomass (recent clear-cut and burned areas, agriculture fields, bogs, wide treeless belts along roads, etc.) could be precisely identified in the radar map. We could not recognize any significant mismatch of data for these polygons.

2. The control based on comparisons of the correspondence of the six Forest cover map classes, provided by forest professionals for 7 independent areas (first 7 territories, identified in Table 6.1) was carried out in the following way: 1) the most reliable available on-ground data were used (air photography and latest forest inventory data from 1998–1999); 2) all questionable cases were checked against initial on-ground data in

map form at the scale of 1:25000; 3) five areas were partially checked directly in the field. From these results we can determine the "user accuracy". A short description of the territories examined is presented in Table 6.1. The correspondence was high for all classes. The statistics P_o (percentage of correctly classified polygons) and κ_w (Weighted Kappa coefficient, a measure of the difference between a classification result and the ground truth data, calculated by formulae (3) from 2.3.2.4 of this Report) were high: the average of P_o is 0.89 with the range for separate territories of 0.75 to 0.94 (Table 6.1), and the average for kappa k_w is 0.91 with the range from 0.73 to 0.97.

Table 6.1 *Correspondence between classes of the Radar map and on-ground data.*

N	No. of Compared Classes	Forest Enterprise	Short Description	No. of Compa-risons	Statistics	
					p_o	k_w
1	6	Emel'janovsky	Plain. Forest steppe zone. Significantly transformed Pine forests. Forest inventory of 1999 based on air photography of 1998.	1155	0.89	0.89
2	6	Shestakovsky	Hilly (up to 250-300 m) plain between Rivers Ilim and Kuna. Transformed Pine and Birch forests. Masked areas along rivers.	733	0.75	0.93
3	6	Birjusinsky	Plain. Significant areas of clear-cut and burns. Air photography of 1998, inventory of 1999.	645	0.92	0.97
4	6	Nizhne-Udinsky	Plain part. Forests are transformed by fire and logging. Significant areas of agricultural land and bogs.	897	0.94	0.97
5	6	Igirminsky	Hilly area. Basically Pine and Deciduous forests. Inventory of 1998.	900	0.94	0.96
6	6	Gremuchinsky -1	Upper terrace (plains with low hills) to the north from the Angara River. Untransformed Pine and deciduous forests. Inconsistency generated by "patching together" of different scenes.	436	0.88	0.73
7	6	Gremuchinsky -2	To the south from Gremuchinsky-1. Land-classes with low biomass are basically presented by bogs and burned areas.	466	0.89	0.91
8	4	Sljudjansky	Basically untransformed mature mountain dark coniferous forests. Southern taiga.	1440032	0.84	0.74
9	4	Primorsky	Hilly and low mountain areas along the Bratsk water reservoir. Pine, Birch and Larch forests.	1439536	0.67	0.76
10	4	Chunsky	Hilly plateau. Pine, Birch and Larch forest. Inventory 1997 with field control 2000 .	1681000	0.79	0.69

3. Overall, the results achieved by the GIS-comparisons for 4 forest classes (final 3 territories, identified in Table 6.1) are lower, but still rather high. Values of P_o varied from 0.67 to 0.84 (the average is 0.76), and for kappa k_w – from 0.69–0.76 (the average is 0.73). One explanation for this lower accuracy could be due to: 1) incomplete georeferencing of compared maps (imagery) due to unexplained reasons. It was concluded that if elements of one edge of a sheet were matched, a shift by 30 to 120 m was observed at the opposite edge of the sheet. This may be generated by either incompatibility of the cartographical products used, or by some inconsistency of the DEM, or other reasons; and 2) as control data were aggregated the real accuracy of the Radar map provided by pixel comparisons was underestimated.

4. It is important to stress that skewed representation of the forest classes overestimates the real accuracy of the map for the first three forest classes. If the most represented class (the class with growing stock >80 m^3 ha^{-1} comprises 55 to 75% of all points compared because the major part of these territories is covered by mature and overmature forests with a high growing stock) is deleted from the evaluation there is a rather weak correspondence for the first three forest classes. This is particularly evident for the territories examined by the GIS method. For instance, P_o for the areas 8,9 and 10 of Table 6.1 are, respectively, 0.63, 0.59 and 0.61.

5. Water as a class was identified correctly for all examined points.

6. The masked areas are defined by relief. We did not find any correlation between masked areas and classes of the Radar map. More than for 50% of mountain forest enterprises like Mansky and Nizhne-Udinsky (southern part) are presented by masked areas for Nevertheless, even relatively low altitude (about 50–

100m) areas could generate masked areas. For instance, for the rather smooth relief of the Igirminsky forest enterprises all masked areas were identified as "shadows" to the east from sharp changes in slope.

7. In one case (sheet D07) the strict boundary between different types of land cover mosaics did not correspond to the actual state of forest cover. One possible explanation is that this boundary was generated by "patching together" different scenes.

As a general conclusion of this evaluation, it can be stated that the Radar Forest cover map has satisfactory quality for practical applications, e.g., for monitoring of reforestation, updating obsolete forest inventory data.

6.2 Earth Observation (EO) Advances

"The working hypothesis is that the radar remote sensing data will contain sufficient information for a set of classifications of images including e.g. 1) land-use land-cover forms; 2) forests by groups of species (coniferous vs deciduous); 3) grouping by density; 4) forests by age groups (young and middle-aged stands vs mature and overmature). Land-cover forms include different types of vegetation (forest, tundra, bogs, shrubs, etc.)." (SIBERIA Proposal, p. 10)

In the two years of the SIBERIA project, 488 ERS images from 122 frames (each consisting of 3 intensity images + 1 Tandem coherence) plus more than 600 JERS-1 images were investigated. The radar backscatter and tandem coherence information was compared to an unprecedented ground-truth database in the history of remote sensing: 54 test areas, each comprising from 40,000 to 150,000 ha and consisting of 700-3000 primary land cover units (stored in GIS-polygons). Hence, the **first advance** to be mentioned is the pure capacity of handling this amount of data between research agencies, universities and SMEs.

The methodological development was governed by two conditions:

- the relatively limited image feature space compared to in-depth analyses on small geographical areas, which e.g. use multitemporal time-series instead of only 4 intensity images (SIBERIA's objective in contrary was the large-area application, which naturally -until now- limits the data sets per location);
- the forest inventory database, which contains (mostly economically) necessary information and cannot *per se* easily be compared to radar signals.

The **second advance** is the intense communication with the users and an increased knowledge of their needs, which is already influencing the feed-back of the EO-members to future sensor parameterisation.

The **third advance** concerns the hypothesis stated in the proposal: the first and third item (landcover and forest density) were, with certain restrictions, met. The second and fourth issues (species composition and age groups) could not be accomplished. Here, the stated hypothesis is a result of over-estimating the ERS temporal information content - as well as missing knowledge about the structure of natural forest stands in the boreal zone:

- the radar information content relates to *Growing Stock Volume* as the only relevant forest parameter,
- the parameter *Age* includes too large natural variations of stands (volume or height vs. age dependent on growing conditions),
- the soil contribution to backscatter signal is an unknown: coherence and intensity vary accordingly,
- fullfillment of forest inventory requirements only small, BUT SIBERIA can contribute to verify/improve global estimates,
- on this basis, a "pragmatic" model-based algorithm can be developed (exponential model to describe the correlation and saturation of ERS tandem coherence vs. volume, similar exponential model for JERS intensity).

The **fourth advance** concerns the experience of the stability of the developed algorithm, the importance of the accuracy assessment and the danger of manipulation. An intensive discussion over several months dealt with the issue of the number of classes. Even amongst the customers the opinions were polarized:

- <u>Do not delete classes</u> – loss of information! Class separations: 0 – 10 m^3/ha, 10-30 m^3/ha has a real physical content (re-growth, would help to separate between steppe and forest boundary), 30-80 m^3/ha and >80 m^3/ha (this is an important boundary to keep).

- Errors are VERY important – they will be picked up by the community for criticism. Hence, combine classes 20-50 and 50-80 for better kappa values. Suggestion for the following classes: O-10 m^3/ha: young disturbed 10-20 m^3/ha: older disturbed, re-growth 20-80 m^3/ha: disturbed (harvest, fire, insects etc.), > 80 m^3/ha: undisturbed, (> 120 m^3/ha: interesting for forest cutting).
- Recommendation from a pure accuracy point of view: only 2 forest classes!

Another issue concluded the discussion: Spatial integrity of the map has a much higher value and is beyond the numbers from accuracy assessment. There is information in the contextual location in the map for classes 20-50 and 50-80. Therefore, six instead of four classes were chosen. Fortunately. Because with every update of the ground-truth database the map accuracies improved. This confirmed, that the methodological algorithm development had reached the best possible solution and the flexible factor for map quality estimations was the accuracy and up-datedness of the ground database.

As a general conclusion, SIBERIA's methodological development has produced and verified that radar remote sensing enables the generation of a land-cover mapping algorithm, that is automatic (because of the large amount of data to be handled), adaptive (because of changes in image properties between scenes, caused by imaging geometry and environmental variations), consistent (so that the assignment of information would not be scene-dependent and overlapping scenes would show no discontinuities), and validated (to assign some degree of confidence to the results).

Further on-going work includes analysis of multitemporal tandem pairs (only available for limited number of test sites) and JERS-1 repeat-pass coherence. The latter one is also existing over the full project area and is an additional, originally not planned product which contains very interesting information, as first analyses showed. The investigation of synergy effects between optical and radar data could not be performed as planned due to limited availability of optical data.

6.3 Conclusions

The SIBERIA proposal lists in its second chapter on Work Content a list of items of special concern to the customers. Table 6.2 compares the stated needs to what has been accomplished at the present state. The table illustrates major advancements, but also topics where SIBERIA's map will serve necessary further investigations.

Table 6.2 *SIBERIA's accomplishments ("√" = accomplished, "+" = crucial advances/further work necessary, "-" = not accomplished)*

Customer's needs (SIBERIA Proposal, p. 6)	*Accompl.*
Actual state, productivity and stability of Russian boreal forests, with special emphasis on the remote northern regions.	+
Sustainable structure of landscapes.	+
Disturbances on areas affected by e.g. forest fires, insect damages, cuttings, air pollution	√
Overall status on the distribution between primary and secondary forests, including harvested areas	-
Species composition regarding coniferous and deciduous	-
Natural regeneration status	√
Rough distribution of volume classes	√
Transportation infrastructure including road network	√
Human transformation of terrestrial biota (natural landscapes) along the Baikal-Amur-Magistrale main railroad	+
Data which can support analyses of long-term succession dynamics, treeline shifting, and permafrost behavior	√
Indicators of surface parameters (temperature, humidity, extent of permafrost) which can be used as variables for forecasting the risk of large-scale disturbances (e.g., forest fire).	-

Before the project started, the following risks of failure had been identified (SIBERIA Proposal, p. 24):

- *how to correct for the influence of the local incidence angle on the backscatter signal,*
- *how to deal with co-registration problems (if any),*
- *how strong are the climatological impacts to the radar signal between swaths?*
- *The main risk to face is the tight timeline of the project.*

All four risks had to be faced during SIBERIA's lifetime. The first and second lead to the masking procedure, which, because of the fourth item "time" resulted in the unfortunate large masking pixels in SIBERIA's Forest Cover Map. For 40% of the project area, where interferometric DEMs could be produced, the masked pixels could have been retrieved from the GTC-products (resulting in 50 m masking pixels), but since time was running late, the global GTOPO30-topographic information had to be applied (resulting in 1000 m masking pixels, i.e. a loss of possibly mapped area by the factor 20).

Finally, sustainability has to be discussed. SIBERIA's forest map is being used at the time of this writing for comparison with climate and fire model results at the Max-Planck-Institute for Biogeochemical Cycles at Jena, at the Modelling Group of CESBIO, and at the Sukachev Forest Institute in Krasnoyarsk in cooperation with the Max-Planck-Institute for Fire Ecology in Freiburg, Germany. The database is part of GOFC (Global Observation of Forest Cover) and GBFM (Global Boreal Forest Mapping) activities. American requests are also listed. The complete database is being archived at the Friedrich-Schiller-University Jena and at every time accessible for data copies. Original satellite data are restricted, the re-sampled image stacks and forest map can be distributed. The final report including all material from SIBERIA's webpage will be distributed on CD internationally.

The Russian customers will use the Forest Cover and the Radar Image Maps to update their database on disturbances. It is extremely relevant, what different types of burning and levels of biomass were identified. The Irkutsk district possesses digitised 1:200.000 maps. These maps will be updated using SIBERIA's maps for the classes forest, water, open and 0-20 m^3/ha class only. The forest enterprise inventories should be updated every 10-15 years, but this cannot be accomplished everywhere under today's economic conditions. During the last 5 years only 7 Mio ha were inventoried (Irkutsk oblast alone encompasses 70 Mio ha, i.e. it would take 50 years until the inventory returns to same site!). In addition, the error factor is 3 to 10 for estimating fire, insect infestation and snow break. All-Russian numbers for forest inventories in 1991: 50 Mio ha (only 5% of total area), 1998: 27 Mio (2.7 %), 2000: 17 Mio ha (1.7%). The techniques applied in the SIBERIA project therefore have large potential to be applied to existing satellite data sets to produce a base map. This would be of great benefit for the Russian forest inventory as well as for the scientific community.

SIBERIA has demonstrated for the first time, the large-area operational generation of a thematic map with Earth Observation techniques purely. Future monitoring of this region with immense environmental, scientific and commercial interest will be possible with Envisat, ALOS and SIBERIA's map as a basis. SIBERIA is an example for a very successful European-Russian cooperation. In the 5th Framework Program, the European Community has granted the continuation of this outstanding international collaboration: SIBERIA-II, Multi-Sensor Concepts for Greenhouse Gas Accounting of Northern Eurasia.

7 Acknowledgements

SIBERIA is a shared-cost action (SCA) financed through the 4th Framework Programme of the European Commission, Environment and Climate, Area 3.3: Center for Earth Observation, Theme 3: Space Techniques Applied to Environmental Monitoring (Contract No. ENV4-CT97-0743-SIBERIA). SIBERIA's work is based on extensive satellite data made available through ESA's 3rd ERS Announcement of Opportunity (Project Number AO3.120 (SIBERIA) and NASDA's JERS initiative "Global Boreal Forest Mapping". The satellite datawere received by a mobile receiving station of the German Remote Sensing Data Center of DLR (DFD), which was deployed for this purpose in Ulaanbaatar, Mongolia. The actvities of VTT Automation in SIBERIA project were partly funded by the Academy of Finland (project 47027), DLR's and later FSU's activities were partly funded by BMBF/DLR-project RD-RE-ERWI50EE9725-50EE9725/7.

This short official acknowledgement does not reflect the tremendous engagement of many individuals from the various agencies. Without the great generous support of DLR, ESA and NASDA the project idea could have not been realized from the beginning. A very crucial person was Klaus Reiniger from DLR-DFD, who immediately and enthusiastically took action to fulfil an extremely tight time-schedule for the deployment of a mobile receiving station in Mongolia.

The SIBERIA team would like to further extend its sincere thanks to Ake Rosenqvist/NASDA (who gave the spark to the project idea through his GBFM initiative), to Wolfgang Keydel, Wolfgang Mett and David Hounam/DLR (who had to suffer through the search of funding), to Klaus Schmidt and Peter Ritter/DLR (who made contacts happen – both count as the first project supporters), to Guy Duchossois, Gunter Kohlhammer and Henri Laur/ESA (who worked hard for an originally not planned Tandem mission), to Masanobu Shimada/NASDA and Norbert Bauer und Rainer Lorenz/DLR (they saved the project goal with their tremendous initiatives to solve never ending JERS transfer format problems between special recorders and special processors), and to Rudolf Winter and Jean-Paul Malingreaux/JRC (who helped to lift-off the project with a first funding).

Very special thanks go to our EC CEO Scientific Officer Martin Sharman, who was from the first conversations an always encouraging contact with a big passion for the science being performed and an open mind for the problems which had to be encountered. He, together with our Financial Officer Katleen Engelbosch, helped us to survive through many contractual problems.

Missing, because working in the background, is the personnel with Prof. Ganzorig in Ulan-Bator, the Russian foresters, DLR's station and ERS's orbit personnel, and all institution's administrative staff that had been involved.

The coordinator would also like to thank the whole SIBERIA Project Team for always being fully dedicated to the overall project goal, always performing fair-play, never putting personal ambitions above the team effort, to have patience and sympathy with each other's (and especially the coordinator's) flaws, for everybody's humour and just being the most wonderful team to work (and play) hard with.

8 References

8.1 Cited Literature

SIBERIA Webpage: http://pipeline.swan.ac.uk/siberia/

ARNOFF, S., 1982: The map accuracy report: a user's view.- Photogrammetric Engineering and Remote Sensing, vol. 48, pp.1309-1312.

ASKNE J., P. DAMMERT, L. M. H. ULANDER, and G. SMITH, 1997: C-band repeat pass interferometric SAR observations of forests.- IEEE Transactions on Geoscience and Remote Sensing, vol. 38.

BALZTER, H., E. TALMON, J. J. YU, S. QUEGAN, D. GAVEAU, M. GLUCK, S. NILSSON, K. TANSEY, A. OESKOG, A. ROTH, and C. SCHMULLIUS, 2000: Accuracy assessment of a large-scale forest map of Central Siberia derived from multi-sensor satellite-borne Synthetic Aperture Radar interferometry (InSAR).- In Accuracy 2000: Proceedings of the 4th International Symposium on Spatial Accuracy Assessment in Natural Resources and Environmental Sciences, edited by G. B. M. HEUVELINK and M. J. P. M. LEMMENS, 12-14 July 2000, (Amsterdam: Delft University Press), pp. 31-34.

BAMLER, R., and P. HARTL, 1998: Synthetic aperture radar interferometry.- Inverse Problems, 14, R1-R54.

BESAG, J., 1986: On the statistical analysis of dirty pictures.- Journal of the Royal Statistical Society B, vol. 48, no. 3, pp. 259-302.

BRUNIQUEL, J., and A. LOPES, 1997: Multi-variate optimal speckle reduction in SAR imagery.- International Journal of Remote Sensing, vol. 18, pp. 603-627.

BRYANT, D., D. NIELSEN, and L. TANGLEY, 1997: The Last Frontier Forests: Ecosystems & Economies on the Edge.- Report from World Resources Institute – Forest Frontiers Initiative.

COHEN, J., 1960: A coefficient of agreement for nominal scales.- Educational and Psychological Measurement, vol. 20, pp. 37-46.

COHEN, J., 1968: Weighted kappa: nominal scale agreement with provision for scaled disagreement or partial credit.- Psychological Bulletin, vol. 70, pp. 213-220.

DEVIJVER, P. A., and J. KITTLER, 1982: Pattern recognition, (London: Prentice-Hall).

DOWMAN, I., 1992: The geometry of SAR images for geocoding and stereo applications.- International Journal of Remote Sensing, vol. 13, pp. 1609-1617.

EINEDER, M., and N. ADAM, 1997: A Flexible System for the Generation of Interferometric SAR Products.- Proceedings of the IGARSS'97.

FFS. 1995: Manual for forest inventory and planning of the Forest Fund of Russia. Volume 1. Field works, 175 pp. Volume 2. Information processing and planning, 180 pp. Federal Forest Service of Russia, Moscow [in Russian].

FOODY, G. M., 1992: On the compensation for chance agreement in image classification accuracy assessment.- Photogrammetric Engineering and Remote Sensing, vol. 58, pp. 1459-1460.

FOODY, G. M., G. PALUBINSKAS, R. M. LUCAS, P. J. CURRAN, and M. HONZAK, 1996: Identifying terrestrial carbon sinks: Classification of successional stages in regenerating tropical forest from Landsat TM data.- Remote Sensing of Environment, vol. 55, pp. 205-216.

FRANSSON, J. E. S., and H. ISRAELSSON, 1999: Estimation of stem volume in boreal forests using ERS-1 C- and JERS-1 L-band SAR data.- International Journal of Remote Sensing, vol. 20, pp. 123-137.

GENS, R., and J. L. VANGENDEREN, 1996: SAR interferometry - Issues, techniques, applications.- International Journal of Remote Sensing, vol. 17, pp. 1803-1835.

GIER A. DE, E. WESTINGA, and S. BEERENS, 1999: User requirements study for remote sensing based on spatial information for the sustainable management of forests.- Final Report. ITC, (Wageningen, The Netherlands), 25 pp.

GONIN, R., S. R. LIPSITZ, G. M. FITZMAURICE, and G. MOLENBERGHS, 2000: Regression modelling of weighted kappa by using generalized estimating equations.- Journal of the Royal Statistical Society Series C-Applied Statistics, vol. 49, pp. 1-18.

HAGBERG, J. O., L. M. H. ULANDER and J. ASKNE, 1995: Repeat pass SAR interferometry over forested terrain.- IEEE Transactions on Geoscience and Remote Sensing, vol. 33, pp. 231-240.

HÄME, T., I. HEILER, and J. SAN-MIGUEL AYANZ, 1998: An unsupervised change detection and recognition system for forestry.- International Journal of Remote Sensing, vol. 19, no. 6, pp. 1079-1099.

HÄME, T., P. STENBERG, and Y. RAUSTE, 2000: A new methodology to estimate forest variables at sub-pixel level.- Proc. of IUFRO, Conference on Remote Sensing and Forest Monitoring. Rogow, Poland, 1 - 3 June 1999, in print.

JANSSEN, L. L. F., and F. J. M. VAN DER WEL, 1994: Accuracy assessment of satellite-derived land-cover data - a review.- Photogrammetric Engineering and Remote Sensing, vol. 60, pp. 419-426.

KIDWELL, K., 1984: NOAA polar orbiter data (TIROS-N, NOAA-6, NOAA-7, and NOAA-8) users guide. (NOAA, Washington DC, USA), 145 pp.

KLEMAN, J., 1986: The spectral reflectance of stands of Norway spruce and Scotch pine, measured from a helicopter.- Remote Sensing of Environment, vol. 20, pp 253-265.

KWOK, R., J. C. CURLANDER, and S. S. PANG,: Rectification of terrain induced distortions in radar imagery.- Photogrammetric Engineering and Remote Sensing, vol. 53, pp. 507-513.

LE TOAN, T., A. BEAUDOIN, J. RIOM, and D. GUYON, 1992: Relating forest biomass to SAR data.- IEEE Transaction on Geosciences and Remote Sensing, vol. 30, no. 2, pp 403-411.

LE TOAN, T., and N. FLOURY, 1998: On the retrieval of forest biomass from SAR data.- Int. Workshop on Retrieval of bio-geophysical parameters using SAR data for land applications, ESTEC, ESA SP-441, pp. 595-600.

LE TOAN, T. et al., 1999: European Forest Observation with Radars (EUFORA).- European Commission Directorate-General XII, ERBENV4CT/960303, Final Report, May 1999, 154 pp.

LOWELL, K., and A. JATON, 2000: Spatial accuracy assessment. Land information uncertainty in natural resources, (Chelsea, MI: Ann Arbor Press).

LUCKMAN, A., J. BAKER, T. M. KUPLICH, C. da COSTA FREITAS YANASSE, and A. FRERY, 1997: A study of the relationship between radar backscatter and regenerated tropical forest for spaceborne SAR instruments.- Remote Sensing of Environment, vol. 60, pp. 1-13.

MA, Z. K., and R. L. REDMOND, 1995: Tau coefficients for accuracy assessment of classification of remote sensing data.- Photogrammetric Engineering and Remote Sensing, vol. 61, pp. 435-439.

MALYSHEVA, N., A. SHVIDENKO, S. NILSSON, S. PETELINA, A. ÖSKOG, 2000: An overview of remote sensing in Russian forestry.- Interim Report IR-00-34. (International Institute for Applied Systems Analysis, Laxenburg, Austria), 83 pp.

MORISETTE, J. T., and S. KHORRAM, 2000: Accuracy assessment curves for satellite-based change detection.- Photogrammetric Engineering and Remote Sensing, vol. 66, pp. 875-880.

NAESSET, E., 1996: Conditional tau coefficient for assessment of producer's accuracy of classified remotely sensed data.- ISPRS Journal of Photogrammetry and Remote Sensing, vol. 51, pp. 91-98.

NAESSET, E., 1996: Use of the weighted kappa coefficient in classification error assessment of thematic maps.- International Journal of Geographical Information Systems, vol. 10, pp. 591-603.

NILSSON, S., A. SHVIDENKO, V. STOLBOVOI, M. GLUCK, M. JONAS and M. OBERSTEINER (2000): *Full Carbon Account for Russia. IR-00-021*. Laxenburg, Austria: International Institute for Applied Systems Analysis.

NISHII, R., and S. TANAKA, 1999: Accuracy and inaccuracy assessments in land-cover classification.- IEEE Transactions in Geoscience and Remote Sensing, vol. 37, pp. 491-498.

NOVAK, L. M., M., C. BURL, and W. W. IRVING, 1993: Optimal polarimetric processing for enhanced target detection,- IEEE Transactions on Aerospace Electronic Systems, vol. 29, pp. 293-305.

OLIVER, C., and S. QUEGAN, 1998: Understanding Synthetic Aperture Radar Images, (Artech House).

PULLIAINEN J., K. HEISKA, J. HYYPPÄ, and M. HALLIKAINEN, 1994: Backscattering properties of boreal forests at C and X bands.- IEEE Transactions on Geoscience and Remote Sensing, vol. 32,no 5, pp 1041-1050.

QUEGAN, S., J. J. YU, and T. LE TOAN, 2000[(a)]: Iterated multi-channel filtering of SAR images.- Proceedings of the IGARSS 2000, Honolulu, USA.

QUEGAN, S., J. J. YU, H. BALZTER, and T. LE TOAN, 2000[(b)]: Combining unsupervised and knowledge-based methods in large-scale forest classification.- Proceedings of the IGARSS 2000, Honolulu, USA.

QUEGAN S., T. LE TOAN, J. J. YU, F. RIBBES, and N. FLOURY, 2000[(c)]: Estimating temperate forest area with multitemporal SAR data.- IEEE Transactions on Geoscience and Remote Sensing, vol. 38, no 2, pp. 741-753.

QUEGAN, S., T. LE TOAN, J. J. YU, F. RIBBES, and N. FLOURY, 2000[(c)]: Multitemporal ERS SAR analysis applied to forest monitoring.- IEEE Transactions of Geoscience and Remote Sensing, vol. 38, pp. 741-753.

RAHMAN, H., G. DEDIEU, 1994: SMAC: a simplified method for the atmospheric correction of satellite measurements in the solar spectrum.- International Journal of Remote Sensing, vol. 15, no. 1, pp. 123-143.

ROTH, A., W. KNOPFLE, M. HUBIG, and N. ADAM, 1998: Operational interferometric SAR products.- Proceedings of the IGARSS'98, 6-10th July 1998, Seattle, USA, vol. 1, pp. 324-326.

ROTH, A., W. KNÖPFLE, B. RABUS, S. GEBHARDT, and D. SCALES, 1999: GeMoS – A System for the Geocoding and Mosaicking of Interferometric Digital Elevation Models.- Proceedings of the IGARSS'99, Hamburg, Germany, 28 June - 2 July 1999, vol. 1, pp. 631-633.

SCHREIER, G., 1993: Geometrical properties of SAR images.- In SAR geocoding: Data and systems, edited by G. Schreier (Karlsruhe: Wichmann), pp. 103-134.

SHIMADA, M., 1996: Radiometric and Geometric Calibration of JERS-1 SAR.- Advanced Space Research, vol. 17, pp. 79-88.

SHIMADA, M., 1999: Verification processor for SAR calibration and interferometry. -Advances in Space Research, vol. 23, pp. 1477-1486

SHVIDENKO, A., S. VENEVSKY, G. RAILE, and S. NILSSON, 1995: A system for evaluation of growth and mortality in Russian forests.- Water, Air and Soil Pollution 82 (1–2), pp. 333–350.

SMIRNOV, A. V., 1969: Forests of Irkutsk oblast. In ZHUKOV, A. B., (ed.), Forests of the USSR. Volume 4. Forests of Ural, Siberia, and Far East, pp. 350-387 [in Russian]

SMITH, G., P. B. G. DAMMERT, M. SANTORO, J. E. S. FRANSSON, U. WEGMULLER, and J. ASKNE, 1998: Biomass retrieval in boreal forest using ERS and JERS SAR.- In International Workshop on the Retrieval of Bio-Geophysical Parameters Using SAR Data for Land Applications, ESTEC, ESA SP-44.

SOKOLOV, V. A., et al., 1997: Backgrounds of management of Siberian forests. Siberian Branch, Russian Academy of Sciences, Krasnoyarsk, 309 pp [in Russian]

SOKOLOV, V. A., I. M. DANILIN, S. K. FARBER, et al., 1998: Problems of sustainable forest use. Siberian Branch, Russian Academy of Sciences, Krasnoyarsk, 230 pp [in Russian]

SOUYRIS, J. C, T. LE TOAN, N. FLOURY, C. C. HSU, and J. A. KONG, 1995: Inversion of forest biomass using SIR C/X-SAR data.- International Workshop on the Retrieval of Bio-Geophysical Parameters from SAR Data, Toulouse, pp. 67-78.

TOUGH, R. J. A., D. BLACKNELL, and S. QUEGAN, 1995: A statistical description of polarimetric and interferometric synthetic-aperture radar data.- Proceedings of the Royal Society of London Series A-Mathematical and Physical Sciences, vol. 449, pp. 567-589.

VAN ZYL, J. J., and C. F. BURNETTE, 1992: Bayesian classification of polarimetric SAR images using adaptive a priori probabilities.- International Journal of Remote Sensing, vol. 13, no. 5, pp. 835-840.

VAN ZYL, J. J., 1993: The effect of topography on radar scattering from vegetated areas.- IEEE Transactions on Geoscience and Remote Sensing, vol. 31, pp. 153-160.

VAN ZYL, J. J., B. D. CHAPMAN, P. DUBOIS, and J. SHI, 1993: The effect of topography on SAR calibration.- IEEE Transactions on Geoscience and Remote Sensing, vol. 31, no. 5, pp. 1036-1043.

VASCHUK, L. N., (ed.), 1997: Forests and forest management of Irkutsk oblast. Irkutsk Forest Management Service, Irkutsk, 287 pp [in Russian]

WEGMÜLLER, U., and C. L. WERNER, 1997: Gamma SAR processor and interferometry software, 3rd ERS Symposium, Florence, 18-21 March 1997.

WIESMANN, A., T. STROZZI, and U. WEGMÜLLER, 1999: JERS SAR processing for the boreal forest mapping project SIBERIA.- Proceedings of the IGARSS'99, Hamburg, Germany, 28 June - 2 July 1999.

WIESMANN A., U. WEGMÜLLER, and T. STROZZI, 1999: JERS SAR processing for the boreal forest mapping project SIBERIA.- Proceedings of the CEOS SAR Workshop, Toulouse, France, 26-29 Oct. 1999, ESA SP-450, 2000a.

WIESMANN A., U. WEGMÜLLER, T. STROZZI, and C.L. WERNER, 2000: The use of JERS SAR within the boreal forest mapping project SIBERIA.- Proceedings of the IGARSS 2000, Honolulu, USA, 24-28 July 2000, 2000b.

ZHUKOV, A. B., I. A. KOROTKOV, V. P. KUTAFEV, et al., 1969: Forests of Krasnoyarsk kray. In Forests of the USSR. Volume 4. Forests of Ural, Siberia, and Far East, edited by A. B. Zhukov, pp. 248-320 [in Russian].

8.2 SIBERIA Project Publications (Status June 2001)

8.2.1 Working Notes (Reference: http://pipeline.swan.ac.uk/siberia/)

1. Coherence (Malcolm Davidson - CESBIO - February 1999).
2. Filtering (S. Quegan and J.J. Yu - SCEOS - February 1999).
3. Analysis of Backscatter and Coherence as Functions of Age - Bratsk site (J.J. Yu and S. Quegan - SCEOS - March 1999).
4. Estimation of Coherence (Nico Adam, Michael Jubig - DLR - October 1998 - Old document from DLR).
5. Image Generation of the DLR Interferometric Processor (Bernhard Rabus, Nico Adam - DLR - October 1998 - Old document from DLR).
6. SUN RASTER file format (DLR - October 1998).
7. Working Note on Calibration using CALIT (Jan Wietmeier - DLR - 25th March 1999).
8. Working Note on Intellectual Property Rights (A. Luckman and K. Tansey - UWS - 29th March 1999).
9. Working Note on Linking Ground Data and SAR Images for Test-site Ust-Illimsk (Heiko Balzter - ITE - 24th April 1999).
10. Analysis of ERS SAR Information Content of the Ulkanskii (Lake Baikal) Test Territory (K. Tansey and A Luckman - UWS - 6th May 1999).
11. State of JERS SAR Processing over SIBERIA (Gamma Remote Sensing - 7th May 1999).
12. Methods of Accuracy Assessment in the Siberia Project (Heiko Balzter - ITE - 21st June 1999).
13. ERS SAR Ordering and Assignation (W. Wagner, DLR-HF, April and May 1999).

14. JERS SAR Prioritisation (W. Wagner, May 1999).
15. Methods of Accuracy Assessment in the Siberia Project (Heiko Balzter - ITE - 21st June 1999)
16. Treatment of extreme topography in GEC and GEC_GLOBE images (Heiko Balzter - ITE - 9th September 1999)
17. Analysis and interpretation of ‘strange’ outliers at the northern Irbeiskii test site (Kevin Tansey - UWS - 20th September 1999)
18. Comparison of slope estimates from the InSAR DEM and GTOPO’30 (Kevin Tansey - UWS - 20th September 1999)
19. Classification of boreal forest (Ust-Illimsk) with maximum likelihood classification (David Gaveau - ITE - 6th October 1999) PDF format (2.4 Mb)
20. Coherence analysis of all processed test sites (Thuy le Toan & Malcolm Davidson - CESBIO - 19th October 1999)
21. Analysis of the information content of three texture measures of ERS amplitude and coherence (Heiko Balzter et al. - ITE - 26th October 1999) PDF format
22. Investigation of image properties in the SIBERIA project (J.J. Yu and S. Quegan - ITE - 26th October 1999) PDF format (2.0 Mb)
23. First results of database analysis for Bolshemurtinskii (W. Wagner, J. Vietmeier, C. Schmullius & A. Holz - DLR - 4th November 1999) PDF format
24. Use of the ERS coherence for forest classification (W. Wagner - DLR - 9th December 1999) PDF format
25. Boxplots of texture statistics against land use class (H. Balzter, D. Gaveau & S. Plummer - ITE - 21st December 1999) PDF format
26. The Iterated Contextual Probability (ICP) classifier (H. Balzter & J. Baker (RSAC) - ITE - 11th January 2000) PDF format
27. Ground offsets during coregistration of JERS-1 and ERS images (H. Balzter & K. Tansey - ITE/UWS - 14th January 2000) PDF format
28. Results of the application of the topography mask to the resampled GTOPO’30 DEM for 2 ERS frames (K. Tansey & A. Luckman - UWS - 14th January 2000)
29. Working note of histogram generation (M. Davidson - CESBIO - 18th January 2000) PDF format
30. Pixel histograms for selected test sites (no supporting text) (D. Gaveau - ITE - 18th January 2000) PDF format
31. Comments and summary: Ground offsets during coregistration of JERS-1 and ERS images (J. Vietmeier & W. Wagner - DLR - 20th January 2000) PDF format
32. Report on coregistration using GAMMA software (K. Tansey - UWS - 31st January 2000) PDF format
33. Boreal Forest INSAR Classification Properties (D. Gaveau - ITE - 1st February 2000) PDF format
34. Extended Accuracy Assessment of Coherence Model(W. Wagner & J. Vietmeier - DLR - 16th February 2000) PDF format
35. Use of ERS Backscattering Coefficient for Forest Classification (W. Wagner & J. Vietmeier - DLR - 18th February 2000) PDF format

Report: Wagner, Wolfgang, Schmullius, C., Balzter, H., Davidson, M., Gaveau, D., et al.: SIBERIA - 1st Progress Report. EC Center for Earth Observation, Project Reports, Contract No. ENV4-CT97-0743-SIBERIA, http://pipeline.swan.ac.uk/siberia/ (1999).

Report: Wagner, Wolfgang, Schmullius, C., Balzter, H., Davidson, M., Gaveau, D., et al.: SIBERIA - 2nd Progress Report. EC Center for Earth Observation, Project Reports, Contract No. ENV4-CT97-0743-SIBERIA, http://pipeline.swan.ac.uk/siberia/ (1999).

Report: Schmullius, C., W.Wagner, A.Roth, J.Vietmeier, U.Marschalk, A.Holz, L.Eriksson, S.Nilsson, A.Shvidenko, M.Gluck, T.LeToan, M.Davidson, S.Quegan, J.J.Yu, A.Luckman, K.Tansey, H.Balzter, D.Gaveau, Y.Rauste, Orrmalm, M. R.Utsi, U.Wegmüller, A .Wiesmann, V.Skudin, L.Vaschuk, V.Sokolov, V.Rozhkov (2000): SIBERIA – 3rd Progress Report. EC Center for Earth Observation, Project Reports, Contract No. ENV4-CT97-0743-SIBERIA, 66 Seiten, http://pipeline.swan.ac.uk/siberia/.

8.2.2 Journals, Conference Papers, Institutional Reports

ANDERSEN, G. and G. Banko (1998): A Satellite Based Study of Ust-llimsk Focusing on Clearcuts. IR-98-087. Laxenburg, Austria: International Institute for Applied Systems Analysis.

ANDERSEN, G.L. (1998) Classification and Estimation of Forest and Vegetation Variables in Optical High Resolution Satellites: A Review of Methodologies. IR-98-085. Laxenburg, Austria: International Institute for Applied Systems Analysis.

BALZTER, H., Talmon, E., Wagner, W., Gaveau, D., Plummer, S., Yu, J.J., Quegan, S., Gluck, M., Shvidenko, A., Tansey, K., Luckman, A. and Schmullius, C. (submitted 03/2001): Accuracy assessment of a large-scale forest map of Central Siberia from Synthetic Aperture Radar. Canadian Journal of Remote Sensing.

BALZTER, H. and Schmullius, C. (2001): Mapping Siberian forests. GIM International 15, 40-43.

BALZTER, H., Talmon, E., Gaveau, D., Yu, J.J., Quegan, S., Gluck, M., Tansey, K., Luckman, A., Wagner, W. and Schmullius, C. (2000): Accuracy assessment issues in the SIBERIA project. Proceedings of the ESA ERS-Envisat Symposium, Gothenburg, 16-20 Oct 2000, CDROM.

BALZTER, H., Talmon, E., Yu, J.J., Quegan, S., Gaveau, D., Gluck, M., Nilsson, S., Tansey, K., Oeskog, A., Roth, A. and Schmullius, C. (2000): Accuracy assessment of a large-scale forest map of Centra**Fehler! Keine Indexeinträge gefunden.**l Siberia derived from multi-sensor satellite-borne Synthetic Aperture Radar interferometry (InSAR). In: Heuvelink, G.B.M. and Lemmens, M.J.P.M. (editors): Accuracy 2000: Proceedings of the 4th International Symposium on Spatial Accuracy Assessment in Natural Resources and Environmental Sciences, Amsterdam, 12-14 July 2000, Delft University Press, 31-34.

BALZTER, H. (2000): Mapping of Siberian forests, CEH Annual Report, p. 27.

BALZTER, H. and Shvidenko, A. (2000): Map accuracy report, SIBERIA forest cover map. Technical report supplementing the map product, DLR, Oberpfaffenhofen, October 2000.

BALZTER, H. (1999): The iterated contextual probability classifier (ICP): An application to forest age classification in Siberia.-IEEE 1999 International Geoscience and Remote Sensing Symposium (IGARSS '99) 28/6-2/7/99, Hamburg.

BANKO, G. (1998) A Review of Assessing the Accuracy of Classifications of Remotely Sensed Data and of Methods Including Remote Sensing Data in Forest Inventory. IR-98-081. Laxenburg, Austria: International Institute for Applied Systems Analysis.

DAMMERT, P. and U. Wegmüller (1999): JERS INSAR DEM quality assessment for a boreal test site.- Proceedings of IGARSS'99, Hamburg, 28 June - 2 July 1999 (D03_03).

ERIKSSON, L., Wiesmann, A., and C. Schmullius (2001): JERS repeat pass coherence for observation of Siberian forest.- LandSAR Conference, 11-14 September, Sheffield (accepted).

ERIKSSON, L., and C. Schmullius (2001): ERS multitemporal coherence for observation of Siberian forest.- LandSAR Conference, 11-14 September, Sheffield (accepted).

ETZROTH, N., Zimmermann, R.; Dempewolf, J.; Ziegler, W.; Vietmeier, J.; Holz, A. (1999): Classification of Central Siberian Forest Types by Combining interferometric Radar Remote Sensing (ERS Tandem Mission, JERS), Topographical Data and Ecophysiological Information. IGARSS'99, 28. June - 02. July 1999, Hamburg, Germany, pp. 720-722.

FROTSCHER, K. & C. Schmullius (2001): A Comparison of SAR-Interferomety- and cartographically generated Digital Elevation Models by errors, accuracies and extracted hydrographic features. - Proceedings of the ERS – ENVISAT Symposium. Looking down to Earth in the New Millennium. 16 – 20 October 2000, Gothenburg, Schweden.

GAVEAU, D.L.A., Balzter, H. and Plummer, S. (2000): Boreal forest InSAR classification properties. Proceedings of the CEOS SAR Workshop, Toulouse, 26-29 Oct. 1999, ESA SP-450, 509-512.

GLUCK, M., G. Banko and W. Vrzal (2000) Harnessing Remote Sensing to Accomplish Full Carbon Accounting: Workshop Report. IR-00-010. Laxenburg, Austria: International Institute for Applied Systems Analysis.

GLUCK, M.J. and R.S. Rempel (1996). The effect of spatial resolution on measurements of landscape structure. Advances in Remote Sensing 4:170–176.

JONAS, M., S. Nilsson, A. Shvidenko, V. Stolbovoi, M. Gluck, M. Obersteiner and A. Öskog (1999) Full Carbon Accounting and the Kyoto Protocol: A Systems-Analytical View. IR-99-025. Laxenburg, Austria: International Institute for Applied Systems Analysis.

KAJII, Y., S. Kato, D.G. Streets, N.Y. Tasai, A. Shvidenko, S. Nilsson, I. McCallum, N.P. Minko, N. Abushenko, D. Altyntsev and T.V. Khodzer (forthcoming) Boreal Forest Fires in Siberia in 1998: Estimation of Area Burned and Emissions of Pollutants by AVHRR Satellite Data. Submitted July 2001 to Journal of Geophysical Research. 12 pp.

LE TOAN, T., H. Balzter, M. Davidson, D. Gaveau, A. Luckman, S.Quegan, C. Schmullius, K. Tansey, W. Wagner and J.J. Yu (2000): Assessing SAR information content for large scale forest mapping in Siberia.- IGARSS 2000, Honolulu.

LE TOAN, T. (2000): Radar Remote sensing of forests.- Invited keynote paper. Proceedings of the Int. Symposium EMEA 2000, 17 pp, Kanazawa, August 2000.

LE TOAN, T., S. Quegan, M. Davidson, J.M. Martinez (2001): Radar remote sensing of forests. Applications using existing satellite SAR data.- Proceedings of The 8th Int. Symposium Physical measurements and Signatures in Remote Sensing, Aussois, January 2001, pp 33-40.

LE TOAN, T. (2001): Contribution of radar remote sensing to the estimates of C budget in forests.- Proceedings of the CEOS SAR Cal-val meeting, Tokyo, April 2001.

LUCKMAN, A., Tansey, K., Schmullius, C., et al., (submitted): The construction of ERS-tandem and JERS SAR image mosaics for large-scale mapping of boreal forest in Siberia. International Journal of Remote Sensing.

NILSSON, S., A. Shvidenko, V. Stolbovoi, M. Gluck, M. Jonas and M. Obersteiner (2000) Full Carbon Account for Russia. IR-00-021. Laxenburg, Austria: International Institute for Applied Systems Analysis.

PETELINA, S.V. (1998) Optical Model of Atmospheric Aerosols in Russian Siberia for Collection of Satellite Data. IR-98-078. Laxenburg, Austria: International Institute for Applied Systems Analysis.

SAKHATSKY, A.I., A.Y. Khodorovsky, I.J. Bujanova and I. McCallum (forthcoming IIASA Interim Report) Classification of space images for forest state identification within the Siberia region – Part 1.

SCHMULLIUS, C., Holz, Andrea,, Vietmeier, Jan, Zimmermann, Reiner, Etzroth, Norbert (1998): SIBERIA - Sar Imaging for Boreal Ecology and Radar Interferometry Applications: First ERS Tandem Results form the IGBP Boreal Forest Transect. - Second International Workshop on Retrieval of Bio- & Geo-physical Parameters from SAR Data for Land Applications, 21-23 October 1998, ESTEC Noordwijk, ESA ESTEC, Retrieval of Bio- & Geo-physical Parameters from SAR Data for Land Applications, p. 365-370, ESA Publications Division.

SCHMULLIUS, C. (1998): SAR Imaging for Boreal Ecology and Radar Interferometry Applications. - International Workshop on Ecological and economic problems in the boreal woodlands of Russia, EU/Sächsisches Staatsministerium für Landwirtschaft, Ernährung und Forsten/TU Dresden, 2-6 July 1998, WorkshopProceedings,p.99-100.

SCHMULLIUS, C., Holz, A.; Vietmeier, J. (1999): Projekt SIBERIA - erste Radarsatellitenaufnahmen der Wälder Sibiriens werden ausgewertet. -In: DLR-Nachrichten - Mitteilungen des Deutschen Zentrums für Luft- und Raumfahrt, Sonderheft Umwelt, Februar 1999 / G12625.

SCHMULLIUS, C., Holz, Andrea, Vietmeier, Jan (1999): SIBERIA - Results from the IGBP Boreal Forest Transect. - International Geoscience and Remote Sensing Symposium, Hamburg, 28 June- 2 July 1999, IEEE, Remote Sensing of the System Earth - A Challenge for the 21st Century, S. 2118-2120, IEEE Inc.

SCHMULLIUS, C., Holz, Andrea, Vietmeier, Jan (1999): Waldkartierung in Sibirien. DLR-Mitt, 92 / G 12625.

SCHMULLIUS, C. (1999): A DLR receiving station in Ulaanbaatar, Mongolia in support of the SIBERIA projet. European Space Agency, Earth Observation Quarterly Supplement, EOQ 61.

SCHMULLIUS, C., W.Wagner, A.Roth, J.Vietmeier, U.Marschalk, A.Holz, L.Eriksson, S.Nilsson, A.Shvidenko, M.Gluck, T.LeToan, M.Davidson, S.Quegan, J.J.Yu, A.Luckman, K.Tansey, H.Balzter, D.Gaveau, Y.Rauste, Orrmalm, M. R.Utsi, U.Wegmüller, A .Wiesmann, V.Skudin, L.Vaschuk, V.Sokolov, V.Rozhkov (2000): SIBERIA - SAR Imaging for Boreal Ecology and Radar Interferometry Applications.- Proceedings FRINGE '99 Advancing ERS SAR Interferometry from Applications towards Operations, Liège, Belgium, 10 - 12 November 1999, ESA Publications Division, SP-478 (CD).

SCHMULLIUS, C. & W. WAGNER (2000): SIBERIA – Kartierung borealer Wälder mit Radarfernerkundung.- Geographische Rundschau, H 3211, Dezember 12, S. 44-48.

SCHMULLIUS, C., Nilsson, S., Shvidenko, A. & E. Vaganov (2001): Russian Forest Inventory Requirements and Remote Sensing Parameters-Operational Aspects evolving from the SIBERIA Project. -Proceedings of the ERS – ENVISAT Symposium. Looking down to Earth in the New Millennium. 16 – 20 October 2000, Gothenburg, Schweden.

SCHMULLIUS, C., J. Baker, H. Balzter, M. Davidson, D. Gaveau, M. Gluck, A. Holz, T. LeToan, A. Luckman, U. Marschalk, S. Nilsson, S. Quegan, Y. Rauste, A. Roth, V. Rozhkov, V. Sokolov, A. Shvidenko, V. Skuding, T. Strozzi, K. Tansey, J. Vietmeier, L. Voloshuk, W. Wagner, U. Wegmüller, A. Wiesmann (2001): SIBERIA – SAR Imaging for Boreal Ecology and Radar Interferometry Applications. Intern. Journal of Remote Sensing (invited paper).

SHVIDENKO, A. and S. Nilsson (forthcoming) Information system for estimating of terrestrial biota impact of budgets of major greenhouse gases. Paper presented to the First International Workshop on Information Technologies Application to Problems of Biodiversity and Dynamics of Ecosystems in Northern Eurasia – WITA 2001, 9–14 July 2001, Novosibirsk, Russia (in press).

SHVIDENKO, A.Z., S. Nilsson, V.S. Stolbovoi, V.A. Rozhkov and M. Gluck (2001) Aggregated Estimation of the Basic Parameters of Biological Production and the Carbon Budget of Russian Terrestrial Ecosytems: 2. Net Primary Production. Russian Journal of Ecology, Vol. 32, No. 2, pp. 71–77. (Translated from Ekologiya, No. 2, 2001 pp. 83–90.)

SHVIDENKO, A.Z., S. Nilsson, V.S. Stolbovoi, M. Gluck, D.G. Shchepashchenko and V.A. Rozhkov (2000) Aggregated Estimation of the Basic Parameters of Biological Production and the Carbon Budget of Russian Terrestrial Ecosystems: 1. Stocks of Plant Organic Mass. Russian Journal of Ecology, Vol. 31, No. 6, pp. 371–378. (Translated from Ekologiya, No. 6, 2000 pp. 403–410.)

TANSEY, K., Luckman, A., Skinner, L., Balzter, H., Strozzi, T., and Wagner, W., (submitted), Classification of Global Forest Volume Resources using ERS Tandem Coherence and JERS Intensity Data. International Journal of Remote Sensing.

TANSEY, K., Luckman, A. and Schmullius, C. (1999): Mapping boreal forest in Siberia with ERS SAR Interferometry. Proceedings of the 25th Annual Conference of the Remote Sensing Society (RSS 99), 8-10 September 1999, Cardiff, Wales, UK.

VRZAL, W. (1999) Information Requirements for Natural Resource Management with Regard to Remote Sensing. IR-99-064. Laxenburg, Austria: International Institute for Applied Systems Analysis.

WAGNER, W., J. Vietmeier, K. Tansey, H. Balzter, C. Schmullius, A. Luckman, S. Quegan, J. J. Yu, D. Gaveau, M. Davidson, T. Le Toan, M. Gluck, A. Shvidenko, An adaptive approach for classifying boreal forest in SIBERIA based on ERS tandem coherence and JERS backscatter data, submitted to Remote Sens. Environment.

WAGNER, W., J. Vietmeier, C. Schmullius, T. Le Toan, M. Davidson, S. Quegan, J.J. Yu, A. Luckman, K. Tansey, H. Balzter, D. Gaveau (2000) The Use of Coherence Information Derived from ERS Tandem Pairs for Determining Forest Stock Volume in SIBERIA, Proc. IGARSS'2000, Honolulu, Hawaii, 24-28 July 2000, pp. 1396-1398.

WAGNER, W., J. Vietmeier, C. Schmullius (2000) Information Content of ERS SAR Interferometric Products for Forest Classification in SIBERIA: A Case Study over the Bolshemurtinskii Forest Enterprise, Proc. IGARSS'2000, Honolulu, Hawaii, 24-28 July 2000, pp. 444-446.

WEGMÜLLER, U. (1999): Automated terrain corrected SAR geocoding, Proceedings of IGARSS'99, Hamburg, 28 June - 2 July 1999 (CC03_02).

WIESMANN, A., T. Strozzi, and U. Wegmüller(1999): JERS SAR and Interferometric Processing for the boreal forest mapping project SIBERIA, Proceedings of IGARSS'99, Hamburg, 28 June - 2 July 1999 (DD01_03).

WIESMANN, A., U. Wegmüller, and T. Strozzi (1999): JERS SAR processing for the boreal forest mapping project SIBERIA.- Proceedings of CEOS SAR Workshop, 26-29 October 1999, Toulouse, France, ESA SP-450, pp. 19-23, March 2000.

WIESMANN, A., Wegmüller U., T. Strozzi, and C. Werner (2000): The use of JERS SARwithin the boreal forest mapping project SIBERIA.-Proceedings of IGARSS 2000, Honolulu, USA, 24-28 July 2000.

WIESMANN, A., Wegmüller U., T. Strozzi, and C. Werner (2000): JERS INSAR coherence over Siberian boreal forest", Proceedings of ERS-ENVISAT Symposium, Gothenburg, Sweden, 16-20 Oct. 2000.

8.2.3 Diplom and Doctoral Theses

ERIKSSON, Leif (to be submitted in 2002): Radar remote sensing of Boreal forests using Envisat, ERS and JERS. - Ph.D. Thesis. Friedrich-Schiller-University Jena, Germany.

ETZROTH, Norbert (to be submitted 2001): Anwendungsmöglichkeiten von SAR-Interferometrie und optischen Fernerkundungsdaten für die Kartierung zentralsibirischer Primärwälder zur Abschätzung von Stoff-Flüssen und –Bilanzen.- Ph.D. Thesis, Georg-August-Universität Göttingen, Germany.

FRISCHEMEYER, Kathrin (1999): Informationsgehalt von Radardaten hinsichtlich der Analyse von Landschaftsstrukturen und Waldverbreitung am Beispiel des Minussinsker Becken (südl. Ostsibirien).- Diplom-Thesis, Georg-August-Universität Göttingen.

FROTSCHER, Karsten (2001): Digital Geländemodelle: Geostatistische Beschreibung und Ableitung hydrologischer Parameter. Eine vergleichende Betrachtung interferometrischer X-SAR/SRTM und ERS-Tandem- sowie kartographischer Modelle.- Diplom-Thesis, Friedrich-Schiller-University Jena, Germany.

LIEBIG, Thorsten (1999): Untersuchung borealer Waldhöhen mithilfe digitaler Höhenmodelle.- Diplom-Thesis, Universität Weihenstephan, Germany

TALMON, E., (2000, in German): Methoden der Fehlerabschätzung in der Fernerkundung am Beispiel einer Klassifikation borealen Waldes in Sibirien mit satellitengestütztem Seitensichtradar (SAR). Diplom-Thesis, Justus-Liebig-Universität Giessen, Germany.

YONG, Jiong-Jiong (2000): Analysis and Classification Methods for Synthetic Aperture Radar Data Applied to Forest Monitoring.- Ph.D. Thesis, University of Sheffield, UK.

8.2.4 SIBERIA Session Overview during ESA's ENVISAT Symposium Gothenburg, 16-20 October 2000

TUESDAY 17 OCTOBER 2000: Forestry (SIBERIA)
Session Chairperson: Christiane Schmullius, Session Co-Chairperson: Henri Laur

9.00 – 9.20	Achim Roth:	ERS Interferometric Processing for Boreal Forest Applications
9.20 – 9.40	Thuy Le Toan:	Assessing ERS and JERS SAR information content for large scale forest mapping in Siberia
10.00 – 10.20	Shaun Quegan:	The classification procedure in SIBERIA: rationale and methodology
10.20 – 10.40	Adrian Luckman:	Global forest classification using JERS and tandem ERS data
10.40 – 11.00	Coffee Break	
11.00 – 11.20	Heiko Balzter:	Accuracy assessment issues in the SIBERIA project
11.20 – 11.40	Christiane Schmullius:	Russian Forest Inventory Requirements and Remote Sensing Parameters-Operational Aspects evolving from the SIBERIA Project

Session Summary
(ERS-Envisat Symposium, SP-461, ESA Publications Division, 2000)

The SIBERIA project (SAR Imaging for Boreal Ecology and Radar Interferometry Applications) aims to image an area of global ecological importance, the central-Siberian forest, using three Earth Observation radar satellites. It was an unprecedented fast and joint effort of the German Aerospace Centre (DLR), the European Space Agency (ESA), and the Japanese Space Agency (NASDA) to collect ERS-1 and -2 and JERS-1 data via a transportable station located in Mongolia. These data (550 ERS-scenes plus 890 JERS-1 scenes) were used in one of the most area-extensive remote sensing projects (1.2 Mio sqkm), to prove the operational use of radar remote sensing for very large-area forest mapping.

The main source of information came from the ERS tandem coherence. It was clearly confirmed that the coherence channel (1-day tandem) was the primary parameter for forest/non-forest delineation. The ERS intensity, even multitemporal, did not provide suitable results for the classification. The final results, derived from ERS coherence and JERS intensity, include classified maps with 3 forest classes of different timber volume. The areas of high relief could not be classified.

The Siberia forest map will help the Russian forest institutions to update obsolete forest inventory data and to monitor reforestation e.g. after fire events.

The session was organised in a logical way, from the data processing description to the presentation of the final classified maps, including the rationale for the applied classification methods. The posters allowed to see various steps of the SIBERIA project and to appreciate some of the final forest maps.

The SIBERIA project was funded by the European Commission within the 4th European Framework Programme.

Appendix A

IIASA
Science for Global Insight

SAR
Imaging for
Boreal
Ecology and
Radar
Interferomerty
Applications

SIBERIA Project Ground Truth Data Workbook
May 1999

A.1 Introduction

This document is a guide to the ground truth data provided to the SIBERIA Project and can be thought of as a *workbook* for our Siberian Field Trip. It is not, however, a definitive report regarding Russian Forest Inventory standards or measurements. Finally, thanks to everyone who contributed questions to our Question & Answer page.

A.2 Forest Inventory

This is a brief description of forest inventory -- a complete review of remote sensing methods used in Russian Forest Inventory is forthcoming. Two types of inventory are completed for Russian forests depending on forest management requirements: on-ground (so called *lesourtroistvo*) Forest Inventory and Planning (FIP) for intensively managed forests and survey of remote unmanaged forests, basically in Siberia and the Far East. The SIBERIA project forests are located in areas inventoried by the first method.

FIP is completed in each Russian Forest Enterprise every 10 to 20 years. Approximately 70 percent of Russian forests are inventoried by FIP. Boundaries of primary inventory units (SKNR) (stands for forested areas although they may be other land classes) are, as a rule, interpreted from 1:10,000 or 1:20,000 scale aerial photos. SKNRs are basically resolved from air photos on the basis of dominant species composition, age, relative stocking, site index, origin, vertical structure, quality of growing stock and forest homogeneity. On ground measurements are used to provide final estimates of variable and verify photo interpretation. Most of the ground truth data in the SIBERIA project area is based on 1:25,000 scale photos. There are three categories of FIP that define details and accuracy of the forest inventory results.

The survey of remote forests is accomplished for the rest of Russia's forested area using a "photo-statistic" or multi-stage sample design. The first stage uses RESURS or COSMOS-based images (1:275,000 scale) to stratify the forest into forest groups (e.g. recently burned forest, mainly larch forest, etc.). Lower stages of the sample design use large-scale (1:2000-1:7000) air photo transects to estimate forest variables. The bottom stage of the sample design involves ground sample plots in which exact measurements of forest variables are made.

A.4 Forest Variable Definitions

Unique

In our attribute data, we have combined forest district (GIR), kvartal (KV), and stand (SKNR) into a Russia-wide unique (UNIQUE) identifier that we use to relate forest data polygons to our databases.

Kvartal (KV)

A kvartal is an administrative area ranging from 50 to 4000 ha. Kvartal boundaries can be natural (e.g. rivers or mountains) or artificial. For example, if you look at the Ust Ilimsk area on the right you see what look like boxes across the forest. These follow an old German system of creating forest compartments as part of the management of the forest. You may see the effect of these administrative units in the cutting patterns in the forest -- harvested areas as a rule follow kvartal boundaries.

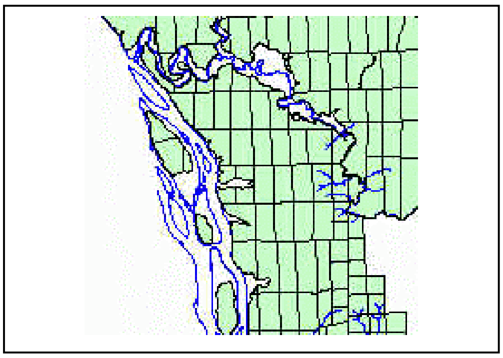

Primary Inventory Unit (SKNR)
Each kvatal is divided into primary inventory units (SKNR) (in forested areas these are sometimes called stands). A SKNR is a relatively homogenous area in terms of tree species composition, age, height origin, site index and relative stocking. Some SKNR boundaries have an ecological origin, etc. (e.g. the edge of an area once burned by fire) and others are kvartal boundaries. The SKNR boundaries are constant but, when we look at the forest according to different attributes (e.g. age or species composition), they may become more or less pronounced. We see this if we, for example, look at a section of the Ermakovsky test area. The image on the left shows the forest displayed according to age (AMZ) whereas the right image shows the proportion of birch (BIRCH_KF). We see that the contrast among the SKNRs is very different.

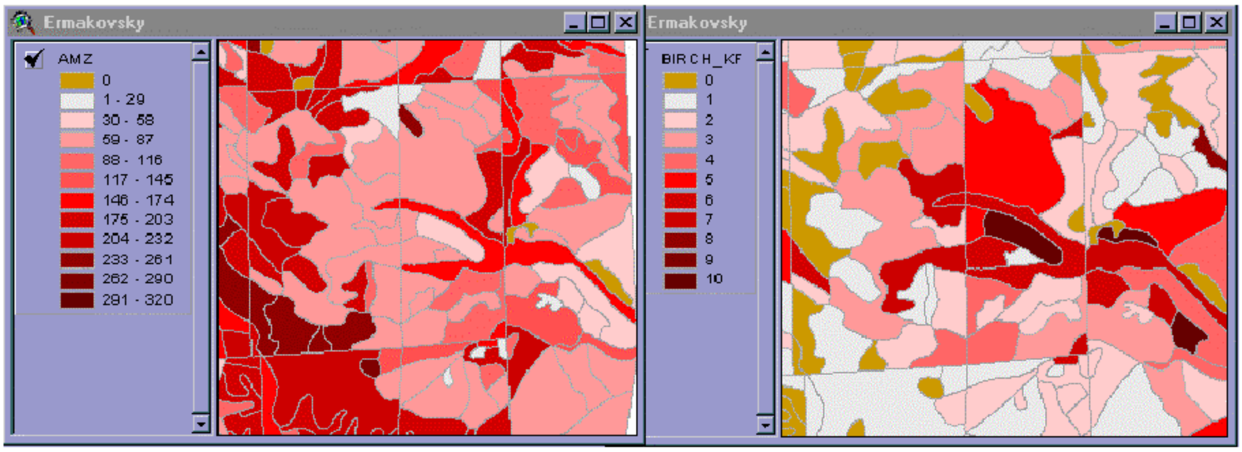

It is important to recognise that SKNR boundaries are based on subjective, human interpretation, usual ly of aerial photos, and that they are not always visible in small-scale satellite-based remotely sensed images, but can often be recognised on large-scale images.

Area (AREA_HA)
This is the vertical projection of the area of the SKNR as reported in the forest inventory. You may notice that the GIS files also contain an "AREA" item. This is the area as measured by the GIS in square meters. The GIS area is sensitive to shifting caused by georeferencing, therefore we advise that the forest inventory area (AREA_HA) be used for analysis purposes.

Land Category (ZK)
These are the basic categories of land for which the entire landscape is classified.
1101 - natural stand
A stand of growing trees resulting from natural regeneration following a forest disturbance. By definition, these stands have relative stocking greater or equal to 10 for young age groups and greater than or equal to 30 for all other age groups.
1102 - unclosed natural forest
Forests with relative stocking of 10 to 40 for young age groups and 10 to 30 for all other age groups *if this condition is a result of climatic conditions* (i.e. altitude or climate), otherwise they are classes as sparse forests (1400)
1104 - low productivity forest
According to "All-Russia Manual", these are mature and overmature exploitable forests of site index *Va* and *V,* and forests of higher productivity if growing stock is less than 40 m^3/ha in European Russia and less than 50 m^3/ha in Siberia. These criteria can be regionally adjusted.

1108 - forest plantation
A stand of growing trees, raised artificially, either by sowing (seeds) or (most commonly) planting. A forest plantation must have at least a relative stocking of 30 for young trees and 20 for mature (less than this it is an unclosed forest plantation). In some plantations, if they have been intensively managed, one may be able to see the trees in rows.

1201 - unclosed forest plantation
This is basically a younger stage of the forest plantation. If you imagine looking down from above on a young forest in which you can still see the forest floor then the canopy is considered "unclosed" (and relative stocking is less than 30 for young trees and 20 for all others). In terms of forest management this means that there is still the possibility of competing vegetation (shrubs, grasses, etc.) to outgrow the planted trees and compete for sunlight and water resources.

1400 - sparse forest
The same relative stocking as in 1102, however, this state is the result of natural (e.g. fire) or human-induced disturbances.

1503 - burned forest
The full name of this category is burned and dead forest. This is a land category that describes areas that have experienced a "stand replacing" fire. This means that the "surviving" trees have a relative stocking of less than or equal to 10. If between 10 and 30 percent (relative stocking) survive the fire then it is classed as a sparse forest (category 1400).

1507 - stand marked for cutting
Stands planned to be cut during the year of forest inventory.

1509 - clear-cut areas
These are areas that are harvested under the clear-cut silvicultural system. They have a relative stocking of less than 10. This is a system of regenerating even-aged forest stands in which new seedlings become established in fully exposed micro-environments after most (some individual trees may remain standing) of the existing trees have been removed. Regeneration can originate naturally or artificially. Clear-cutting may be done in blocks, strips or patches. Once regrowth occurs the area could be classed into unclosed forest plantation (1201). Check the inventory update date of the test territory (this information is located on each test territory page) to verify before what date this harvest occurred.

Other - non-defined.
2102 - agriculture, hay
2103 - agriculture, pasture
2110 - stream
2308 - lake
2507 - bogs
2505 - exposed rock
2512 - talus
2540 - quarry or gravel pit

Relative Stocking (SKAL)
Let's break relative stocking down into two parts -- "relative" and "stocking". Stocking is an expression of the adequacy of tree cover on an area in terms of basal area. Basal area is the area of the cross section of a tree trunk near its base, usually 1.3m above the ground (also called breast height). Basal area is a way to measure how much of a site is occupied by trees. The term basal area is used to describe the collective basal area of trees per hectare. Relative stocking is a comparison of the stocking of a particular stand to what the ideal stocking would be under perfect management conditions. The ideal conditions are a function of site quality and can vary according to the species composition and age of the stand. There are yield tables developed for Russia that would describe fully stocked stands.

Growing Stock Volume (TUR1H)
In general, growing stock volume (TUR1H) is the STEM volume for all living species in a stand. Specifically, however, only in young stands are all stems considered. In all other stands trees must be greater or equal to 6 cm at "breast height" (1.3 m) to be included in the growing stock. The trees that are excluded from this measurement only represent about 1 percent of the volume -- so it OK to say that this variable considers all trees. It is expressed in cubic meters per hectare.
NOTE: The Ust Ilimsk database has volume in 10m3/ha units!!

Age of Dominant Species (AMZ)
This can be considered as the age of the stand expressed in years. Age *groups* are region-specific calculations that take into account forest site quality, dominant species and legislative requirements. In general, however, the age groups for the SIBERIA project area can be defined using simply the age of the dominant species. The table below shows the age thresholds for the age groups in our project area.

Species	Young	Middle-aged	Immature	Mature	Overmature
Pine, spruce, fir & larch	1-40 years	41-80 years	81-100 years	101-140 years	>140 years
Cedar	1-80 years	81 - 160 years	161 - 200 years	201 - 240 years	>240 years
Aspen & birch	1-20 years	21-50 years	51-60 years	61-70 years	>70 years

Composition (KF)
Composition is the proportion of a species in a stand on a scale of 1 to 10 (e.g. PINE_KS = 1 means 10 percent of the growing stock of the trees in the main canopy layer of the stand are pine)

Height (H)
An estimate of the average tree height of the dominant species in the stand. Expressed in meters.

Diameter (D)
An estimate of the average tree diameter of the dominant species in the stand based on a quadratic average. The diameter is measured at 1.3m or "Breast height". Expressed in decimetres.

A.4 Forest Variable Relationships

In this section we discuss the relationships among the variables with particular attention to how these relationships affect remotely sensed measurements.

Age, volume and stocking

In general, stand volume increases with age until maturity is reached after which the stand starts to loose volume through death and decay. When examining stand volume it is important to also look at the relative stocking of the stand. For example, we can consider three stands with the same volumes:

Stand	Age	Age Group	Relative Stocking	Composition	Volume
1	200	Overmature	40%	60% pine, 40%larch	150
2	60	Immature	70%	10%pine, 30%larch, 60% birch	150
3	50	Middle age	90%	100% birch	150

This does not follow the pattern we would expect until we consider stocking. These stands have different ages (and are in different age groups) but the general pattern is that the older stands have lower relative stocking. This affects the expected relationship between age and volume, however, if we calculate what the volumes *would be* if these stands were *fully stocked* (i.e. SKAL = 10) then stand one would have 375 m^3/ha, stand two 214 m^3/ha and stand three 167 m^3/ha. We can plot the forested stands from the Ust-Ilimsk test territory this way to also see this relationship.

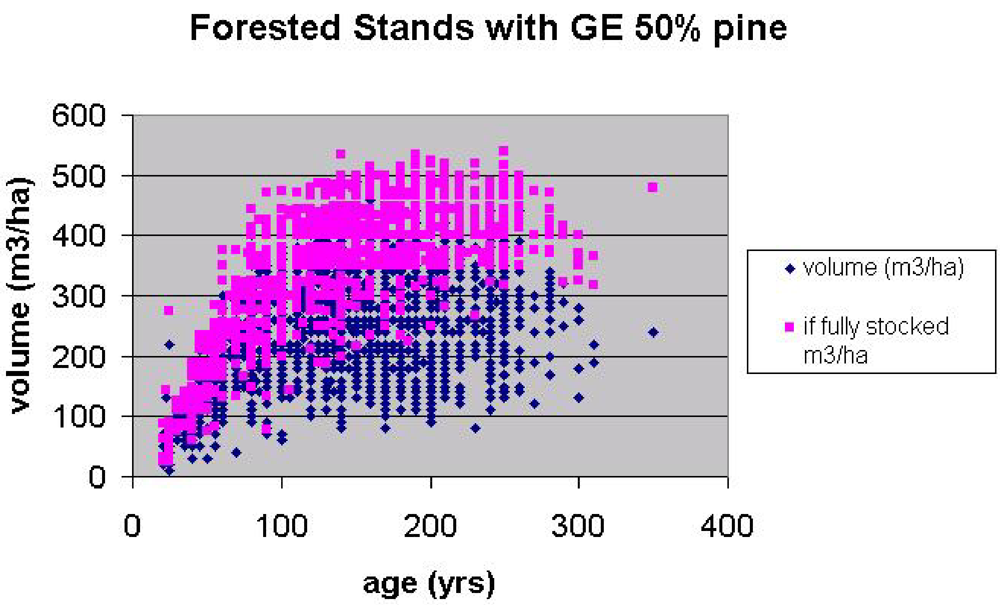

Species and Canopy Characteristics

The canopy structure of forests varies according to species composition, age, relative stocking and height. Radar-based measurements can also be affected by season and weather conditions. The following figure shows the basic form for individual trees (from Racey *et al*. 1996).

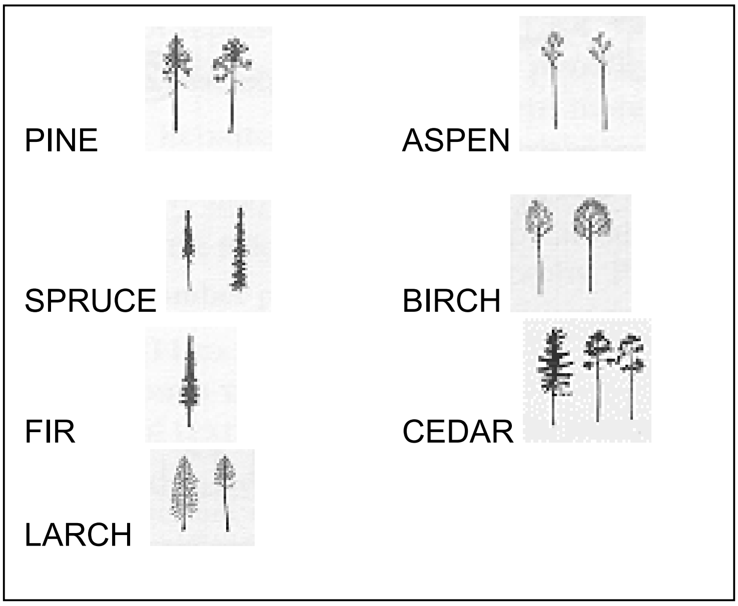

Here are some hypothetical cross-sections of forest stands (from Racey *et al*. 1996)

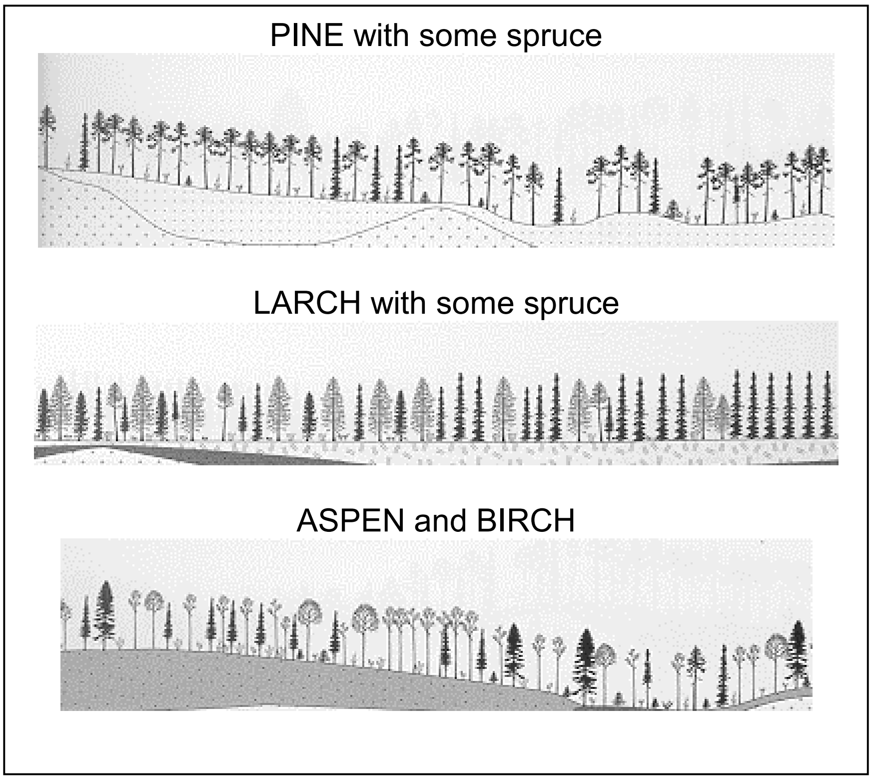

Disturbed Areas

One of the most important information requirements is to know the extent and type of forest disturbance. Forest can be disturbed naturally by biotic (e.g. fires or wind) or biotic (e.g. insects and disease) sources and through human-caused activities (e.g. harvesting, pollution). Probably the most easily detected disturbances in the SIBERIA study area are clear-cut harvesting and forest fires. The forest data must be carefully queried, however, to these areas. For example, to find recently disturbed areas in the Ust Ilimsk test territory, we should use the select clear cut stands (ZK = 1503), unclosed forest or plantations (ZK = 1102 or 1201), burned and sparse forest (ZK = 1509 and 1400) and forest stands with a young age (e.g. AMZ < 10). The figure below shows this selection and compares it to SPOT XS4 and ERS data for the same area.

Some notes:

- Some clear-cut areas still have standing trees.
- Burned areas generally have many standing dead trees.
- There may only be undetectable (remotely sensed) differences between clear-cut, plantation and young forests.
- Some clear-cut areas are not indicated in the ground truth due to the age of the data.
- Wetlands may have similar physiognomic features to recently disturbed areas and may actually have "dry surfaces" during the summer months.

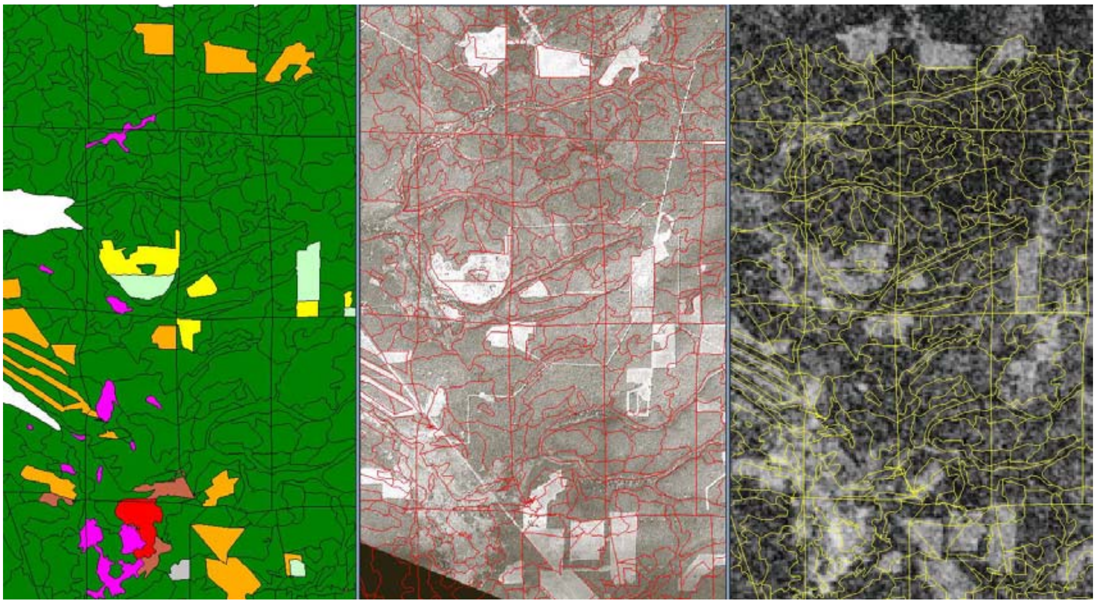

Left to right, forest map (mustard = clear cut areas, pale green = plantation, yellow = forest < 10 years, red = burned areas, pink = bogs and brown = not classed), SPOT XS4 and ERS1 coherence images with forest map polygons.

A.5 Forest Variable Estimate Accuracy

Here are the required inventory standards as described in the Russian Forest Inventory handbook. As the table below shows, the required inventory accuracy increases, as stands become ready to harvest. In general, however, one can see that the required accuracy is between 10 and 20 percent.

WHEN?	Growing stock - within XX percent	basal area (used for stocking) within XX percent	height within XX percent	composition within X percent (1 = 10 %)	diameter within XX percent
Stands to harvested	15	12	8	1	10
Stands to be thinned (pre-commercial)	20	16	10	1.5	10
All other stands	20	16	10	1.5	12

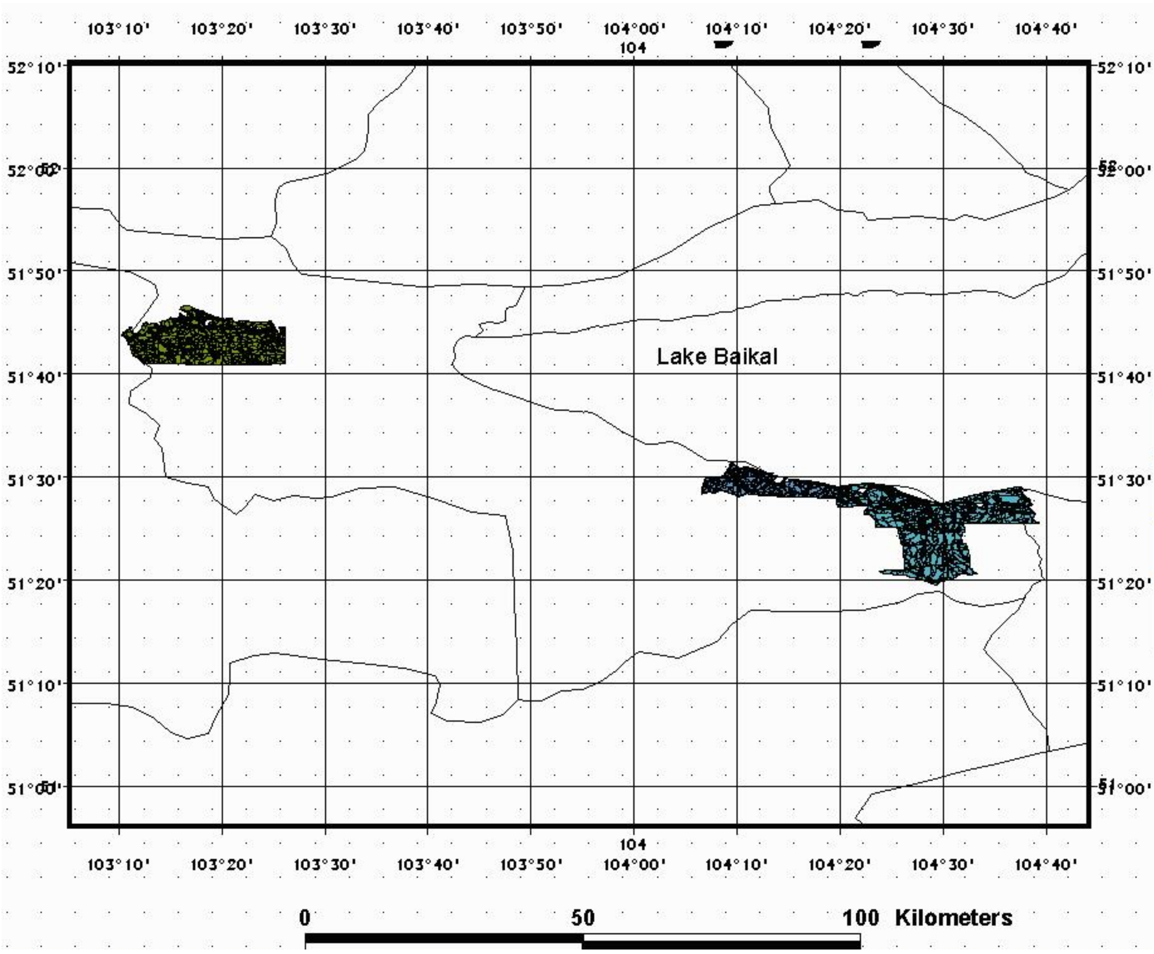

Baikal Field Trip Sites

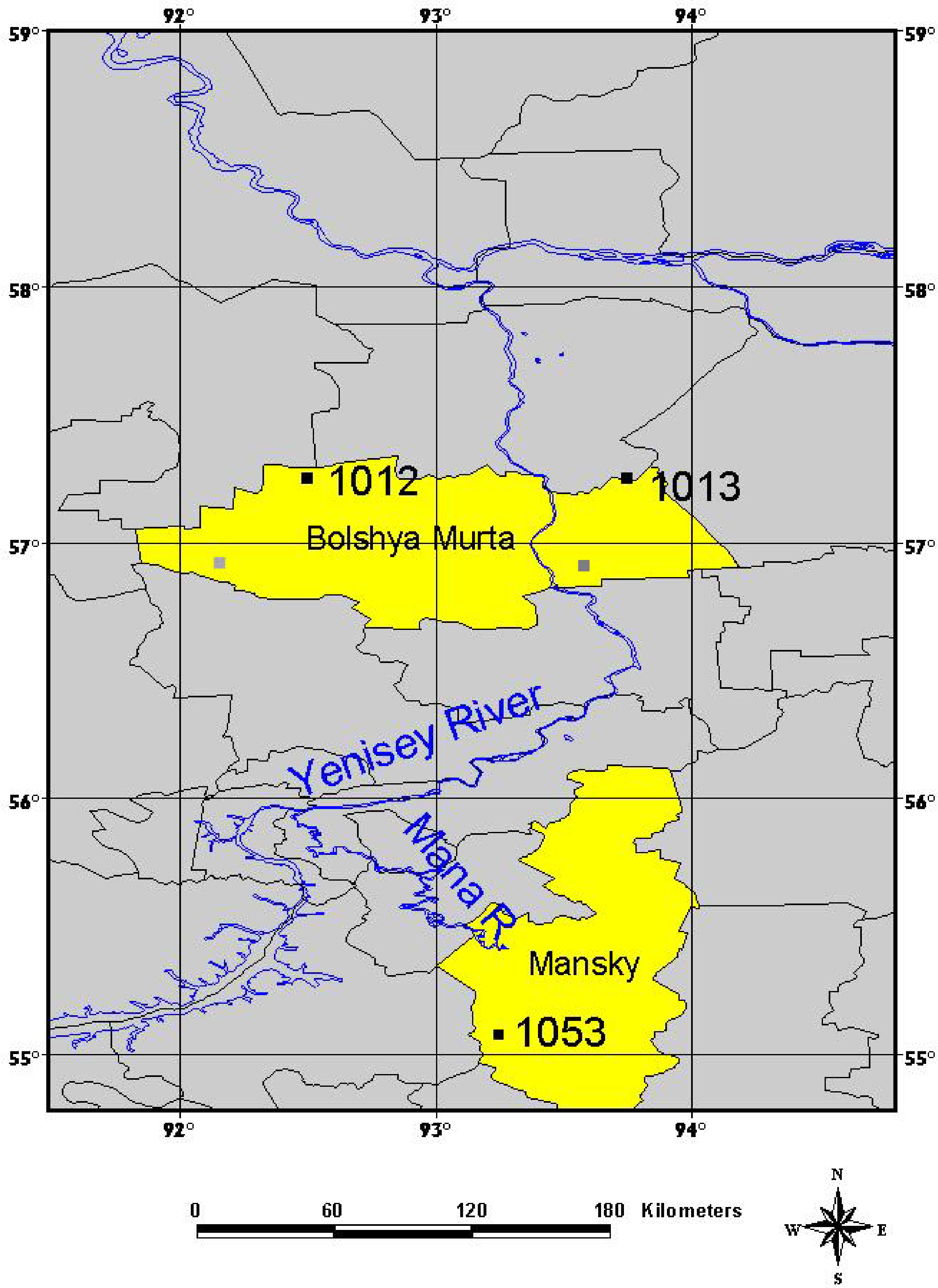

Krasnoyarsk Field Trip Sites

Appendix B: SIBERIA Excursion Documentation

(original notes by A. Holz, edited by C. Schmullius)

PARTICIPANTS:

Anatoly Shvidenko/IIASA, Vjacheslav Rozhkov/Moscow, Michael Gluck/IIASA, Thuy Le Toan/CESBIO, Malcolm Davidson/CESBIO, Shaun Quegan/SCEOS, Jiong-Jiong Yu/SCEOS, Adrian Luckman/UWS, Kevin Tansey/UWS, John Baker/NERC, David Gaveau/NERC, Yrjö Rauste/VTT, Christiane Schmullius/DLR, Wolfgang Wagner/DLR, Jan Vietmeier/DLR, Andrea Holz/DLR.

SUNDAY, MAY 30, 1999, MOSCOW

Arrival of team members at Moscow International Airport Sheremetevo II. Transport to Hotel Minsk (on Tverskaja street near city center). Visit of Red Square. Departure from Hotel at 17 h to the National Airport Domodedevo. Take-off for Krasnoyarsk at 22:50 h local time (Moscow: 2 hours time difference from Central European Daylight-Savings Time, Krasnoyarsk: 6 hours time difference to CEDST).

MONDAY, MAY 31, 1999, KRASNOYARSK

Arrival: 07:15 h local time at Krasnoyarsk Airport. Transport to Hotel "Oktjabrskaja", prospect Mira 15, Krasnoyarsk.

15:00 Institute for Geology, Landuse and Nature Resources

Presentation by Dr. Vladimir Sokolov, SIBERIA-Partner:
Forest can be divided in 4 different categories (see also viewgraphs that have been provided as handouts):

- Forest with highest protection and possible future activity = forest far north in Krasnoyarsk Kray. Practically no harvest until now, but permafrost region. Protection needed.
- Developing forest areas north of Krasnoyarsk, rich forest, forest is exploited.
- Stabilising forest use around Abakan, no logging because of forest's stabilising function.
- Exhausted forest resources around Krasnoyarsk.

In the forests of Krasnoyarsk Kray are mainly 7 species: fir, spruce, pine, cedar, larch, aspen, birch.

Forest stem volume in Krasnoyarsk Kray is more then 6 billion m^3 of coniferous forest. 53 million cubic meters per year can be harvested and the forest still stays sustainable. Actual numbers 1993: 13 million m^3, 1995: 9 m^3, plan for 2000: 16 m^3. Territory is huge and remote sensing and other methods are useful to keep inventory up-to-date.

The total SIBERIA project area covers 6 different ecoregions. Forest management practices are changed according to the local conditions. These regions also need inventory methods adjusted to the ecology. The primary inventory units for different ecosystems here in Krasnoyarsk Kray are typically about 25-30 ha.

Leskhoz = Russian forest enterprise, that is a management unit with separate budget etc. There are 57 different forest enterprises in the Krasnoyarsk Kray.

16:00 "State East Siberian Forest Management Enterprise, Federal Forest Service of Russia", Krupskaya 42.

Presentations given by Dr. Victor Skudin (SIBERIA Partner) and Dr. Vajaskan.
This enterprise started about 40 years ago with airphotos for logging information. Forest inventory intervals: 10-15 years. Goldmining and other activities are also observed. The goal is to improve the forest management. Questions to be answered are e.g. how much soil is destroyed etc. Airphotos at scales of 1: 60 000 and 1: 25 000 were presented. In 1994, big forest losses to infestation by Siberian Moth.

Today maps are produced digitally with Russian GIS-software. Formats are compatible to other systems like ArcInfo. This has been started 3 years ago. Forest enterprise maps are at the scale of 1:250,000 and 1:25,000 (this scale is confidential material). No relief is printed on maps, because topography is secret information.

Other sources of remote sensing data are used as well like: NOAA/AVHRR, Russian satellite systems like Resurs etc. But so far no satisfactory results were achieved with remote sensing data.

In 1980, big clear-cut areas were observed with air photography. This was mainly important for State Agencies to estimate tax payments.

Inventory technique: single areas are outlined on air photography, then every sector is visited and forest parameters measured.

Tour through the institute:
In one room the forest maps are produced. Smallest unit is called "blanchet", like the French word. Scale 1:1,000. Stand = smallest unit, can be forest or clear cut etc.
Maps are compatible to topographical maps with Russian coordinate system (S42). Basis are topographical maps and airphotos at 1: 25.000 scale. Airphotos are acquired on infrared film. From the airphoto interpretation, polygones are derived for the GIS. Then maps are produced. Each polygon is connected with an online info sheet (attribute file). Resulting maps are in Gauss-Krueger projection. (Question: why are the maps in Gauss-Krueger while everything else is in S42?) DEM's are not produced, see remark above.
Five different forest enterprises are served by this institute. 4 Mio hectares have been digitised this year within 6 months and with 20 people.

18:00 Internal SIBERIA Team-Meeting: (about progress of last two months since Swansea-meeting)
DLR: Within 2 month, repeat-pass JERS-1 data from the 1998-acquisition will be available. Meteorological data for all test sites for this field trip have been investigated and presented in temperature and precipitation time-plots. We had problems with JERS co-registration to ERS DEM.
IIASA: Will provide biomass for each stand, but must be calculated first from various stand tables.
USW: Time intensive software providing has to change (e.g. filtering software for different computer platforms and operations systems). Worked on GIS and co-registration to SAR data.
CESBIO/SCEOS: Bolshaya Murta color-composite for field trip, handout for Prdivinsky test site. Keep concentrated on low productivity, since high biomass saturates the SAR-data. Note: mistakes happened earlier because of different scales/units in GIS.

TUESDAY, JUNE 1, 1999, BOLSHAYA MURTA

8:00 Departure to Bolshaya Murta. On our way North, we saw the transition zone between taiga and steppe = forest steppe, with the typical black steppe soil (Tschernosem).

10:20 Arrival at Bolshaya Murta State Forest Enterprise

Presentation by Director Victor Padgornov:

This region belongs to the South-Taiga vegetation zone. 540 000 ha forest, allowable harvest is 1 Mio m^3 per year. Actually just 20% are cut. The enterprise includes 7 forest districts, 2 wood processing plants and 1 production unit for repair of electrical equipment. Total staff 200 employees, including 95 "state forest guards", about 40 are staff engineers and technicians, 50 are quarter-rangers, 85% of the staff are graduated. The number of staff could be kept even after the economic decline of Russia. In 1995, one of the first GIS-systems for forest management has been developed here.

Forest protection and reforestation is the major task.. Reforestation is natural. 25 years ago, prescribed forest burning was forbidden, but large amount of dry material (left-over logging material) is dangerous fuel for forest fires. Now prescribed burning is scientific experiment with American foresters.

In the past, 85-90% of the logging activities were clear-cuts. Since selective harvest has started, productivity increased: 200-300 m^3 was usual, now > 400 m^3. Two techniques: regular selective harvest and gradual selective harvest. Best tree age for harvest: 100 years. Range of age classes differ with species: coniferous species have 6 age classes (each 20 years), birch has 6 age classes (each 10 years).

In 1991, last forest inventory. Major tree species spruce and fir, on Eastern side after big forest fires: birch. Very good coniferous re-growth. Young stands = low productive areas < 50 t/ha. Also big forest losses after Siberian Moth infestation in the 50's and 60's. Here, 30 – 100 m^3 dead material on ground. Areas that have been destroyed by insects can be identified as clear-cuts in remote sensing images. A GIS is established and updated regularly, partially by airphotos, most by ground inspections.
In this enterprise also co-operation with Americans on carbon budget analysis – 1000 test plots all over Taiga.

What is economic future? Demand for high-quality industrial wood. Big part of forest is overmature, but only 20% of allowable cuts can be done due to economical situation. Hope, that Krasnoyarsk paper plant will increase production. Major problems are on political level, not on the local activities.

Lunch in Bol'shaya Murta.

Transport to key area 1012, about 57° 17'N, 92° 39'E.

Succession with small, young *Betula pendula* after clear-cut, very few *Salix*. Inventory Unit 25. Underground very wet, with puddles, herbaceous undergrowth, mainly grass. Airphotos of this area from 1990 show that here was a total clear-cut, no vegetation. Residuals are *Pinus sibirica, Picea sibirica* and *Abies sibirica* (for common names, see Table B-1). Species composition here as indicated in GIS: 40 % Spruce, 20 % Fir, 20 % Cedar, 20% Birch. How the clear-cut areas look depends on the post-harvest treatment (burning etc.).

The ground-truth is established as follows:
1. on airphotos, boundaries of homogeneous forest stands are delineated as polygons,
2. each polygon is then inspected on the ground and the following parameters measured (list not complete, compare GIS):

- average tree height and dbh (diameter at breast height = 1.35 m per definition) for each species that is listed as dominant;
- relative stocking, scaled from 0 – 10: for example 8 means 80% of possible stocking (only trees are included which have a minimum dbh of 6.1 cm, trees of a dbh < 6.1 cm belong to undergrowth;
- main species in undergrowth are registered as well;
- “bonitet“ is registered only for dominant species;
- age.

This is Quartal No. 10: 270 m³/ha growing stock, undergrowth is herbaceous: lots of moss, farn, trefoil, horse-tail, rubus arcticus (a kind of raspberry), very wet ground.

Walk to a second clear-cut area. Here, residuals of former stand visible. Without fire this will be a coniferous stand again, now this stand is covered mainly by *Betula* (4 m height). In the forest inventory this area is possibly marked as clear-cut since the inventory was made several years ago.

Further walk into undisturbed forest: mainly *Pinus sibirica* with 80%. *Pinus sibirica* is very valuable wood and can only be harvest under very controlled conditions due to old Soviet regulations.

Dinner and overnight-stay in Bol’shaya Murta.

WEDNESDAY, JUNE 2, 1999, PREDIVINSKY

Transport to Predivinsk on the Eastern shore of Yenisey

Visit of forest enterprise “logging land and wood processing enterprise”

Meeting with Director Dr. Vladimir Michaelevitch, also associated Professor at the University in Krasnoyarsk.

The enterprise was founded in 1930. Main tasks are logging and construction work. Here is the basis station for technical wood processing of the University of Krasnoyarsk. Today the enterprise is in a horrible economic situation – the main task is to survive. One method: economic diversification. Products are: special medicine oil from *Abies*, agricultural production unit, honey production, licences for gold mining, providing road constructions, wood transportation ships. The enterprise has special social enterprises like kindergarten, cafes, shops etc.. Everything possible is done here, to keep the staff and to maintain the social structure. “If Russians would prefer Russian products, Predivinsky would be ahead!”. Forest harvest per year: 160 – 170.000 m³, of which 30 % *Picea*, 30% *Abies*, 20% *Populus*, 10% *Betula*, 10% other species. The enterprise is also starting to produce log with western standard. But wood has to be transported 6000 km to any market: to the West (Europe) or to the east (Japan).

A long-term project exists with American scientist on sustainable forest management (financing through World Bank: 60 Mio USD). In the past, harvesting occurred mainly unorganised – large amounts of dead material was left in the logged areas, which is a dangerous amount of fuel for forest fires. Nowadays, natural reforestation with various species. Since this region belongs to the transition zone between steppe and forest, forest regrowth has permanently to be monitored.

There are 970 employees in this enterprise. The forest area only of this enterprise covers 22.000 km^2 = 2,2 Mio ha (that is about half the size of the forest in France) – Finland has 50 Mio ha, Russia 68 Mio ha. 3 Mio people are employed in Russia in the forest industry. Lesosibirsk, a big city on the Yenisey further North, is more or less completely based on forest industry. Demand for domestic products exists, but companies cannot pay!

Transport to ground-truth site NE of Predivinsky, approximately at 50°12'N, 93°42'E (site N 3).

Walk to Quartal 23 on border between 22 and 23. The two stands are the same, the border is artificial. It is the border between low biomass and natural low productivity, cleared about 35 years ago. Main species are *Pinus sylvestris, Betula, Sorbus*. Initially it was *Betula* and as undergrowth coniferous, but eventually a coniferous forest will establish if no fire occurs. In case of fire, *Betula* and *Pinus sylvestris* will survive and in 100 years just *Pinus sylvestris* will be left. The residuals of *Pinus sylvestris* here are about 250 years old. Sensitivity to fire in order: *Abies* (very sensitive), *Picea, Larix, Pinus sylvestris* (not very sensitive to fire).

Drive to next stop further north: house surrounded by pasture, west of it low biomass/high coherence area (biomass ca. 30 t/ha, scrubs and little trees not higher than 3 m, mainly *Betula* and *Salix*). South of the house: pasture and forest (natural stand, No. 21). Comparison with ERS images shows that forests of less than 50 t/ha can be distinguished. The low biomass area was cleared 20 years ago, about 1973-1975. This area thus is younger but has same biomass than the above regrowth site in Quartal 23. Result: age is not a discriminator! Possible explanation is difference in regeneration. In 1981, a plantation was planted, because regeneration was bad. Belt of mother-trees (=residuals) is visible behind the low biomass area and was also recognised on the SAR image.

End of September (time of SAR images): no leaves on trees. Litter fall is finished at end of September.

Drive back to Predivinsky: short stop at place where log piles (clearly visible on ERS image, high coherence).

Early dinner in Predivinsky, ferry over Yenisey, transport back to Krasnoyarsk.

Observations: huge fields with islands of forest and bare black soil/Tschernosem (soil had been ploughed shortly, remainders of last harvest visible); wind-erosion protection using tree lines (3-4 rows of *Populus*).

21.00 Reflection Measurement Station

Measurements of forest reflectance and brightness with different spectrometers and radiometers. Small forest plantations (ca. 10 m x 50 m ?) with different species compositions had been planted between two measurement towers. Sensors were moved along a wire between these towers. Height of towers approximately 30 meters, distance ca. 500 m. This remote sensing experimental station had been operating from 1960-85.

22.00 Arrival in Krasnoyarsk

THURSDAY, JUNE 3, 1999, KRASNOYARSK:

9.30 Visit of the "Sukachev Forest Institute, Siberian Division of the Russian Academy of Sciences".

Introduction by Dr. Abaimov
The Sukachev Forest Institute is the oldest in the structure of the Academy of Sciences. Founded 1944 in Moscow. 350 employees, including 100 scientists, 30 professors and 80 PhD students, so more than 25% are PhD students. There are also branches in Tomsk and Novosibirsk. It includes the Siberian International Centre for Ecological Boreal Research. A receiving station for remote sensing data exists (NOAA/AVHRR, and Russian sensors).
During the last ten years, 30 scientific projects have been undertaken with institutes from the USA, Switzerland, Japan, Korea, Sweden, Norway, Poland, and Germany. Publications in international journals. In the past 25 years, more then 200 books have been published.

Presentation by the Deputy Director Dr. Fedor Pleshikov

There are two levels of monitoring: regional level (Siberia) and local level (selected regions of Siberia). Remote sensing data is used: NOAA/AVHRR, Kosmos, Landsat-TM, Resurs, Spot. GIS is used for regional subsystems.

A map of forest transformation was presented: changed/damaged regions, based on remote sensing data. The area of pine forest decreased, area of young stands increased twice. Forest fires are the main problem, detailed maps exist since 1987-93. Further map presentations on:
- classification with 4 different classes of transformation;
- analysis of dynamics of forests during the last 20 years;
- stages of reforestation and productivity of regeneration stages;
- maps of fire temperature extracted from AVHRR;
- index of fire danger. 50% of fires could be reliably recognised by NOAA/AVHRR;
- maps of Siberian Moth damage (forecast possibilities are also investigated).
-

Work in the IGBP-NES Transect has been started in the last years. Several observation stations are located in this area. Thematic maps 1: 50 000 have been prepared. In a circle of 1 ha around each observation station intensive measurements took place. Measurement stations are distributed all along the Transect. With RESURS, maps of forest productivity were generated and verified including maps of biomass and storage of soil organics. Special investigations along the Angara river to investigate restoration of vegetation after fire.

Presentation by Dr. Vyacheslav Cherkashin (manager of GIS group)

Map generation on local and regional scale. Map sector O-46 is the most investigated part around Krasnoyarsk.
- Maps of Russian forest, soil maps, vegetation and climate etc. exist at scale 1: 1 Mio.
- Dendrochronology maps are used for prediction of forest productivity.
- Maps of carbon content in vegetation and soil.
- Regional maps on species composition and age structure, landscape, forest types.
- Maps of fire history and classes of biological regimes were used to generate a fire danger map at 1 : 1 Mio.

Major case study for ecological management: Bol'shaya Murta, because of extensive moth infection in 1994-96 and large areas have changed from coniferous to deciduous. Here, maps are available at 1: 250.000. Landscape maps in "3D" and maps of possible fire-succession vegetation. SPOT and airphotos are used, remote sensing methods in general are exploited since 1976. The GIS also consists of 1: 25.000 maps.

Different levels for maps scales:
- local level 1: 500 000 to 1: 100 000
- subregional level 1: 100 000 to 1: 1 000 000
- regional level 1: 1 000 000 and smaller

Presentation by Dr. Christiane Schmullius

Overview of objectives and status-quo of the SIBERIA Project.

Presentation by Dr. Thuy LeToan

What can we extract from radar information? First started with physical models of trees (*Pinus nigra*), establishment of a tree growth model: 4 orders of branches, 9000 cylinders, position, orientation etc. are considered. Scattering contributions were estimated on *Pinus pinaster*.

Backscatter coefficient increases with phytomass, saturation at about 100 t/ha for L-band (50 t/ha for C-band). Comparison of classification results for different classes of clear-cuts with SPOT data from Yrjö Rauste. First results from ERS data.

Presentation by Guest-Professor Nobuyuki Abe, Niigata University, Japan
Study along the Yenisey in the region of Tuva, with OPS-Sensor on JERS-1. Classification of different tree species (*Pinus sylvestris, Pinus sibrica*) and their density. NDVI from different tree species. Co-operation between Sukachev Forest Institute and the Niigata University, Japan since 5 years.

Presentation by Dr. Slava Kharuk
He was one of the main investigators for the Spectral Reflectance Measurements Station, we had visited. He is a co-operation partner of Jon Ranson, NASA Goddard Space Flight Center. Images from SIR-C/X-SAR used for classification of vegetation.

Lunch at Academy-Restaurant

15:00 Federal Forest Service, Forest Committee for the Krasnoyarsk Region

Meeting with Director Dr. Vladimir N. Vekshin
6% (!) of the World's growing stock belongs to Krasnoyarsk Kray. Total land area is 14 % of Russian territory. 160 Mio ha total forest land. Coniferous forest is more than 60 %. 57 different administrative levels belong to this forest agency, 52 forest enterprises (biggest forest enterprise is near the arctic circle = Taimyr, 22 Mio ha), national parks, forest protection centre. 5500 employees, 3500 forest guards. Krasnoyarsk Kray covers very diverse geographical regions, since it stretches almost from 50 – 80 degrees latitude.

Main tasks: fire protection, reforestation, insect protection, harvest. Wood harvest: 53 Mio m^3 = 25 Mio ha during Soviet Era by selective logging. Perestroika caused decline to 6 Mio ha. 50% export to Japan, China, Chita, Buriatia and Mongolia.

40.000 ha have been burned out. 25 planes are used for forest fire fighting. 500 people are employed. All forest is federal property. 95% of this forest is managed by this Committee. The State's responsibility: to protect forest! 1000 – 1500 forest fires per year = 100–120.000 ha. Last year only 12.000 ha burnt (very lucky because cold and rainy May and June and good preparation of people). Most important are prophylactic measurements, e.g. education in schools. Of 400 fires this year, 95% were caused by people, 25% in May and June by dry lightning. In July and August mainly dry lightning causes forest fires. Along the front of clouds lightning is produced: a line of fire along this track. Helicopters are following this line.

Only 40% of Krasnoyarsk Kray are under fire protection and thus observation. Every 10-12 years airphoto campaigns. To update, the data from the SIBERIA-project even in the scale of 1: 1 or 2 Mio would be very useful (even a forest/non-forest map) because of the size and difficult access to major parts of the district.

Siberian Moth "interval" every 10-12 years. 1 Mio ha was destroyed. Forest treated with two insecticides: Desos (French) and Dipel (American). Forest Patological Service works on better predicting how many moths are where.

11.-12.000 ha annually new planted forest. Existing undergrowth is protected. 100 nurseries for seedlings. 6 – 7 Mio ha harvested area from these plantations.
Krasnoyarsk Kray is the geographical centre of Russia, therefore unfortunately highest prices for transport (markets to the East and the West are 6000 km away). Only high quality wood can be sold, for example the Angara pine (Ангарская сосна). This pine has to be 120 years old for harvest. Wood rings show very regular pattern. Natural reforestation only.

In the former Soviet Union, 30% of all forest enterprises had higher debts than benefits. Benefits of healthy industry went to “sick”. This ensured 100% employment and management of forests. Regionally varying cost for transport was compensated by the Ministry of Transport. State regulations existed. A lot of wood was exported to republics like Tchetchenia. The demand for wood is still high, but there are now new custom regulations, that make it impossible to export wood to these independent states. Major problems are outside forestry: political and economical problems in Russia.

16.30 Free time in Krasnoyarsk

18.00 Internal SIBERIA Methodology Meeting

- Preparation of Mansky field site visit (originally planned location cannot be visited due to landslide – we have to use full-frame image prints, cannot use zooms).
- Discussion on classification rules.
- Discussion on GIS-parameters: necessity of biomass calculations.

20.00 Dinner (Restaurant close to Hotel)

FRIDAY, JUNE 4, 1999, MANSKY

8.00 Transport to Narva on the Mana River, southeast of Krasnoyarsk

11.00 Visit of the Mansky Forest Enterprise

Without further introduction who we are and what we are here for, we rushed in the door and asked a lot of questions and started a big discussion:

> “On our ERS images are big areas with medium coherence, sharply seperated from areas with low coherence. Both seem to be forest. But what is the difference? What are the causes for the different coherence values?”

Answers: In this area there have been several burnings. 1990 has been a very serious fire, after that only slow regeneration, and a new fire in 1997, but smaller and less intense than 1990. Since 1993, sites in the middle of the ERS scene (where coherence is medium) have been harvested. The topographical map was produced 1984. Large (medium coherence) region underwent harvesting in the 70’s. Two weeks ago all that forest burnt again.

In the coherence image, the recognisable areas from West to East: Closed Cedar Forest – “border” - *Picea, Abies, Betula* (heavily harvested forest 1975 - 1980’s).

Introduction to the Enterprise by its quarter-ranger

The area of this forest enterprise is 418.000 ha and has 70 workers. The enterprise owns a wood mill. Wood processing for local population. 500 ha per year is planted forest. 10.000 m3 is the current forest harvest. Forest fire protection: 100 guards, 12 chemical stations. 1 Helicopter and 12 personal. This is one of the few airstations for fire fighting.

Mansky is divided into two forest regions: mountain and plain forests. The forest consists basically of *Picea* and *Abies*, and further of *Betula* and Cedar. The boundary is basically formed by harvest due to ecological conditions. The Western forests mainly consist of Cedar stands, that strictly and only used for pine nut harvest.

25./26.05.99 a ground-fire went throughout 25 km of forest. It destroyed 70% of our GIS key area. A visit today it is not possible.

12.00 Embarkment onto two boats and transport to “Garden Eden” (93°34' E, 55°42' N)

Along the riverbanks (hilly terrain) mixed forest consisting of *Pinus sylvestris, Larix, Betula, Picea., Pinus sibirica*, further *Populus* and *Picea* (*P.sibirca* mainly on steep slopes. Question of nutrients and drainage?). Where flat terrain (meadows): mainly *Betula* and *Salix*, especially on the islands in the river only *Salix*.

After lunch, transport down the Mana river to the village Bolshaya Ungut (93°25' E, 55°44' N). Short lecture by Thuy LeToan: in the ERS images, here at the village high amplitude and high coherence are visible - roofs of houses can cause high backscatter, even from wooden houses with wooden roofs.

A retired forest fire engineer who has worked here for 40 years gave us some information. In 1997, a very severe fire occurred and the regeneration of the forest was very slow. During the 1970-1980’s intensive harvests. Therefore 1975, houses for about 400 people were build. Mainly *Picea, Abies* and some Cedar grew here before the harvest and the fire. Nowadays this is not longer an industrial zone, it is strictly protected. This zone stretches until the boarder which is recognisable in the ERS images.

Spontaneous organisation of visit of burnt forest north of the Mana river (93°22' E, 55°50' N). Only one 4-wheel drive vehicle was available. Participants: LeToan, Quegan, Schmullius, Shvidenko, Gluck, and 2 forest guards. Visit of 1990-fire area, where it meets the less severe 1997-fire area. The severe fire in 1990 had totally burned the forest. Now, nine years later, re-growth consisting of bushes and small birch trees (height < 2 m) was visible. This area has very high coherence values. Next to it, is a region of medium coherence. This had been undisturbed forest until the ground-fire went through it in 1997. Very interesting is the fact, that although the top of the canopy was still green (not burned) and only the lower ¾ of the tree were burned, this area can be recognised due to higher coherence. The fire-boarder runs along a valley with riparian vegetation (very moist, local swamps). This boarder is easily visible on the coherence image (running diagonally from SW to NE) due to medium versus low coherence areas.

19.30 Dinner (fresh fish, local schnaps, beautiful singing)

01.00 Arrival in Krasnoyarsk

SATURDAY, JUNE 5, 1999, KRASNOYARSK –DIVNOGORSK

10.00 City Tour, Visit of Yenisei Dam

13.00 Lunch

15.00 Visit of Botanical Garden at Sukachev Forest Institute

Lecture by Prof. Anatoly Shvidenko:

500 tree and shrub species in Russia. 7 tree species cover 85 % of Siberia: larch, birch, spruce, aspen, cedar, Scotch pine, fir: *Abies, Picea, Pinus sylvestris, Pinus sibirica, Larix, Betula, Populus*. 80-82% are coniferous forests.

Larch covers about 35%, forming the Northern and Southern tree line. *Larix sibirica* and *Larix dahurica* survives temperatures of –60°C and up to +21°C monthly mean temperature. Larch has a growing stock volume of about 100-300 cubic meter per hectare. The average for all Russian tree species is about 180 m^3/ha. The average leaf-on time period is from mid-May until beginning of October.

Of Birch, 30-35 different subspecies exist. They are divided into softwood and hardwood. Hardwood species, e.g. *Betula ermanii* only East of Lake Baikal. Siberian species: *Betula pendula* (or *varucosa* – old name). Litter fall is about 1st of September. Only 3-5% of forest harvest is birch.

SUNDAY, JUNE 6, 1999, TRANS-SIBERIAN RAILWAY FROM KRASNOYARSK TO IRKUTSK:

13.00 Departure to Train Station
15.00 Departure of Train N250

MONDAY, JUNE 7, 1999, IRKUTSK

11:00 Arrival in Irkutsk: Welcome by Dr. Leonid Vaschuk, Irkutsk Regional Forest Management Service, SIBERIA-partner.

13.00 Transport to Russian Academy of Science in Irkutsk, Biophysical Institute.

Presentation by Dr. Leonid Vaschuk Irkutsk Regional Forest Management Service, SIBERIA-partner.

Irkutsk region contains 58 forest enterprises, which are managed by the State Forest Department. Total forest land 65.7 Mio ha plus one national park and two national forest reserves. 80% of Irkutsk Oblast is covered with forest. 9.2 Mio m^3 growing stock, of which 5.4 Mio m^3 are available for harvest. 2 % of the World's forest belongs to Irkutsk Oblast. 6.4 % of the harvest belongs to highly valuable wood. Dominant species are coniferous, covering 45 Mio ha. 5.4 Mio m^3 of mature forest, ready for harvest. 2100 forest fires in 1998. 38 forest fires today and yesterday registered. 45 fires probably by now. 98% are ground-fires, 2% are crown fires. 80% of all fires are human caused.

The amount of harvested wood dropped, maximum was in 1988. 40.7 Mio ha harvested in 1988. 12.6 Mio ha harvested in 1998. This is typical for the entire country. In the former Soviet Union, Irkutsk produced 10-11% of all Russian wood production.

Presentation by Dr. Christiane Schmullius

Overview of objectives and status-quo of the SIBERIA Project.
Discussion: Forest enterprises have to update their ground-truth every year on the basis of air photography. Question about defoliation monitoring - LeToan: defoliation should be better seen with shorter wavelengths than ERS.

Presentation by Prof. Vjacheslav Rozhkov, Dokuchaev Soil Institute, Moscow, SIBERIA-Partner

This institute controls the SIBERIA GIS-Database. Soil maps of all areas are available in the scale of 1: 100.000 to 1: 5 Mio. Landscape maps are now available at some scales.

Presentation by Prof. Mikheev, Geography Institute of the Siberian Branch of the Akademy of Science

Laboratory since 20 years, development of remote sensing methods, cartography, research on natural environments ecological investigations with remote sensing. Some work has been done in Krasnoyarsk Kray also, but now mainly in Irkutsk.. Unfortunately no radar data available. Basically optical data from Russian systems used. Mainly dealing with forest.

Presentation of GIS project for Olchon island. RESURS data is here available since October 1995. Also, some Landsat and SPOT images.

Presentation by Prof. Shamov, Institute of Plant Physiology:

The institute possesses several laboratories for ecological and dendrochronological research. Biological indicator system for biosystems along the Baikal. No remote sensing methods are used until now. Close co-operation with Geographical institute. The maps presented were generated at the Geographical Institute. Threat-maps for different insects at scale 1: 7.5 Mio. in co-operation with a Moscow forest department. Protection of endangered plants. Investigation of pollution, e.g. from Baikalsk paper mill. About 20% of damaged needles are in highly polluted areas.

17.00 Irkutsk City Tour

20.00 Internal SIBERIA Methodology Meeting

Lessons learned. Preparation of Baikal field site visit.
Brief lecture by Dr. LeToan: Coherence drops with increasing growing stock volume. In slopes this relationship becomes unclear, measurements are very scattered. The drop of coherence can be caused by bad geometry. If there is no DEM, then there is no correction of coherence as well. High coherence areas can appear in areas of dense vegetation due to geometrical aspects.

TUESDAY, JUNE 8, 1999, IRKUTSK – LAKE BAYKAL

9.00 Logistics (changing money, buying airtickets)
10.00 Departure to Lake Baykal
13.00 Lunch in Slyudyanka

14.00 Transport to Marble Quarry “Pereval” (103°30' E, 51°40' N)

Presentation by Company Geological Advisor

The marble is transported in a cable car over a distance of about 3 km. 2000 tonnes are transported per day at the moment. Marble is used for cement and decorative purpose. What it is used for depends on the mineral composition. The exploitation is done above-ground. 1 tonne costs about 2 USD at the moment. Lake Baikal is 460 m above sea level, our stop at about 1500 m at the top of the quarry.

The forests in the surrounding of the quarry consist mainly of cedar (*Pinus sibirica*). Cedar needs moisture and good soils, it is a typical tree for more humid areas. Wind exposition is also important. Other tree species of a mixed cedar forest are *Picea* and *Larix*.

16.00 Slyudyanka Forest Enterprise

Presentation by Forest Quarter-Ranger

A production plant for wild berries existed, but was closed due to economical problems. This Forest Enterprise is the most southern one of the Irkutsk Oblast. Its East-West extension is about 120 km, bordering to the East the Buryat Republic. Fires are mainly caused by people due to their economic situation. Unemployed people use more the forests for hunting and collecting plant and berries. The slope exposition has in the Slyudyanka area not a very strong impact, but this impact is increasing towards South (to Mongolia) up to extreme cases where the north-slope is forest-covered and the south-slope forest-free.

Cedar (*Pinus sibirica*) is the dominant species in 60 % of the forests. 80% of the total area is covered by forest. Protection of fire and insects is the main task. 2000 m^3 of wood are processed. Cedar nuts are collected as a selling product, only every 4-5 years. Forest is within Baykal watershed protection zone, so harvest is prohibited. Just selective log harvest for local demand and sanitary cutting.

After the Baykalsk Cellulose Kombinat started working in 1962, the fish population as well as berry harvest and forest vitality were strongly impacted.

18.00 Visit of Nature Museum, Slyudyanka

Very interesting museum with a good collection of local minerals and presentation of regional animals. (We expressed our thanks in the guest-book and Anatoly gave a donation to the museum since they are momentarily not able to pay the electricity bill.)

19.00 Transport to Guesthouse in Tibilti/Ckotimport (103°10' E, 51°50' N)

Driving East from Slyudyanka along the road to the Tunka basin, we passed one of the ground-truth sites: GIS Key Area 19 next to the road, Polygon 176 and 171. In this wetland site, *Betula* and *Pinus sylvestris* are dominant. The wetland area along the road shows on the coherence image high values. Small ridges into the swamp with higher forest densities can also be recognised with lower coherence values.

Long discussion about clustering of GIS-polygons based on other GIS-parameters (e.g. landscape, soils). Explanation of phytomass = ALL parts of tree including roots. In GIS data, look for dominant species and %-values, because e.g. a birch forest with cedars will be called "cedar forest", due to economical importance of cedar.

21.00 Dinner, Sunset over Tunka Cordilleres, Campfire

WEDNESDAY, JUNE 9, 1999, FORESTS VISITS AT SW-SHORE OF LAKE BAYKAL

9.00 Transport to Cedar Forest and Upland Area (103°25' E, 51°45' N)

For cedar nut production, re-growth is supported by planting cut branches. After 15 years, the cedars are producing nuts. These cedars are 65 years in average. Undergrowth mainly horse-tail and grass. On the opposite slope a slope-bog is visible, caused by varying geological/pedological layers.

Drive further up-hill into the forest until bridge (polygon 87, Stand 2.): forest damaged by Siberian Moth. 7-8 years ago a ground-fire took place. The north side of this valley has low coherence, high backscatter: dense forest with mainly *Pinus sylvestris* and some *Pinus sibirica, Betula, Picea.* Comments: probably more backscatter from stems on slopes, as they can be seen very well, better than on flat areas (Quegan), backscatter cannot be used here because of the slope influence (LeToan).

11.30 Transport to Tourist Camp "Cneshnaya"

13.30 Lunch at Camp

14.30 Departure for Field Visits (104°30' E, 51°30' N)

The series of visited ground-truth sites during the following two days, familiarised the team with various low biomass cover types, where the coherence images showed high coherence values. This approach seemed to be the most fruitful, because so far the lesson had to be learned, that with ERS-images alone no discrimination of closed forest could be done. Therefore, the emphasis was now on understanding high-coherence surface types.

First stop along road, west of Vuidrino

Different *Betula* stands. North of the road young re-growth. No exact answer on age (inventory list said 40 years, but stand looked younger). Ground-truth verification failed due to braking American equipment. South of the road also *Betula* forest, older and with coniferous re-growth.

The inventory measurements were prepared by airphotos. Polygons were verified in the field with geodetical instruments. Roads and other artificial features are also used for boarder determination. Species composition, biomass, height etc. have been measured.

Walk into forest (Area 19)

The inventory has been done 15 years ago, now only birches are here. Average age is 30 years, average height 8 meters, relative stocking 0.5, growing stock volume 35-45 cubic meters per hectare.

Some few meters further on we have the next stand: 50% *Betula*, 30% Cedar, 20% *Picea* and *Pinus*. Forest stand is marked as Cedar! *Explanation*: where coniferous species together build 50 % of the stand, there conifers are dominant by definition. Here, the dominant conifer is Cedar, therefore the stand is marked accordingly (even though as a single species only 30%). Birch is not interesting for forest harvest.

Some meters further on, 3 polygons meet:: very young birch (behind is a polygon with older birch stands), one with bog and the one with 30 % cedar, which was just visited.

Second bus stop further West

Large bog: sphagnum moss, wool grass, single very small birch trees. These are quite old: 15 years. Northwest of the bog, railroad tracks of the Trans-Siberian railway.

Third bus stop at Bridge over Xara Murin near Village Murino

15 years ago this was a hayfield, now small *Betula*, *Salix* (30 %) and shrubs. Phytomass: 10-15 to/ha.

Walk to Riparian Area along River
Mosaic of meadows (very wet), old-growth of aspen and bogs.

18.30 Return to Tourist Camp and Dinner

TUESDAY, JUNE 10, 1999, BAYKALSK AND LAKE BAYKAL

9:00 Departure for Field Visits

Bus Stop between Colsan and Murino at indigenous forest: Forest classification types: virgin, natural and anthropogenically influenced forest.

The succession stages of forests after burning are:
1. first 20 years only *Betula*
2. *Picea* and *Cedar* are growing below *Betula*
3. 100 years late, birch forest has turned into coniferous forest

Betula is generally not a dominant species, just for a short period after burning or clear-cut. Here, 30-35% *Pinus sibirica*, 30-35% other coniferous, 40-30% *Betula*. Exposition-dependent differences visible: cedar prefers the warmer slopes.

Field visit to high-coherence area (burnt forest) on hill slope, South of Colsan (104°10' E, 51°30' N)

In the late 60's strong fires, 1996 again fire (partly only ground-fire). Three years ago, 3 parallel power lines have been built (visible on ERS images). In GIS, *Betula* and *Salix* less than 1 m height, now 3 Meter. The ground-fire in 1996 was not very severe, 1997 grass started to re-grow. The fire was burning from the river up-hill. About 30 ha have been destroyed.

13.00 Lunch in Baykalsk

14.00 Visit of Baykalsk Cellulose Combinat

16.30 Embarkment on Forest Department Vessel to cross Baykal

17.30 Internal SIBERIA Methodology Meeting

Protocol of Remarks:

- Better preparation would have been necessary, but JERS data was not been available (LeToan).
- SSC will only produce frames where ERS-Tandem + Amplitude 3 (summer 1998) + JERS are available and the quality is good (Schmullius).
- Good, if we get 1 or 2 classes inside the forest, outside 3 or 4 classes (bogs, burnt areas, water, urban areas) (Quegan).
- Keep experimenting with unsupervised classification, find something robust and simple (LeToan).
- Use additional information, e.g. elevation model with 1km resolution (Luckman).
- Degree of slope is a limit of processing, it is not known yet but for sure the area around Baikal will be on that limit (Quegan).
- JERS must be the key as longer wavelength means a more stable coherence (Baker).
- 1-1.5 dB difference is expected between leaf-off/leaf-on situation. But there is more to learn, since different species behave different in time and geographical location. Look at the histograms to distinguish classes (especially for non-forest classes: agriculture, shrubs, bare soil). Focus on low productivity and low biomass areas. IIASA has no non-forest information, so algorithms have to be transferred to SSC, with which to classify only about 5 landcover-classes (not various agriculture/pasture-classes) (LeToan, Quegan).
- Coherence values will not be the same from one image to another! (LeToan)
- No idea how variable the coherence is for low biomass, we only looked on a few places (Quegan).
- We have to develop together the methodology for SSC, everyone can test on own testsites and develop ideas (Wagner)
- Concentrate on non-forest, since we have a detection problem distinguishing forest classes (Quegan).
- Put infos about own analyses on the web, that everybody can learn (Luckman).
- Pay attention to forest that is not in polygons, since it is under agricultural management (Quegan).

Actions to take for further image analysis:

- Use stock volume and then biomass for every polygon you select!
- Use for every polygon the following parameters in this order:
  - stock volume
  - biomass
  - % of deciduous forest, % of coniferous forest
  - slope
  - strange flag (something contradictory, for example high coherence but forest)
- Calculate change in amplitude and coherence.
- Select first images with strange values first and with anomalies to understand variation and problems.

Decisions:

- Use GTOPO-30 as input and info.
- All teams build up a SIBERIA database: need to understand statistics of backscatter and coherence for low/high biomass classes, growing stock classes.
- *Questions*:

- Has biomass to be calculated for all polygons? Answer: Biomass will be calculated by IIASA for representative (necessary) polygons – not all.

- Are component biomass calculations useful? Answer: perhaps –since ERS and JERS backscatter originates from different parts of canopy.

19.00 Arrival at Palavinnui-Beach (104°20' E, 51°50' N)

(...who could ever forget this last night on the shore of Baykal, despite rain and lightning...)

FRIDAY, JUNE 11, 1999, LAKE BAIKAL - LISTVJANKA

9:00 h departure with the boat to Listvjanka (near the start of the Angara river). Arriving at about 11 h, with following **visit of the Limnological Museum**. The afternoon was spent in a hotel the hill side of Listvjanka. 20:00 back to Irkutsk by bus.

SATURDAY, JUNE 12, 1999, IRKUTSK – MOSKAU

05:25 h departure (by bus) to the Irkutsk Airport.
07:00 h Flight to Moscow Sheremetevo I
end of journey

Scientific name:	**common name in English:**	**common name in German:**	**common name in Russian:**
Coniferous:			
Abies sibirica	fir	Tanne	пихта
Picea sibirica or abies or obovata	spruce	Fichte	ель
Pinus sylvestris	scotch pine	Kiefer	сосна
Pinus sibirica	cedar	sibirische Kiefer	седр
Larix dahurica, sibirica and sukachova	larch	Lärche	лиственница
Deciduous:			
Populus tremula	aspen	Zitterpappel oder Espe	тополь
Populus balsamifera?	?	Pappel (?)	осина
Betula pendula	common birch	Hänge-Birke	береза
Betula pubescens	birch mainly in bogs	Moor-Birke	береза
Salix	willow	Weide	ива
Alnus	alder	Erle	ольха
Sorbus sibirica	rowan-tree or mountain-ash	Eberesche oder Vogelbeerbaum	рабина

Major Siberian Tree Species

Appendix C: SIBERIA's False Color Composite Mosaic (p. 116)
Appendix D: SIBERIA's Forest Cover Map Mosaic (p. 117)
Appendix E: Example of a Radar Image Mapsheet (p. 118)
Appendix F: Example of a Forest Cover Mapsheet (p. 119)

Appendix G: The SIBERIA Project Team Member List (p. 120)

DLR-HF	Prof. Christiane Schmullius, Dr.Wolfgang Wagner, Jan Vietmeier, Andrea Holz, Deutsches Zentrum für Luft- und Raumfahrt, Institut für Hochfrequenztechnik, P.O. Box 11 16, D – 82230 Wessling, Germany; Phone +49.(0)8153.28-2337, Fax +49.(0)8153.28-1449, e-mail: chris.schmullius@dlr.de
FSU	Seit 01/00: Leif Eriksson, Friedrich-Schiller-Universität, Institut für Geographie, Loebdergraben 32, 07743 Jena, Phone +49.(0)3641.948877, Fax +49.(0)3541.948852, e-mail: c.schmullius@geogr.uni-jena.de
DLR-DFD	Dr. Achim Roth, Ursula Marschalk, Deutsches Zentrum für Luft- und Raumfahrt, Deutsches Fernerkundungsdatenzentrum, Muenchener Str. 20, D-82230 Wessling, Germany; Phone +49.(0)8153.28-2706, Fax +49.(0)8153.28-1445, e-mail: achim.roth@dlr.de
IIASA	Prof. Sten Nilsson, Prof. Anatoly Shvidenko, Michael Gluck, Ian McCallum, International Institute for Applied Systems Analysis, Schlossplatz 1, A – 2361 Laxenburg, Austria; Phone +43.(0)2236.807-229, Fax +43.(0)2236.71313, email: nilsson@iiasa.ac.at
CESBIO	Dr. Thuy Le Toan, Dr. Malcolm Davidson, Universite Toulouse III - Paul Sabatier, Centre d'Etudes Spatiales de la Biosphere, 18, avenue Edouard Belin, F - 31401 Toulouse, France; Phone +33.561.556671, Fax +33.561.558500, email: thuy.letoan@cesbio.cnes.fr
SCEOS	Prof. Shaun Quegan, Dr. Jiong-Jiong Yu, Sheffield Center for Earth Observation Science, Hicks Building, Hounsfield Road, Sheffield, S3 7RH, Great Britain; Phone +44.114.222-3778, Fax +44.114.222-3809, email: s.quegan@sheffield.ac.uk
UWS	Dr. Adrian Luckman, Dr. Kevin Tansey, Department of Geography, University of Wales, Singleton Park, Swansea, SA2 8PP, Wales/UK; Phone +44.1792.295524, Fax +44.1792.295955, email: a.luckman@swansea.ac.uk
NERC	Dr. John Baker, Dr. Heiko Balzter, David Gaveau, Institute of Terrestrial Ecology, Natural Environment Research Council, Abbots Rifton, Huntingdon, PE17 2LS, Cambridgeshire, United Kingdom; Phone +44.1487.773381, Fax +44.1487.773277, email: j.r.baker@nerc.ac.uk
VTT	Dr. Einar-Arne Herland, Dr. Tuomas Häme, Dr. Yriö Rauste, VTT Technical Research Center, P.O. Box 13002, Otakaari 7B, Espoo, FIN-02044 VTT, Finland; Phone +358.9.456-4799, Fax +358.9.456-6475, email: einar-arne.herland@vtt.fi
SSC	Dr. Torbjörn Westin, Marianne Orrmalm, Roland Utsi, SSC Satellitbild Aktiebolag, P.O. Box 4207, 17104 Solna, Sweden, Phone +46.8.6276462, Fax +46.8.984975, email tw@ssc.se.
Gamma	Dr. Urs Wegmueller, Dr. Andreas Wiesmann, Gamma Remote Sensing Research and Consulting AG, Thunstrasse 130, CH – 3074 Bern, Switzerland; Phone +41.31.951-7005, Fax +41.31.951-7008, email: gamma_rs@pingnet.ch
ESFIPE	Dr. Victor Skuding, East Siberian Forestry Inventory and Planning Enterprise, Krupskoi 42, 66062 Krasnoyarsk, Russia; Phone +7.3912.452830, Fax +7.3912.453224
IFS	Dr. Leonid Voshtshouk, Irkutsk Regional Forest Management Service (IFS), Gor'Kogo 31, 664011 Irkutsk, Russia; Phone +7.3952.335975, Fax +7.3952.243155
IFRAS	Prof. Vladimir Sokolov, Department of Forest Inventory and Management, Academgorodok, 66036 Krasnoyarsk, Russia; Phone +7.3912.494635, Fax +7.3912.433686